


THESIS APPROVED BY

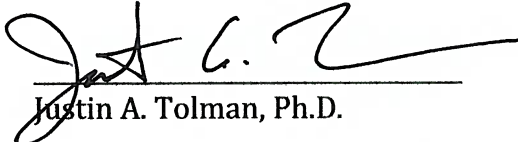
05/13/2015
Date



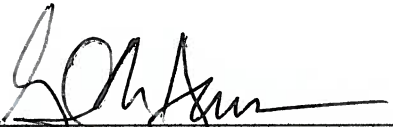
Harsh V. Chauhan, Ph.D.



Somnath Singh, Ph.D.



Justin A. Tolman, Ph.D.



Gail M. Jensen, Ph.D., Dean

**DRUG-POLYMER AND DRUG-LIPID MISCIBILITY FOR THE DEVELOPMENT OF
AMORPHOUS SOLID DISPERSIONS AND SOLID LIPID NANOPARTICLES**

By

Anne Trivino

A THESIS

**Submitted to the faculty of the Graduate School of the Creighton University in
Partial Fulfillment of the Requirements for the degree of Master of Science in
the Department of Pharmacy Sciences**

Omaha, NE

May 2015

© Anne Trivino, 2015

Abstract

Flutamide (FLT) is an anticancer agent used in the treatment of prostatic carcinoma. FLT amorphous solid dispersions (SDs) and solid lipid nanoparticles (SLNs) were prepared to overcome limited solubility. Investigation of drug-polymer and drug-lipid miscibility was carried out to enhance drug performance by assessing solubility and particle size. Miscibility was then correlated to performance to determine successful preparation of FLT SDs and SLNs.

Four polymers used to prepare SDs included polyvinylpyrrolidone K90 (PVP), hydroxypropyl methylcellulose (HPMC), eudragit (EPO), and polyethylene glycol 8000 (PEG). Miscibility of drug and polymer at 90:10, 70:30, and 50:50 w/w (drug:polymer) was assessed through modulated differential scanning calorimetry (MDSC). FLT SDs were characterized by powder X-ray diffraction (PXRD). Molecular interactions were determined using infrared and Raman spectroscopy and molecular modeling using Jaguar. Polymer precipitation inhibition efficiency and dissolution studies were conducted at 0.1 mg/mL and 0.05 mg/mL (70:30 w/w).

Glyceryl monoleate (GMO), Precirol® (glyceryl distearate, PRE), glyceryl monostearate (GMS) and COM® (glyceryl dibehenate, COM) were prepared with Gelucire (GEL) 44/14 or 50/13 as surfactant at 5:2 w/w (lipid:surfactant) and 2:1 w/w (FLT:lipids/surfactants). Miscibility of lipid and surfactant mixtures with and without FLT were investigated using MDSC. SLNs with and without drug-loading were prepared by ultrasonication and characterized for particle size. Drug-loaded SLNs were lyophilized and characterized in a similar manner.

Miscibility between FLT-PVP and FLT-PEG was observed in MDSC results. PXRD indicated the formation of FLT-PVP amorphous SDs, while FLT-PEG formed a crystalline eutectic mixture. Molecular modeling studies confirmed potential interactions formed between FLT-PVP and FLT-PEG. PVP and PEG were shown to be the most efficient FLT precipitation inhibitors and displayed enhanced dissolution profiles.

Miscibility between GMO and GMS with GEL 50/13 was observed in MDSC results in the presence or absence of FLT. The particle size of SLNs prepared from GMO and GMS was found to be <100 nm compared to >200 nm obtained from PRE and COM. Similar trends regarding particle size were seen upon lyophilization.

Miscibility of FLT with polymers and lipids demonstrated enhanced performance suggesting FLT SDs and SLNs would result in increased solubility and bioavailability.

Preface

Abstracts

1. Trivino, A., Bernick, J., Chauhan, H. Effects of lipids and surfactant miscibility on the particle size of solid lipid nanoparticles. American Chemical Society Midwest Regional Meeting, Omaha, NE. October 2012. Poster.
2. Trivino, A., Bernick, J., Chauhan, H. Molecular modeling of drug polymer interactions for amorphous stabilization of poorly soluble anticancer drug flutamide. American Association of Pharmaceutical Sciences Annual Meeting and Exposition, San Antonio, TX. November 2013. Poster.

Publications

1. Meng, F., Trivino, A., Prasad, D., Chauhan, H. (2015). Investigation and correlation of drug polymer miscibility and molecular interactions by various approaches for the preparation of amorphous solid dispersions. *European Journal of Pharmaceutical Sciences*, 71(0), 12-24.
2. Trivino, A., Chauhan, H. (2015). Drug-excipient compatibility for the formulation development of solid lipid nanoparticles. *American Pharmaceutical Review*, 18(20), 24-28.

Dedicated to my loved ones

ACKNOWLEDGEMENTS

I would like to express my sincere gratitude to the Creighton University Pharmaceutical Sciences faculty and staff for their unwavering support and encouragement throughout the program. First, I would like to thank my advisor, Dr. Harsh Chauhan, for his continual guidance, patience, and willingness to teach me. I would also like to thank my committee members, Dr. Somnath Singh and Dr. Justin Tolman, for their valuable suggestions toward my research. I am grateful for all of their expertise, time, and assistance with the preparation of my manuscript and defense. Additionally, I would like to thank Dr. Somanth Singh for overseeing my progress and ensuring the completion of the program requirements. Thanks to Daniel Munt for all his help with conducting experiments and Dawn Trojanowski for her encouragement.

To my lab partners, Jonathan Bernick, Urvi Gala, and Fan Meng, thank you for your support and encouragement throughout this project. I appreciate all your input and contributions to this research. My special thanks to Anne Grana and my fellow graduate students who have shared their knowledge, friendship, and encouragement, all of which has made this a memorable experience.

I would like to express my utmost gratitude to my family and friends for their continual love, support, and inspiration. Above all, I would like to thank God for his unwavering faithfulness and grace.

TABLE OF CONTENTS

Abstract	iii
Preface	v
Dedication	vi
Acknowledgements	vii
Table of contents	viii
List of figures	xv
List of tables	xvii
List of common abbreviations	xviii
Chapter 1 Introduction	1
1.1 Solid Dispersions	4
1.1.1 Definition	4
1.1.2 Advantages	5
1.1.3 Disadvantages	6
1.2 Solid Lipid Nanoparticles	7
1.2.1 Definition	7
1.2.2 Advantages	8
1.2.3 Disadvantages	9
1.3 Flutamide	10
1.3.1. Indications	10
1.3.2 Physiochemical properties	11
1.3.3 Pharmacokinetics	11
1.3.4 Pharmacology	12

1.4	Polymers	14
1.4.1	Polyvinylpyrrolidone K90	14
1.4.1.1	Physiochemical state and appearance	14
1.4.1.2	Glass transition temperature	15
1.4.1.3	Molecular weight	15
1.4.1.4	Solubility	15
1.4.1.5	Density	15
1.4.1.6	Viscosity	15
1.4.2	Hydroxypropyl Methylcellulose	15
1.4.2.1	Physiochemical state and appearance	16
1.4.2.2	Glass transition temperature	16
1.4.2.3	Molecular weight	16
1.4.2.4	Solubility	16
1.4.2.5	Density	16
1.4.3	Eudragit	16
1.4.3.1	Physiochemical state and appearance	17
1.4.3.2	Glass transition temperature	17
1.4.3.3	Molecular weight	17
1.4.3.4	Solubility	17
1.4.3.5	Density	17
1.4.3.6	Viscosity	18
1.4.4	Polyethylene Glycol 8000	18
1.4.4.1	Physiochemical state and appear	18

1.4.1.2	Glass transition temperature	18
1.4.4.3	Molecular weight	18
1.4.4.4	Solubility	19
1.4.4.5	Density	19
1.4.4.6	Viscosity	19
1.5	References	19
Chapter 2	Drug-lipid and drug-polymer miscibility for the development of amorphous solid dispersions and solid lipid nanoparticles	22
2.1	Amorphous solid dispersions	23
2.1.1	Role of polymers in the development of amorphous solid dispersions	23
2.1.2	Drug-polymer miscibility	25
2.2	Solid lipid nanoparticles	25
2.2.1	Role of lipids in the development of solid lipid nanoparticles	26
2.2.2	Role of polymers in the development of solid lipid nanoparticles	27
2.2.3	Drug-polymer miscibility	27
2.2.4	Drug-lipid miscibility	28
2.3	Hypothesis and specific aims	30
2.3.1	Hypothesis	30
2.3.2	Specific aims	30
2.3.3	Materials and methods	31
2.3.3.1	Specific aim 1	31
2.3.3.1.1	Preparation of physical mixtures	31

2.3.3.1.2	Determination of miscibility	31
2.3.3.1.3	Preparation of amorphous solid dispersions	31
2.3.3.1.4	Characterization of amorphous solid dispersions	32
2.3.3.2	Specific Aim 2	33
2.3.3.2.1	Preparation of physical mixtures	33
2.3.3.2.2	Determination of miscibility	33
2.3.3.2.3	Preparation of solid lipid nanoparticles	33
2.3.3.2.4	Characterization of solid lipid nanoparticles	34
2.3.3.2.5	Determination of miscibility	34
2.3.3.3	Specific Aim 3	34
2.4	Conclusion	35
2.5	Future directions	35
2.6	References	35
	Chapter 3 Preparation and characterization of flutamide amorphous solid dispersions	38
3.1	Introduction	39
3.2	Material and methods	41
3.2.1	Materials	41
3.2.2	Methods	41
3.2.2.1	Preparation of physical mixtures (PMs)	41
3.2.2.2	Thermal analysis of flutamide, polymers, and physical mixtures	42
3.2.2.2.1	Thermogravimetric analysis (TGA)	42
3.2.2.2.2	Modulated differential scanning calorimetry analysis of PMs	42

3.2.2.3 Solubility Parameter Calculations	42
3.2.2.4 Preparation of solid dispersions (SDs)	43
3.2.2.5 Characterization of solid dispersions	43
3.2.2.5.1 Modulated differential scanning calorimetry (MDSC) analysis of SDs	43
3.2.2.5.2 X-ray powder diffraction (xPRD)	43
3.2.2.5.3 Infrared (IR) Spectroscopy	44
3.2.2.5.4 Raman spectroscopy	44
3.2.2.6 Molecular modeling studies	44
3.2.2.7 Flutamide precipitation studies	45
3.2.2.8 Flutamide dissolution study	46
3.3 Results and Discussion	47
3.3.1 Physiochemical properties of flutamide and polymers	47
3.3.2 Thermal analysis of flutamide, polymers, and physical mixtures	47
3.3.2.1 Thermogravimetric analysis	47
3.3.2.2 Modulated differential scanning calorimetry (MDSC) analysis of PMs	49
3.3.2.1 Drug Polymer Miscibility: First Heating Cycle (2 °C/min)	49
3.3.2.2.2 Drug Polymer Miscibility: Second Heating Cycle (\pm 0.2°C/min)	55
3.3.3 Solubility parameters of FLT and polymers	59
3.3.4 Characterization of solid dispersions	60
3.3.4.1 Thermal analysis of flutamide SDs	60
3.3.4.2 pXRD of pure FLT, polymers, PMs and SDs	62

3.3.5	Molecular interactions	65
3.3.5.1	IR spectroscopy of pure FLT, polymers, PMs and SDs	65
3.3.5.2	Raman spectroscopy of pure FLT, polymers, PMs and SDs	68
3.3.5.3	Molecular modeling	70
3.3.6	Precipitation inhibition studies	73
3.3.7	In vitro dissolution studies of FLT SDs	77
3.8	Conclusions	80
3.9	References	81
Chapter 4 Preparation and characterization of flutamide solid lipid nanoparticles		85
4.1	Introduction	87
4.2	Materials and Methods	88
4.2.1	Materials	88
4.2.2	Preparation of lipids and surfactants physical mixtures	89
4.2.3	Modulated differential scanning calorimetry (MDSC)	89
4.2.4	Preparation of nanoparticles	89
4.2.5	Characterization of nanoparticles	90
4.2.5.1	Particle size	90
4.2.5.2	Raman spectroscopy of lipids and surfactants	91
4.2.6	Stability studies	91
4.3	Results	92
4.3.1	Physiochemical properties of FLT, lipids and surfactants	92
4.3.2	Thermal Analysis	94

4.3.2.1 DSC for pure lipids and surfactants	94
4.3.2.2 Miscibility study of pure lipids and surfactants (GEL 44/14, 50/13)	96
4.3.2.3 Miscibility study of FLT with lipids and surfactants (GEL 50/13)	98
4.3.3 Particle size analysis	99
4.3.3.1 Unloaded solid lipid nanoparticles	99
4.3.3.2 Drug loaded solid lipid nanoparticles	100
4.3.4 Raman spectroscopy of lipids and surfactants	101
4.3.5 Stability studies of drug loaded solid lipid nanoparticles	103
4.4 Discussion	104
4.5 Conclusion	106
4.6 References	107
Chapter 5 Correlation of drug-polymer miscibility to solubility of amorphous solid dispersions and drug-lipid miscibility to particle size of solid lipid nanoparticles	109
5.1 Summary and conclusions	110
Chapter 6 Future directions	115
6.1 Potential future studies	116

LIST OF FIGURES

Figure 1	Nanoparticle drug incorporation models	7
Figure 2	Structural formula of flutamide	11
Figure 3	Metabolism of flutamide to its active moiety, 2-hydroxyflutamide	12
Figure 4	Structural formula of polyvinylpyrrolidone	14
Figure 5	Structural formula of hydroxypropyl methylcellulose	16
Figure 6	Structural formula of eudragit	17
Figure 7	Structural formula of polyethylene glycol	18
Figure 8	The effects of lipids in prepared SLN on drug absorption	26
Figure 9	Pharmaceutical and pharmacologic implications of evaluating drug-lipid miscibility in solid lipid nanoparticles	29
Figure 10	Graphical abstract of drug-polymer and drug-lipid miscibility for the development of amorphous SDs and SLNs	30
Figure 11	TGA of pure drugs and polymers	48
Figure 12	Example of MDSC thermogram from first heating cycle	49
Figure 13	DSC thermograms of pure FLU, FLU-PVP 90:10, FLU-PVP 70:30, FLU- PVP 50:50	52
Figure 14	Depression of melting point (initiation) of flutamide in presence of various polymers. Comparison of theoretical and experimental Enthalpy (melting) of pure flutamide observed in presence of polymers	53
Figure 15	Example of MDSC thermogram from second heating cycle	55

Figure 16	MDSC thermograms of 2 nd heating cycling of FLT-polymer physical mixtures at 70:30 w/w drug to polymer concentration	58
Figure 17	MDSC thermograms of FLT-polymer SDs (73:30 w/w): pure FLT , FLT-PVP, FLT-HPMC, FLT-EPO, FLT-PEG	61
Figure 18	XRPD of pure FLT, polymers, physical mixtures (70:30 w/w) and solid dispersions (70:30 w/w)	64
Figure 19	IR spectra of pure FLT, PMs, SDs	66
Figure 20	Raman spectra of pure FLT, PMs, and SDs	69
Figure 21	Molecular modeling results depicting hydrogen bonds formed between FLT-polymer complexes after geometric optimization	72
Figure 22	Flutamide precipitation in absence and presence of various polymers (70:30 w/w)	75
Figure 23	Precipitation inhibition efficiency of polymers	76
Figure 24	Dissolution profiles of pure FLT, PMs, and SDs (70:30 w/w)	79
Figure 25	MDSC thermograms of pure lipids and surfactants	95
Figure 26	MDSC thermograms of lipid-surfactant physical mixtures	97
Figure 27	MDSC thermograms of pure FLT, FLT-lipid, FLT-surfactant	99
Figure 28	Particle size of unloaded solid lipid nanoparticles	100
Figure 29	Raman spectra of pure lipids, surfactants and PMs	102
Figure 30	Particle size of loaded solid lipid nanoparticles on Day 1 and Day 14	103
Figure 31	Summary of the methods and results of FLT SDs	111
Figure 32	Summary of the methods used to prepare FLT SLNs	113

LIST OF TABLES

Table 1	Physiochemical properties of FLT and polymers	47
Table 2	Solubility parameter calculations of FLT	60
Table 3	Solubility parameters of FLT and polymers	60
Table 4	Summary of PXRD and MDSC results	65
Table 5	Peak positions of functional groups present in IR spectra for FLT and FLT binary SDs	67
Table 6	Raman peak assignments of FLT and FLT-polymer SDs	70
Table 7	Molecular modeling results of FLT and monomers	73
Table 8	Physiochemical properties of FLT, lipids and surfactant	92

LIST OF COMMON ABBREVIATIONS

FLT	Flutamide
SDs	Solid dispersions
SLNs	Solid lipid nanoparticles
PVP	Polyvinylpyrrolidone K90
HPMC	Hydroxypropyl methylcellulose
EPO	Eudragit
PEG	Polyethylene glycol 8000
MDSC	Modulated differential scanning calorimetry
PXRD	Powder X-ray diffraction
GMO	Glyceryl monooleate
PRE	Precirol®, Glyceryl distearate
GMS	Glyceryl monostearate
COM	Compritol®, Glyceryl dibehenate
PWSAD	Poorly water soluble anticancer drugs
API	Active pharmaceutical ingredient
LHRH	Luteinizing hormone-releasing hormone
PMs	Physical mixtures
ATR	Attenuated total reflectance
TGA	Thermogravimetric analysis
IR	Infrared

CHAPTER 1

Introduction

Introduction

Advancements in oral chemotherapy in recent years have altered clinical management of cancer by providing effective therapeutic alternatives and significantly improving patients' quality of life. The benefits of oral chemotherapy over traditional parenteral agents stem from ease of administration, convenient dosing regimens, decreased side effect profile, and reduced medical expenses (Mei et al, 2013). Despite these advantages, many new chemical entities and existing chemotherapeutic drugs pose a challenge for the pharmaceutical industry to design stable products capable of delivering chemotherapy.

Many anticancer agents exhibit high lipophilicity and low water solubility (Sultana, 2013). These properties of poorly water soluble anticancer drugs (PWSAD) limit their clinical use due to concerns with safety and efficacy. According to the Biopharmaceutics Classification System (BCS), a drug is classified as poorly soluble when the highest dose strength is not soluble in 250 mL or less of an aqueous media over a pH range of 1 to 7.5 at 37°C (O'Driscoll Griffin, 2008). PWSAD are often composed of structures with high lattice energy. As a result, thermodynamic stability hinders drug dissolution and release. Moreover, the inability for PWSAD to form interactions with water makes these agents unsuitable for oral administration. (Narvekar et al, 2014).

Further development of PWSAD is needed to mitigate the issues that arise during research and development. The aforementioned problem concerning drug dissolution is significant because dissolution rate is dependent upon solubility. Poor

solubility results in limited bioavailability of orally administered chemotherapy (Kawabata et al, 2011). In these instances, dose escalation would allow the drug to reach therapeutic concentrations. However, toxicity or adverse drug-related events may occur as a result of unnecessary ingestion of large amounts of excipient. Additionally, increased costs associated with manufacturing may result due to the need for more active pharmaceutical ingredient (API) in the final product (Kawabata et al, 2011). Both factors may affect patient compliance, which is crucial to the prevention of disease progression.

Drug delivery and drug stability are two problem areas that require more focus to refine the formulation design of PWSAD. Therapeutic drug concentrations must be achieved in order for these agents to be efficacious. Due to low bioavailability, dose escalation provides a less than ideal solution. Aside from the impact on the pharmacologic profile of these PWSAD, dose escalation complicates drug manufacturing because of drug loading. A high drug load is difficult to achieve and may cause decreased flowability or increased granulation during manufacturing (Kawabata et al, 2011). Furthermore, PWSAD may exhibit poor encapsulation as a result of influential factors, such as method of preparation or usage of certain solvents, surfactants, or excipients. (Narvekar et al, 2014).

Versatile formulation methods have been employed to overcome these biopharmaceutical challenges. The physiochemical properties of the PWSAD as well as the physiological environment in which they will be exposed have been taken into consideration in order to formulate better-quality drugs. This study focused on two of these innovative approaches, SDs and solid lipid nanoparticles.

1.1 Solid Dispersions

1.1.1 Definition

The preparation of SDs is one method to enhance the formulation of poorly water soluble drugs, thereby improving oral bioavailability. SDs incorporate one or more active ingredients within an inert carrier in the solid state (Janssens Van den Mooter, 2009). Active ingredients are often poorly water soluble drugs embedded in hydrophilic carriers. Properties of these carriers influence the drug release profile of these agents.

Crystalline carriers were first used to prepare SDs. They were found to display improved thermodynamic stability through the formation of a eutectic mixture in which a crystalline drug is dispersed within a crystalline carrier (Baird Taylor, 2012). However, drug release rates were not ideal. The desire to improve drug release profiles led to the production of second generation SDs, in which amorphous carriers were employed.

Amorphous SDs are categorized as either solutions or suspensions depending on the interaction of the poorly soluble drug and carrier used in the formulation process. A homogenous solution is created when both the drug and carrier are completely miscible and soluble. The strong interaction between both components dissolves the crystalline drug to produce an amorphous product (Baird Taylor, 2012; Vasconcelos et al, 2007). On the contrary, an amorphous solid suspension is produced when the carrier has low solubility or has a high melting point. Small drug particles are dispersed in a polymeric carrier in this type of dispersion (Baird Taylor, 2012). Amorphous SDs are further able to decrease drug

particle size with the aid of a water soluble carrier to provide increased bioavailability.

Advances in solid dispersion preparation have employed the use of surfactants. The surfactant has been shown to prevent crystallization or precipitation. This is ideal in order for the particle size to remain low without agglomerating into large, undissolved crystalline drug (Vo et al, 2013). Addition of the surfactant allows the amorphous solid dispersion to remain stable for an extended duration of time while simultaneously improving bioavailability.

1.1.2 Advantages

Improving drug stability through solubility enhancement is possible through the use of SDs. Unlike other methods, such as chemical or formulation changes, SDs are easier to produce and apply to various drug agents. This method leads to solid, oral dosage forms, which are more convenient and commonly preferred by patients (Qian et al, 2010).

The benefit of SDs is the ability to alter carriers or properties of the particles in order to achieve improved bioavailability. Particle size reduction allows for the poorly soluble drug to be molecularly dispersed throughout a highly soluble carrier. This creates a high surface area for these particles resulting in increased dissolution rate. Improved wettability through the reduction of particle size and inclusion of surfactants in some SDs further aids the enhancement of drug solubility (Craig, 2002; Janssens Van den Mooter, 2009). Similarly, SDs formulated with polymers increase particle porosity. This parameter results in higher dissolution rate and improved drug release profile (Qian et al, 2010; Vo et al, 2013). Amorphous SDs

have the added benefit of being in an irregular formation. The absence of a crystal lattice means no energy is required to promote the dissolution process (Vasconcelos et al, 2007).

1.1.3 Disadvantages

Though SDs paved the way for future improvements in drug development, there are still issues with formulation. A main concern is stability of the products. The amorphous solid dispersion may undergo crystallization upon storage if exposed to environmental changes, such as temperature or humidity (Newman et al, 2012). Increased drug mobility through the absorption of moisture may cause phase separation, crystallization, or conversion from an amorphous to more stable crystalline form (Brough Williams, 2013). The amorphous form is more thermodynamically unstable and therefore have a tendency to convert to a more stable form through recrystallization (Laitinen, et al, 2013). These changes to the amorphous state would ultimately result in decreased solubility and dissolution rate.

Another disadvantage of SDs is manufacturing. SDs can be prepared using melt methods or solvent evaporation. The main concern with melt methods is that exposure to high temperatures may cause degradation of the incorporated drug. Furthermore, the drug and carrier may remain immiscible due to the increased viscosity of the polymeric carrier at these high temperatures (Craig, 2002). In contrast to melt methods, solvent evaporation techniques pose other manufacturing issues. In order to prepare SDs, organic solvents, which are often associated with toxicity, are often used. Moreover, this method is relatively more costly than

alternative methods, more sensitive to changes in the conditions necessary for solvent evaporation, and more difficult to obtain the uniform final product (Vasconcelos et al, 2007).

1.2 Solid Lipid Nanoparticles

1.2.1 Definition

SLN are comprised of solid lipids and surfactants (Müller et al, 2000). Lipids used in the formulation process include triglycerides, fatty acids, steroids, or waxes. The addition of surfactants help stabilize the lipid dispersion to prevent particle aggregation (Mehnert Mäder, 2001).

SLN can be generated using various techniques, such as high pressure homogenization, microemulsions, emulsification-evaporation technique, water/oil/water double emulsion method, or ultrasonication (Wissing et al, 2004). The resultant product can incorporate the desired drug in one of three models. The drug can be molecularly dispersed throughout a solution, present on the exterior of a nanoparticle or encapsulated within the core of the nanoparticle (Müller et al, 2000).

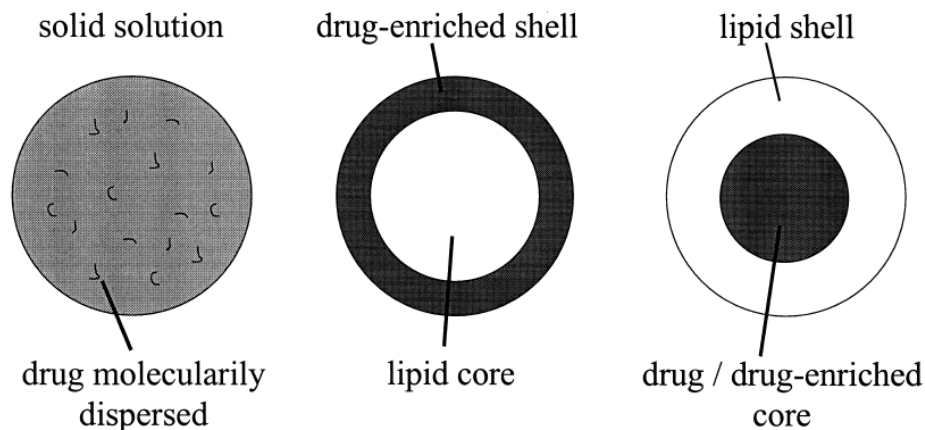


Figure 1. Nanoparticle drug incorporation models (Müller et al, 2000)

SLN are an alternative colloidal drug delivery system composed of submicron colloidal size between 50 to 1000 nanometers (Fricker et al, 2010). The reduction in particle size subsequently leads to an increase in surface area that ultimately enhances both dissolution rate and provides more suitable conditions for controlling the pharmacokinetic profile of the newly formulated dosage form (Merisko-Liversidge, 2008).

1.2.2 Advantages

The benefits of formulating poorly water soluble agents as SLN include the ability to provide controlled drug release and enhance drug targeting to limit adverse effects, increase drug stability, incorporation of both lipophilic and hydrophilic agents, elimination of a toxic carrier, avoidance of organic solvents, and feasibility of large scale production (Mehnert Mäder, 2001).

Previous production of polymer based nanoparticles provided the benefit of numerous chemical modifications, however, concurrent use led to issues with scale up and cytotoxicity due to the presence of organic solvents. To avoid these problems, SLN utilize physiological lipids, which eliminate toxicity concerns (Fricker et al, 2010).

Lyophilization and spray drying are two methods to aid in improved stability of prepared nanoparticles. Chemical and physical factors affect stability, but the goal of these procedures is to prevent degradation reactions, such as hydrolysis, and preserve the particle size of these SLN (Mehnert Mäder, 2001). Lyophilization produces a solid form of SLN that can be prepared as pellets, tablets, or capsules. This technique increases the stability of SLN, thereby avoiding crystal growth by

Ostwald ripening, and resists changes in temperature that may occur during shipping and storage (Mehnert Mäder, 2001). Spray drying offers a more cost effective alternative for converting SLN to a dry product.

Large-scale production of SLN is made feasible through use of high-pressure homogenization (HPH). Unlike other instances in which scaling up leads to problems, the use of large machines results in better quality products with homogenous particle size distribution (Muchow et al, 2008). Large-scale machinery provide the added benefit of ease of transfer, less fluctuation of pressure, and more effective temperature control (Muchow et al, 2008).

1.2.3 Disadvantages

Though the nanometer-sized particles provide beneficial pharmacokinetic and pharmacodynamic properties, the increase in surface area promotes a thermodynamically unstable state. Thus the nanoparticles may convert to a more stable form by spontaneous agglomeration (Merisko-Liversidge, 2008). Similarly, the lipids used to formulate SLN are crystalline in nature. Solid-liquid transitions that are time and temperature-dependent may result in polymorphic changes. These modifications can be controlled by altering the components of SLN, such as emulsifiers or the incorporated drug. Failure to consider the potential for conversion to a more stable state may result in negative consequences related to decreased stability and increased crystallinity (Bunjes, 2010).

Another disadvantage of SLN is inadequate drug loading capacity (Wissing et al, 2004). Loading capacity is defined as the percentage of drug incorporated into the SLN in relation to the total weight of the lipid phase (Muchow et al, 2008).

Successful inclusion of a drug into a carrier system can be determined by its loading capacity. Solubility and miscibility of both the melted drug and lipid, chemical and physical structure of the solid lipid complex, as well as, the polymorphic state of the lipid are just some factors that affect loading capacity (Müller et al, 2000). The crystalline structure of lipids leads to limited space for drug incorporation as the drug may be situated between the crystalline lattice, fatty acid chains, or amorphous clusters in crystal imperfections (Muchow et al, 2008).

1.3 Flutamide

The purpose of this study was to enhance the solubility of a poorly water soluble anticancer agent, FLT, using amorphous SDs and solid lipid nanotechnology. This study investigated that improved formulation of FLT with these methods will augment drug bioavailability to ultimately produce a more stable, therapeutically efficacious drug.

1.3.1. Indications

FLT (Eulexin™) is an antiandrogen agent indicated for the treatment of both local and metastatic prostate cancer. Patients with stage B₂ to C prostate cancer should start treatment with FLT and goserelin, a luteinizing hormone-releasing hormone (LHRH) agonist, eight weeks prior to starting radiation and continuing throughout radiation therapy. The treatment of stage D₂ prostate cancer should begin with both FLT and an LHRH agonist. Combination therapy should continue for metastatic prostate cancer until disease progression.

FLT has off-label uses for acne vulgaris and hirsutism in women. However, little evidence is available to support these off-label indications. The risk for hepatotoxicity limits its use.

1.3.2 Physiochemical properties

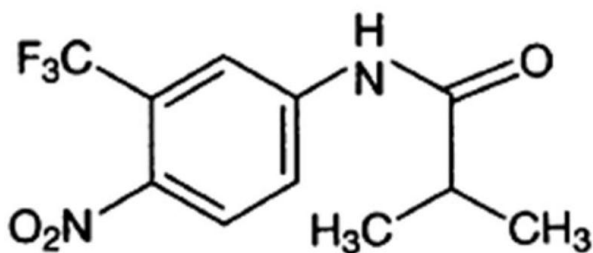


Figure 2. Structural formula of flutamide

FLT or 2-methyl-*N*-[4-nitro-3-(trifluoro-methyl)phenyl] propanamide is an acetanilide, nonsteroidal antiandrogen. Its chemical structure is $C_{11}H_{11}F_3N_2O_3$ with a pKa of 13.12. FLT is available as a pale, yellow crystalline powder and has a molecular weight of 276.2 g/mol. FLT is freely soluble in methanol and ethanol, but insoluble in water or other solutions with a pH of 1 to 6. The partition coefficient (log P) of FLT is 3.7. The melting point of FLT is 114°C. Mass solubility is 28×10^{-3} g/L and the contact angle for wettability of FLT is 57°.

FLT is commercially available as a 125 mg oral capsule.

1.3.3 Pharmacokinetics

2-hydroxyflutamide is the active drug of FLT. Absorption in the gastrointestinal tract is rapid and complete following oral administration with time to peak occurring at about two hours. The bioavailability of FLT is not affected by the administration of food. The parent drug is 94 to 96% protein bound, while 2-

hydroxyflutamide is 92 to 94% protein bound. The drug is distributed and appears to concentrate in the prostate. Following a single oral dose of 250 mg, steady state plasma concentrations of 24 to 78 ng/mL and 1556 to 2284 ng/mL are detected for the parent and active drug, respectively. FLT is metabolized by the liver into six or more metabolites. The active drug is metabolized to 2-hydroxyflutamide primarily by CYP1A2. Excretion of these metabolites is primarily via the urine with approximately 4% elimination via feces over a 72 hour period. The half-life of 2-hydroxyflutamide is about six hours. The half-life is slightly prolonged in patients with renal dysfunction and is approximately 9.6 hours in the elderly population.

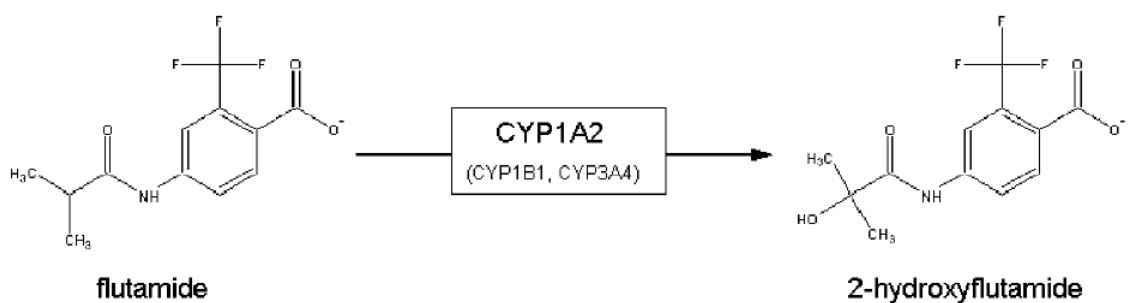


Figure 3. Metabolism of FLT to its active moiety, 2-hydroxyflutamide (Sissung et al, 2006)

1.3.4 Pharmacology

FLT is a nonsteroidal antiandrogen whose mechanism of action is mediated by the inhibition of androgen uptake and/or androgen binding of testosterone and dihydrotestosterone to the targeted prostatic tissue. These tumors are androgen-sensitive and respond to FLT therapy due to its counter effect of androgens.

The usual dosage for FLT for the treatment of prostatic carcinoma is 250 mg every eight hours. The maximum daily dosage of FLT in adults is 750 mg.

The safety and efficacy of FLT in pediatric and adolescent populations has not been established. No dosage adjustments are required for elderly populations or patients with renal function impairment. While no adjustments are necessary for mild to moderate hepatic impairment, the use of FLT in patients with severe hepatic dysfunction is contraindicated.

FLT carries a black box warning for hepatic injury due to postmarketing reports of hospitalization due to liver failure. A majority of the cases occurred within the first three months of initiation of therapy and is reversible in some incidences upon discontinuation of therapy. Patients with reported hepatic injury present with elevated serum transaminase levels, hepatic encephalopathy, jaundice, and in rare cases death. Baseline liver function tests should be obtained prior to beginning treatment with FLT and routinely thereafter.

FLT is classified as pregnancy category D and is not indicated for use in women.

Commonly experienced adverse reactions include hot flashes, galactorrhea, decreased libido, diarrhea and impotence. A mild or transient increase in lactate dehydrogenase or serum aminotransferases may also occur.

FLT is a substrate of both CYP1A2 and CYP3A4 and is a weak inhibitor CYP1A2. FLT therapy should be monitored if used with concurrent agents that undergo extensive hepatic metabolism due to the potential for drug-drug interactions.

1.4 Polymers

Polymers are commonly used excipients in the pharmaceutical industry to develop drugs that are difficult to formulate due to complications related to permeability, stability and solubility (Mei et al., 2013). Selection of the appropriate polymer for drug conjugation relies on the physicochemical properties of both components to successfully develop a safe and efficacious dosage form. The four polymers utilized in this study included polyvinylpyrrolidone K90 (PVP), hydroxypropyl methylcellulose (HPMC), eudragit (EPO), and polyethylene glycol 8000 (PEG). The physicochemical properties of these polymers are discussed below.

1.4.1 Polyvinylpyrrolidone K90

Polyvinylpyrrolidone is mainly used in the formulation of solid dosage forms, however, it can also serve as a disintegrant, dissolution enhancer, suspending agent, or tablet binder. When mixed with polyvinylpyrrolidone, the solubility of various poorly water soluble drugs is increased.

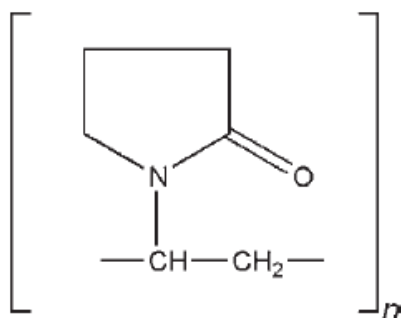


Figure 4. Structural formula of polyvinylpyrrolidone

1.4.1.1 Physicochemical state and appearance

White to cream colored, fine, hygroscopic powder; slight odor to odorless

1.4.1.2 Glass transition temperature

176.9°C

1.4.1.3 Molecular weight

1000000 g/mol

1.4.1.4 Solubility

Soluble in acids, chloroform, ethanol (95%), ketones, methanol, and water; insoluble in ether, hydrocarbons and mineral oil

1.4.1.5 Density

1.18 g/cm³

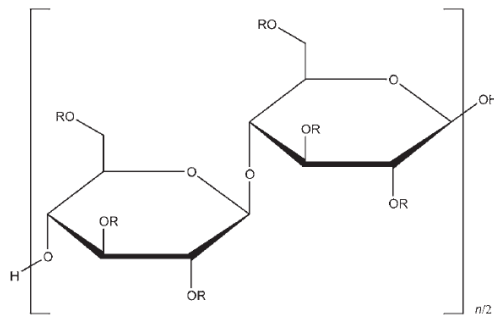
1.4.1.6 Viscosity

53.0 mPas in ethanol (95%); 90.0 mPas in propan-2-ol

1.4.2 Hydroxypropyl Methylcellulose

Hydroxypropyl methylcellulose is used in a variety of pharmaceutical formulations, including oral, ophthalmic, nasal, and topical products.

In solid oral products, hydroxypropyl methylcellulose is used as a tablet binder, coating agent, or as a matrix for the development of an extended release product. In contrast, hydroxypropyl methylcellulose is utilized as a suspending or thickening agent for liquid oral dosage forms.



where R is H, CH₃, or CH₃CH(OH)CH₂

Figure 5. Structural formula of hydroxypropyl methylcellulose

1.4.2.1 Physiochemical state and appearance

White or cream-colored, fibrous or granular powder; odorless; tasteless

1.4.2.2 Glass transition temperature

149°C

1.4.2.3 Molecular weight

10000-1500000 g/mol

1.4.2.4 Solubility

Soluble in cold water and mixtures of ethanol and dichloromethane, methanol and dichloromethane, and water and alcohol; insoluble in hot water, chloroform, ethanol (95%), ether

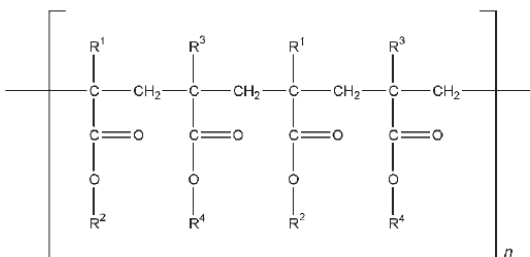
1.4.2.5 Density

1.326 g/cm³

1.4.3 Eudragit

Eudragit is a polymethacrylate, which is primarily used as film-forming agent. Eudragit is also used as a tablet binder or tablet diluent. Eudragit E is used as an insulating film former and is soluble in gastric fluid with a pH less than 5.

Polymethacrylates are utilized in larger quantities to control the release of a drug from a tablet matrix. These polymers may also be used to form matrix layers of transdermal delivery systems or gel formulations for rectally administered products.



For *Eudragit E*:
 $R^1, R^3 = CH_3$
 $R^2 = CH_2CH_2N(CH_3)_2$
 $R^4 = CH_3, C_4H_9$

Figure 6. Structural formula of eudragit

1.4.3.1 Physiochemical state and appearance

White, free-flowing powder

1.4.3.2 Glass transition temperature

49.2°C

1.4.3.3 Molecular weight

100000-250000 g/mol

1.4.3.4 Solubility

Soluble in ethanol (95%), methanol, and propan-2-ol

1.4.3.5 Density

0.815 g/cm³

1.4.3.6 Viscosity

3-6 mPas

1.4.4 Polyethylene Glycol 8000

Polyethylene glycols (PEGs) are used in the formulation of parenteral, topical, ophthalmic, oral and rectal products. They have also been used in controlled release systems as biodegradable polymeric matrices. PEGs are categorized as an ointment base, plasticizer, solvent, suppository base, and tablet or capsule lubricant.

When formulated as SDs or nanoparticles, PEGs can be used to improve the solubility and increase dissolution rate of poorly water soluble compounds, thereby improving oral bioavailability of these agents.

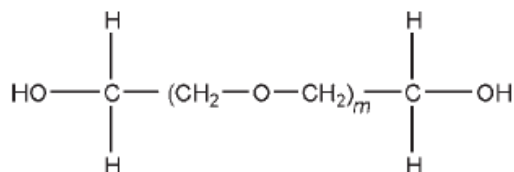


Figure 7. Structural formula of polyethylene glycol

1.4.4.1 Physiochemical state and appearance

White to off-white colored, waxy flakes; slight, sweet odor

1.4.4.2 Melting temperature

63°C

1.4.4.3 Molecular weight

7000-9000 g/mol

1.4.4.4 Solubility

Soluble in acetone, dichloromethane, ethanol (95%), methanol, water; slightly soluble in aliphatic hydrocarbons and ether; insoluble in fats, fixed oils, and mineral oil

1.4.4.5 Density

1.08 g/cm³

1.4.4.6 Viscosity

260–510 mPas

1.5 References

Baird, J. A., & Taylor, L. S. (2012). Evaluation of amorphous solid dispersion properties using thermal analysis techniques. *Advanced Drug Delivery Reviews*, 64(5), 396-421.

Brough, C., & Williams III, R. O. (2013). Amorphous solid dispersions and nano-crystal technologies for poorly water-soluble drug delivery. *International Journal of Pharmaceutics*, 453(1), 157-166.

Craig, D. Q. M. (2002). The mechanisms of drug release from solid dispersions in water-soluble polymers. *International Journal of Pharmaceutics*, 231(2), 131-144.

Flutamide. Clinical Pharmacology [database online]. Tampa, FL: Elsevier; 2014.

Flutamide. Facts & Comparisons eAnswers [database online]. Indianapolis, IN: Clinical Drug Information, LLC; 2014.

Flutamide. Lexicomp [database online]. Hudson, OH: Lexicomp; 2015.

Flutamide prescribing information. Parsippany, NJ: Actavis Pharma, Inc; 2014.

Fricker, G., Kromp, T., Wendel, A., Blume, A., Zirkel, J., Rebmann, H., Müller-Goymann, C. (2010). Phospholipids and lipid-based formulations in oral drug delivery. *Pharmaceutical Research*, 27(8), 1469-1486.

Janssens, S., & Van den Mooter, G. (2009). Review: Physical chemistry of solid dispersions. *Journal of Pharmacy and Pharmacology*, 61(12), 1571-1586.

- Kawabata, Y., Wada, K., Nakatani, M., Yamada, S., & Onoue, S. (2011). Formulation design for poorly water-soluble drugs based on biopharmaceutics classification system: Basic approaches and practical applications. *International Journal of Pharmaceutics*, 420(1), 1-10.
- Laitinen, R., Löbmann, K., Strachan, C. J., Grohgan, H., & Rades, T. (2013). Emerging trends in the stabilization of amorphous drugs. *International Journal of Pharmaceutics*, 453(1), 65-79.
- Mehnert, W., & Mäder, K. (2001). Solid lipid nanoparticles: Production, characterization and applications. *Advanced Drug Delivery Reviews*, 47(2-3), 165-196.
- Mei, L., Zhang, Z., Zhao, L., Huang, L., Yang, X., Tang, J., & Feng, S. (2013). Pharmaceutical nanotechnology for oral delivery of anticancer drugs. *Advanced Drug Delivery Reviews*, 65(6), 880-890.
- Merisko-Liversidge, E. M., & Liversidge, G. G. (2008). Drug nanoparticles: Formulating poorly water-soluble compounds. *Toxicologic Pathology*, 36(1), 43-48.
- Muchow, M., Maincent, P., & Muller, R. H. (2008). Lipid nanoparticles with a solid matrix (SLN, NLC, LDC) for oral drug delivery. *Drug Development and Industrial Pharmacy*, 34(12), 1394-1405.
- Müller, R. H., Mäder, K., & Gohla, S. (2000). Solid lipid nanoparticles (SLN) for controlled drug delivery – a review of the state of the art. *European Journal of Pharmaceutics and Biopharmaceutics*, 50(1), 161-177.
- Narvekar, M., Xue, H., Eoh, J., & Wong, H. (2014). Nanocarrier for poorly water-soluble anticancer Drugs – Barriers of translation and solutions. *AAPS PharmSciTech*, 15(4), 822-833.
- Newman, A., Knipp, G., & Zografi, G. (2012). Assessing the performance of amorphous solid dispersions. *Journal of Pharmaceutical Sciences*, 101(4), 1355-1377.
- O'Driscoll, C. M., & Griffin, B. T. (2008). Biopharmaceutical challenges associated with drugs with low aqueous solubility—The potential impact of lipid-based formulations. *Advanced Drug Delivery Reviews*, 60(6), 617-624.
- Qian, F., Huang, J., & Hussain, M. A. (2010). Drug-polymer solubility and miscibility: Stability consideration and practical challenges in amorphous solid dispersion development. *Journal of Pharmaceutical Sciences*, 99(7), 2941-2947.
- Rowe, R., Sheskey, P., Quinn, M. American Pharmacists Association. (2009). *Handbook of pharmaceutical excipients*. London: Pharmaceutical Press.

Vasconcelos, T., Sarmiento, B., & Costa, P. (2007). Solid dispersions as strategy to improve oral bioavailability of poor water soluble drugs. *Drug Discovery Today*, 12(23-24), 1068-1075.

Vo, C. L., Park, C., & Lee, B. (2013). Current trends and future perspectives of solid dispersions containing poorly water-soluble drugs. *European Journal of Pharmaceutics and Biopharmaceutics*, 85(3, Part B), 799-813.

Wissing, S. A., Kayser, O., & Müller, R. H. (2004). Solid lipid nanoparticles for parenteral drug delivery. *Advanced Drug Delivery Reviews*, 56(9), 1257-1272.

CHAPTER 2

Drug-polymer and drug-polymer miscibility for the development of amorphous solid dispersions and solid lipid nanoparticles

2.1 Amorphous solid dispersions

SDs are a type of drug delivery system in which an active pharmaceutical ingredient (API) is dispersed within an inert carrier or matrix (Kawakami, 2012). SDs can be prepared using different techniques to obtain various combinations of an amorphous, crystalline, or molecularly dispersed API and carrier. This study focuses on amorphous SD prepared by solvent evaporation method.

Amorphous SD can be classified as a solution or suspension, where the drug and carrier are miscible forming a homogenous mixture or where the drug is present as small particles dispersed in an amorphous carrier, respectively (Vasconcelos et al, 2007). The amorphous state of the drug delivery system accounts for increased solubilization and low thermodynamic stability (Vo et al, 2013). The absence of a crystalline lattice means no energy is required for dissolution to occur leading to a faster release rate.

SDs are one approach to overcome poor water solubility. Advantages of using SD include a reduction in particle size, enhancement of drug wettability, porosity, and dissolution rate, as well as, conversion of a crystalline API to an amorphous state (Janssens Van den Mooter, 2009; Vo et al, 2013). Moreover, many carriers used to produce SD are commonly used and well-studied pharmaceutical excipients diminishing the need for further toxicity studies (Leuner Dressman, 2000). Overall, formulation with SD improves drug bioavailability.

2.1.1 Role of polymers in the development of amorphous solid dispersions

Polymers act as the matrix for molecular dispersion of an API, system stabilizer, and solubilizer. Drug and polymer interactions formed prevent

nucleation, thereby leading to enhanced absorption and improved stability (Ivanisevic, 2010; Vo et al, 2013). However, given that the amorphous state is higher in free energy, physical instability of the system and concerns with drug crystallization do arise. Thus, the addition of polymers can act as stabilizers by reducing molecular mobility. This is made possible by increasing the glass transition temperature of the system (Prasad et al, 2014; Rumondor et al, 2009). Polymer inclusion is also known to decrease the thermodynamic driving force, increase the energy barrier and interrupt drug-drug interactions, thereby limiting the potential for drug crystallization (Rumondor et al, 2009).

It is evident that selection of the most suitable polymeric carrier is dependent upon its physiochemical properties. Synthetic polymers, such as PVP and PEG, along with a natural polymer, HPMC are commonly used for the preparation of SD. These polymers are soluble in organic solvents and therefore are ideal candidates for use in the solvent evaporation method. PEG is crystalline in nature and has a low melting point in comparison to PVP, which has a high glass transition temperature and is amorphous in nature. Both these polymers are available in an array of molecular weights. High molecular weight polymers are often associated with decreased solubility and high viscosity (Vo et al, 2013). While increased viscosity may enhance stability due to decreased tendency for recrystallization, it may also prevent the drug from becoming molecularly dispersed with the carrier leading to a slowed dissolution rate.

2.1.2 Drug-polymer miscibility

Miscibility between SD drug and polymer is important because of its effect on physical stability of the system. When both components are miscible, drug recrystallization is less likely to occur (Marsac et al, 2009). Studies conducted by Ivanisevic evaluated the physical stability of twelve amorphous SDs. It was conclusive that miscible amorphous SD involving various ratios of PVP and API, including ketoconazole, felodipine, nifedipine, and indomethacin, showed no crystallization and improved shelf-life (Ivanisevic, 2010).

2.2 Solid lipid nanoparticles

SLN are a type of a carrier system that employs solid lipids as a matrix for drug delivery (Müller et al, 2000). The drug is molecularly dispersed within the lipid matrix and the system is stabilized with an emulsifier (Martins et al, 2007). Nanoparticles distributed within the matrix have a mean particle size in the range of 50 to 1000 nanometers (Bunjtes, 2010; Fricker et al, 2010). This reduction in particle size along with drug incorporation throughout the lipid matrix influence the improved pharmaceutical features of SLN.

SLN combine the added benefits of their counterpart carrier systems while minimizing potential formulation problems. The advantages of SLN include improved drug-carrier stability, protection of incorporated drug from degradation along with enhanced tolerability, controlled drug delivery, and site-specific targeting (Wissing et al, 2004). The production of SLN allows for the incorporation of both lipophilic and hydrophilic drugs, which expands the market for this drug delivery system. Formulation using physiologic lipids eliminates the need for

organic solvents, thus mitigating the potential for carrier toxicity. The ease of large-scale manufacturing of SLN complements the progression of this drug delivery system (Mehnert Mäder, 2001).

2.2.1 Role of lipids in the development of solid lipid nanoparticles

Poorly water soluble anticancer drugs have limited bioavailability. In contrast to polymeric drug carriers, lipids are more physiological and biocompatible carriers that may aid in the resolution of this issue. Moreover, the reduction in size of SLN can be attributed to enhanced particle adhesion to the gut wall, a location more suitable for the drug release and absorption. Apart from promoting absorption, lipids are degraded by gut enzymes leading to the production of micelles. Solubility enhancement occurs during this process as the drug dissolved within the lipid matrix is incorporated into micelles. Upon lipid degradation, the drug is absorbed (Bunjjes, 2010). This process is depicted in Figure 8.

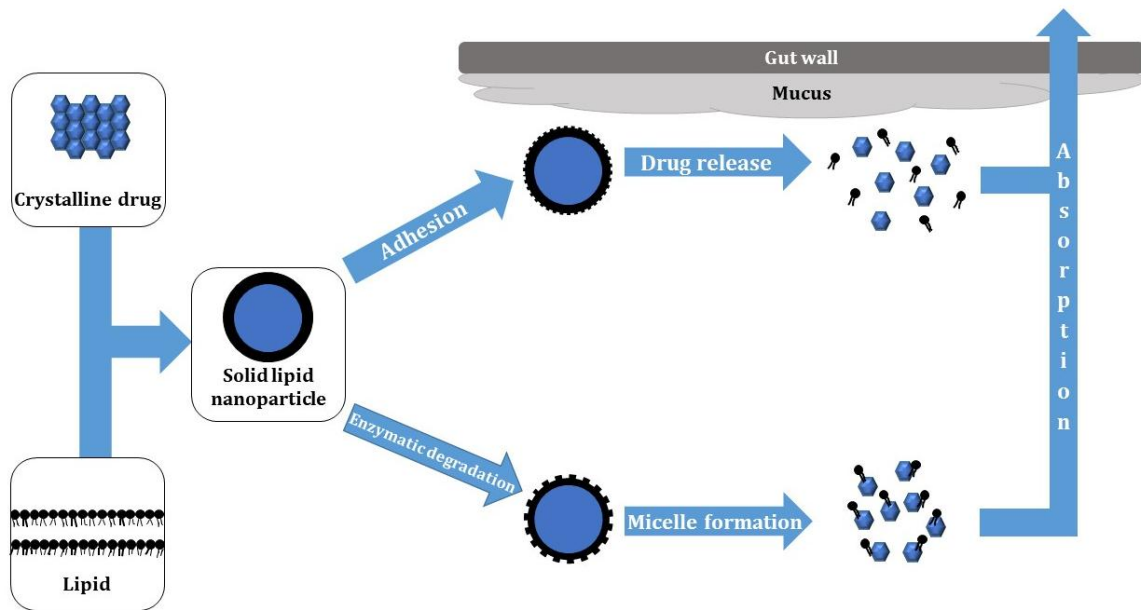


Figure 8. The effects of lipids in prepared SLN on drug absorption

The solid lipids used to prepare SLN are crystalline in nature and serve as the matrix in which an immobilized drug is molecularly dispersed. Stability of SLN are influenced by the bulk properties and length of their composite lipids. Short lipid chains with less branching degrade more quickly in comparison to long lipid chains with more branching (Blasi et al, 2007). The selection of lipids for SLN is thus significant to enhance the solubility and stability of the carrier system.

2.2.2 Role of polymers in the development of solid lipid nanoparticles

The use of polymers in the formulation of nanoparticles has fallen out of favor due to toxicity concerns, high cost for biodegradable polymers and difficulty with large-scale production (Joshi Müller, 2009). Despite these drawbacks, polymers have been used as surfactants to stabilize SLN. Poloxamer and tween 80 are two examples of surfactants approved for use that are generally well tolerated eliminating toxicity concerns (Joshi Müller, 2009).

Surface coating with polymers, such as polyethylene glycol (PEG), is used to increase biodistribution by modifying hydrophobic particles located on the surface of SLN and stabilizing them. As an amphiphilic copolymer, PEG is capable of orienting its hydrophobic residues near the lipophilic SLN core. The strength of the bonds formed between SLN and polymer determine SLN stability, prevention of agglomeration, and dispersability. Surface modification also provides increased transport and site-specific drug targeting (Uner Yener, 2007).

2.2.3 Drug-polymer miscibility

Miscibility of various drug-polymer complexes have been reported through the analysis of component interactions. To improve the physical stability of the

drug, it must be mixed with a polymer to modify the environment surrounding the drug to provide more favorable conditions. Similarly, the polymer is capable of altering the physical properties of the drug, which may lower the thermodynamic tendency for crystallization (Marsac et al, 2006).

Polyvinylpyrrolidone (PVP) has been shown to form hydrogen bonds with nifedipine, a drug containing a nitrogen-hydrogen functional group. These interactions were shown to decrease molecular mobility stabilizing the drug carrier system. However, despite these changes, it was noted that preparation method, temperature, and drug-polymer composition influence miscibility (Yuan et al, 2014).

2.2.4 Drug-lipid miscibility

Figure 9 depicts the pharmaceutical and pharmacologic implications of evaluating drug-lipid miscibility in SLNs. Lipid-based formulations can be used to increase drug absorption by increasing solubilization, enhancing permeability, reducing drug metabolism by inhibiting hepatic enzymes, and improving transport via inhibition of efflux transporters and escalation of chylomicron production (O'Driscoll Griffin, 2008). The miscibility of a drug and excipient is dependent upon the interactions formed between the drug (solute) and excipient (solvent) (Shah Agrawal, 2013).

Mixed glycerides, such as glyceryl monooleate (GMO), serve as a popular solvent for poorly water soluble drugs. GMO is a waxy, long-chain glyceride useful in formulating liquid dosage forms. Sorbitan fatty acids (Spans) have similar physical properties to GMO. These polar oils, also known as co-surfactants, promote miscibility due to the presence of hydroxyl groups (Pouton Porter, 2008). Co-

surfactants decrease interfacial tension between two immiscible components to improve thermodynamic stability and thus miscibility (Heurtault et al, 2003).

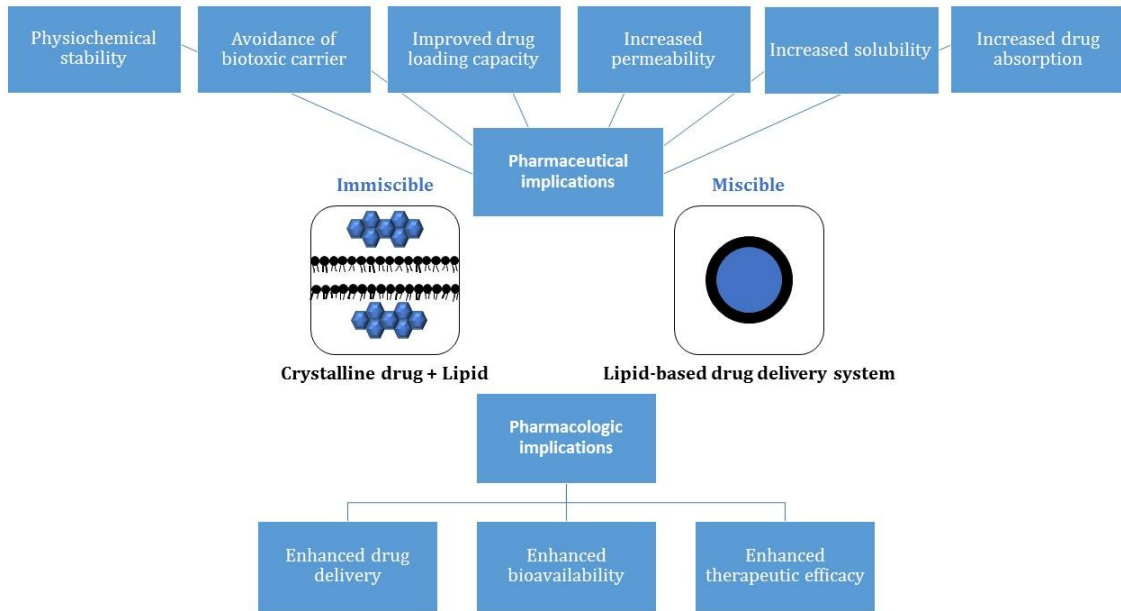


Figure 9. Pharmaceutical and pharmacologic implications of evaluating drug-lipid miscibility in solid lipid nanoparticles

2.3 Hypothesis and specific aims

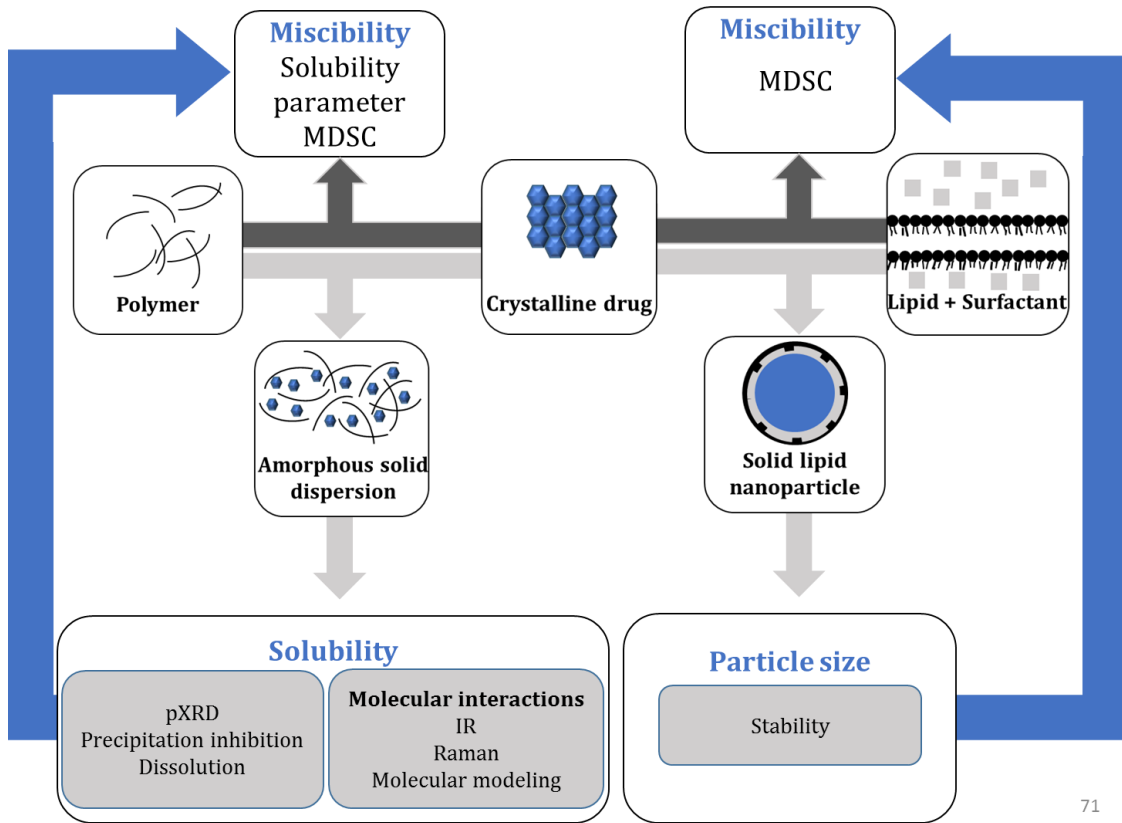


Figure 10. Graphical abstract of drug-polymer and drug-lipid miscibility for the development of amorphous SDs and SLNs

2.3.1 Hypothesis

Drug-polymer miscibility improves the solubility of amorphous SDs and drug-lipid miscibility reduces the particle size of SLNs.

2.3.2 Specific aims

1. To prepare and characterize FLT amorphous SDs
2. To prepare and characterize FLT SLNs
3. Correlate results of miscibility studies to solubility of amorphous SDs and particle size SLNs

2.3.3 Materials and methods

2.3.3.1 Specific aim 1

To prepare and characterize FLT amorphous SDs

2.3.3.1.1 Preparation of physical mixtures

Mixtures of FLT with polymers (PVP, HPMC, EPO, PEG) were prepared at 90:10, 70:30, and 50:50 (drug: polymer) weight ratio. Homogenous blending of accurately weighed amounts of drug and polymer was accomplished by geometric dilution.

2.3.3.1.2 Determination of miscibility

MDSC settings for drug-polymer PMs were as follows: The initial cycle for all samples were heated at 5°C/min from 30-200°C. Inert atmosphere was maintained by nitrogen at a flow rate of 40 mL/min. A second and third cycle was run under MDSC solely for 70:30 (drug:polymer) molar ratio. Modulated temperature was set to $\pm 20^\circ\text{C}/\text{min}$. The sample was initially heated to 150°C followed by a cooling cycle to 40°C and finally reheated to determine if recrystallization occurred.

2.3.3.1.3 Preparation of amorphous solid dispersions

FLT and polymer SDs were prepared at 70:30 (drug:polymer) molar ratio. Weighed amounts of drug and polymer were placed in a 50 mL round bottomed flask to which 5 mL of methanol was added to the mixtures containing PVP and PEG. To ensure complete dissolution of the mixtures containing HPMC and EPO, 2.5 mL of dichloromethane and 2.5 mL of methane were used as co-solvents. Solvent evaporation technique under reduced pressure created by a RotaVapor R-215

(Buchi, Flawil, Switzerland) was used to prepare SDs. Rota evaporation was carried out at 67°C at 0-50 mbar with a rotation speed of 150 rpm for 15 minutes or until a dry product remained. SDs were vacuum dried at room temperature overnight.

2.3.3.1.4 Characterization of amorphous solid dispersions

Powder X-ray diffraction (pXRD) was used to study drug crystallinity and identify the precipitated polymorphic form. The pXRD patterns were collected in the angular range of $1 < 2\theta < 40^\circ$ in step scan mode and analyzed by EVA software.

Attenuated total reflectance (ATR) mode was used to obtain IR spectra using Bruker Vertex series 80 V IR spectrometer (Billerica, MA). Fifty scans were collected for each sample over a wave number region of 400-4000 cm^{-1} . IR spectroscopy was used for characterization of the precipitate and to explore the drug polymer interactions.

Raman spectra were obtained using Bruker Vertex series 80 V Raman spectrometer and data processing was performed using OPUS software (Billerica, MA). Data acquisition was done using an exposure time of 10 seconds for 10 accumulations and a laser power setting of 400 mW at 785 nm. Raman spectroscopy was used for characterization of precipitate and to explore the drug polymer interactions in various mixtures and dispersions along with IR spectroscopy.

Molecular modeling studies using Jaguar were carried out to understand drug polymer interactions.

2.3.3.2 Specific Aim 2

To prepare and characterize FLT SLNs

2.3.3.2.1 Preparation of physical mixtures

Drug-lipid physical mixtures were prepared in 5:3 w/w ratio (lipid: surfactant) and 2:1 w/w (FLT: lipids/surfactants) by co-melting them at 85-90°C. The mixture was homogenized using a cyclomixer. Solid lipid used included glyceryl monooleate, Precirol, glyceryl monostearate, and Compritol. Gelucire 44/14 and 50/13 were used as the surfactant.

2.3.3.2.2 Determination of miscibility

MDSC settings for drug-lipid PMs were as follows: The nitrogen flow rate was set to 40 mL/min with a ramp rate of 2°C/min. Three cycles were performed. During cycle 1, the temperature was increased from room temperature to 90°C. The sample was then cooled from 90°C down to -40°C during cycle 2. Finally, a temperature increase back to 90°C occurred during cycle 3.

2.3.3.2.3 Preparation of solid lipid nanoparticles

Nanoparticles were prepared using 500 mg of lipid (GMO, PRE, GMS, COM) and 200 mg of surfactant (GEL 50/13, 44/14). Accurately weighed lipid and surfactant were placed in a screw-capped vial and laid on a hot plate at 90°C until melted. To ensure complete melting of COM, the temperature was increased to 125°C. Once melted, 20 mg of FLT was added to the lipid and surfactant. A total of 10 mL of distilled water heated to the same temperature as the obtained mixture was added dropwise to create a primary emulsion. A stir bar was placed in the screw-capped vial to assist with mixing. Ultrasonication of the primary emulsion was

performed using the Sonicator 3000 (Misonix, Farmingdale, New York) at 18W with an output setting of 4.0 for 5 minutes to create a secondary emulsion. This method was performed in triplicate.

2.3.3.2.4 Characterization of solid lipid nanoparticles

Particle size of the prepared secondary emulsions were obtained to characterize the FLT nanoparticles. Data was acquired from a ZetaPlus, Zeta Potential Analyzer (Brookhaven Instruments Corp., Holtsville, New York). To attain these values, 10 μ L of the secondary emulsion was placed in a test tube and diluted with 10 mL of water. The test tube was placed on a Genie 2 vortex (Fisher Scientific, Hampton, New Hampshire) to ensure homogenous mixing and then sonicated for 5 minutes using a Sonicator FS60 (Fisher Scientific, Hampton, New Hampshire).

Raman spectra were obtained using Bruker Vertex series 80 V Raman spectrometer and data processing was performed using OPUS software (Billerica, MA). Data acquisition was done using an exposure time of 10 seconds for 10 accumulations and a laser power setting of 400 mW at 785 nm.

2.3.3.2.5 Determination of miscibility

MDSC thermograms for amorphous SDs and SLNs were obtained in a similar manner to the drug-polymer and drug-lipid PMs.

2.3.3.3 Specific Aim 3

Correlate results of miscibility studies to solubility of amorphous SDs and particle size SLNs

Results from the drug-polymer miscibility studies were examined for enhanced solubility of FLT. Comparative analysis was performed between FLT PMs versus FLT amorphous SDs. A similar analysis was performed for the FLT SLNs. Particle size was the major parameter assessed to determine overall performance of this carrier system.

2.4 Conclusion

Preparation of amorphous SDs and SLNs successfully enhanced the miscibility of the poorly water soluble anticancer agent, FLT. These studies demonstrated good miscibility between GMO and GMS prepared SLNs with the addition of GEL as the surfactant. PVP and PEG were found to provide stabilization and efficient precipitation inhibition of the FLT SDs.

2.5 Future directions

Amorphous SDs and SLNs displayed improved stability and miscibility, two important factors necessary for improved physiochemical properties and drug delivery of FLT. The success of these drug delivery systems can be utilized to produce a superior oral dosage form of FLT. The benefits of these formulations would include increased bioavailability, targeted drug accumulation, limited side effect profile and enhanced patient compliance.

2.6 References

Blasi, P., Giovagnoli, S., Schoubben, A., Ricci, M., & Rossi, C. (2007). Solid lipid nanoparticles for targeted brain drug delivery. *Advanced Drug Delivery Reviews*, 59(6), 454-477.

Bunjes, H. (2010). Lipid nanoparticles for the delivery of poorly water-soluble drugs. *Journal of Pharmacy and Pharmacology*, 62(11), 1637-1645.

- Fricker, G., Kromp, T., Wendel, A., Blume, A., Zirkel, J., Rebmann, H., Müller-Goymann, C. (2010). Phospholipids and lipid-based formulations in oral drug delivery. *Pharmaceutical Research*, 27(8), 1469-1486.
- Heurtault, B., Saulnier, P., Pech, B., Proust, J., & Benoit, J. (2003). Physico-chemical stability of colloidal lipid particles. *Biomaterials*, 24(23), 4283-4300.
- Ivanisevic, I. (2010). Physical stability studies of miscible amorphous solid dispersions. *Journal of Pharmaceutical Sciences*, 99(9), 4005-4012.
- Janssens, S., & Van den Mooter, G. (2009). Review: Physical chemistry of solid dispersions. *Journal of Pharmacy and Pharmacology*, 61(12), 1571-1586.
- Joshi, M. D., & Müller, R. H. (2009). Lipid nanoparticles for parenteral delivery of actives. *European Journal of Pharmaceutics and Biopharmaceutics*, 71(2), 161-172.
- Kawakami, K. (2012). Modification of physicochemical characteristics of active pharmaceutical ingredients and application of supersaturatable dosage forms for improving bioavailability of poorly absorbed drugs. *Advanced Drug Delivery Reviews*, 64(6), 480-495.
- Leuner, C., & Dressman, J. (2000). Improving drug solubility for oral delivery using solid dispersions. *European Journal of Pharmaceutics and Biopharmaceutics*, 50(1),
- Marsac, P., Li, T., & Taylor, L. (2009). Estimation of Drug-Polymer miscibility and solubility in amorphous solid dispersions using experimentally determined interaction parameters. *Pharmaceutical Research*, 26(1), 139-151.
- Marsac, P., Shamblin, S., & Taylor, L. (2006). Theoretical and practical approaches for prediction of Drug-Polymer miscibility and solubility. *Pharmaceutical Research*, 23(10), 2417-2426.
- Martins, S., Sarmiento, B., Ferreira, D. C., & Souto, E. B. (2007). Lipid-based colloidal carriers for peptide and protein delivery--liposomes versus lipid nanoparticles. *International Journal of Nanomedicine*, 2(4), 595-607.
- Mehnert, W., & Mäder, K. (2001). Solid lipid nanoparticles: Production, characterization and applications. *Advanced Drug Delivery Reviews*, 47(2-3), 165-196.
- Muchow, M., Maincent, P., & Muller, R. H. (2008). Lipid nanoparticles with a solid matrix (SLN, NLC, LDC) for oral drug delivery. *Drug Development and Industrial Pharmacy*, 34(12), 1394-1405.

- Müller, R. H., Mäder, K., & Gohla, S. (2000). Solid lipid nanoparticles (SLN) for controlled drug delivery – a review of the state of the art. *European Journal of Pharmaceutics and Biopharmaceutics*, *50*(1), 161-177.
- O'Driscoll, C. M., & Griffin, B. T. (2008). Biopharmaceutical challenges associated with drugs with low aqueous solubility—The potential impact of lipid-based formulations. *Advanced Drug Delivery Reviews*, *60*(6), 617-624.
- Pouton, C. W., & Porter, C. J. H. (2008). Formulation of lipid-based delivery systems for oral administration: Materials, methods and strategies. *Advanced Drug Delivery Reviews*, *60*(6), 625-637.
- Prasad, D., Chauhan, H., & Atef, E. (2014). Amorphous stabilization and dissolution enhancement of amorphous ternary solid dispersions: Combination of polymers showing drug-polymer interaction for synergistic effects. *Journal of Pharmaceutical Sciences*, *103*(11), 3511-3523.
- Rumondor, A. F., Ivanisevic, I., Bates, S., Alonzo, D., & Taylor, L. (2009). Evaluation of drug-polymer miscibility in amorphous solid dispersion systems. *Pharmaceutical Research*, *26*(11), 2523-2534.
- Shah, M., & Agrawal, Y. (2013). High throughput screening: An in silico solubility parameter approach for lipids and solvents in SLN preparations. *Pharmaceutical Development and Technology*, *18*(3), 582-590.
- Uner, M., & Yener, G. (2007). Importance of solid lipid nanoparticles (SLN) in various administration routes and future perspectives. *International Journal of Nanomedicine*, *2*(3), 289-300.
- Vasconcelos, T., Sarmiento, B., & Costa, P. (2007). Solid dispersions as strategy to improve oral bioavailability of poor water soluble drugs. *Drug Discovery Today*, *12*(23–24), 1068-1075.
- Vo, C. L., Park, C., & Lee, B. (2013). Current trends and future perspectives of solid dispersions containing poorly water-soluble drugs. *European Journal of Pharmaceutics and Biopharmaceutics*, *85*(3, Part B), 799-813.
- Wissing, S. A., Kayser, O., & Müller, R. H. (2004). Solid lipid nanoparticles for parenteral drug delivery. *Advanced Drug Delivery Reviews*, *56*(9), 1257-1272.
- Yuan, X., Sperger, D., & Munson, E. J. (2014). Investigating miscibility and molecular mobility of nifedipine-PVP amorphous solid dispersions using solid-state NMR spectroscopy. *Molecular Pharmaceutics*, *11*(1), 329-337.

CHAPTER 3

Preparation and characterization of flutamide amorphous solid dispersions

Our major goal was to successfully formulate poorly soluble anticancer drug FLT utilizing solid dispersion technology. FLT precipitation inhibition was correlated in solution to the amorphous stabilization of FLT in the solid state. Precipitation studies were carried out using a BioTek plate reader using various FLT drug concentrations. The precipitation of drug was observed with time in absence and presence of different polymers. Four polymers: PVP K90, HPMC, Eudragit EPO and PEG 8000 were studied at different drug to polymer ratios. Miscibility studies between drugs and polymers were carried out using Modulated Differential Scanning Calorimetry (MDSC). SDs were prepared by using solvent evaporation technique and were characterized by Powder X-ray Diffraction (PXRD) and MDSC. Infrared and Raman Spectroscopy were used to investigate the possible drug-polymer interactions in obtained dispersions. Molecular modeling studies using Jaguar were carried out to understand drug polymer interactions. The physical stability of the SDs was studied at 25°C for one month.

3.1 Introduction

Many potential poorly soluble drugs result in decreased drug dissolution rate following oral administration and consequently, show reduced bioavailability (Kolašinac et al., 2012). The added challenge for anticancer drugs is that they are often associated with high toxicity. There is a significant need in designing and developing new formulations for poorly soluble anticancer drugs due to the prevalence of cancer and availability of limited drug delivery systems. Present drug development delivery techniques remain insufficient due to their inability to improve bioavailability. The use of novel drug delivery systems, such as SDs have

great potential to overcome the physiochemical limitations of anticancer drugs. The technique has been successfully utilized to improve oral formulations; increase their dissolution rate, absorption, wettability, and overall bioavailability. SDs are molecular mixtures of drugs in hydrophilic carriers in which drug release profile is driven by polymeric properties. Thus, it is important to have good miscibility between drug and polymers to enhance solubility and stability (Sarmiento, 2007). In solid dispersion technology, drugs are usually present in amorphous form which are more soluble and exhibit faster dissolution rates since the absence of a crystal lattice means no energy is required for this process to occur (Taskinen, 2010).

The prospects of therapeutic efficacy for FLT are minimal due to its low bioavailability. This may be due to poor wettability, low permeability, and rapid first pass hepatic metabolism. As a high-dose anticancer drug, FLT exhibits a limited dissolution rate due to larger particle size and low concentration at the absorption surface (Elkhodairy, 2010). Therefore, novel drug delivery systems, such as SDs, may be utilized to increase drug dissolution and achieve high drug concentrations at its target site of action.

In this study, polyvinylpyrrolidone (PVP) K90, hydroxypropyl methylcellulose (HPMC), Eudragit (EPO) and polyethylene glycol (PEG) 8000 are used as polymers. These polymers are commonly used in the preparation of SDs and were selected due to their contrasting physiochemical properties. Polymers improve the physical stability of amorphous drug in SDs by reducing the molecular mobility or by interacting with the functional groups on the drug (Sarmiento, 2007). All polymers used in this study are hydrophilic carriers and increase wetting of

poorly soluble drug and thereby improve dissolution of the molecularly dispersed matrix-incorporated drug (Elkhodairy, 2011; Millqvist, 2010). PVP, HPMC, EPO and PEG are regarded as non-toxic and non-irritant (Jones, 2004).

The objective of the present study was to form soluble and stable SDs. SDs are characterized by PXRD, MDSC while IR, Raman, and molecular modeling studies were used to study the drug polymer interactions.

3.2 Material and methods

3.2.1 Materials

FLT was purchased from TGI American (Portland, Oregon). The various polymers used were EPO from Degussa (Parsippany, New Jersey), PEG 8000 from Sigma (St. Louis, Missouri), PVP from Spectrum (New Brunswick, New Jersey) and HPMC from Dow Company (Midland, Michigan). Solvents used included methanol purchased from Fischer Scientific (Fair Lawn, New Jersey) and dichloromethane from Sigma (St. Louis, Missouri). All materials were used as received.

3.2.2 Methods

3.2.2.1 Preparation of physical mixtures (PMs)

Mixtures of FLT with polymers were prepared at 90:10, 70:30, and 50:50 (drug: polymer) weight by weight ratios. Homogenous blending of accurately weighed amounts of drug and polymers were accomplished by geometric dilution. All PMs were stored at room temperature in screw-capped vials until use.

3.2.2.2 Thermal analysis of flutamide, polymers, and physical mixtures

3.2.2.2.1 Thermogravimetric analysis (TGA)

Thermal analysis of pure drug and polymers was performed using a differential scanning calorimeter (TGA/DSC 60, Shimadzu, Kyoto, Japan). Drugs or polymers were placed in open aluminum pans and bathed in a nitrogen atmosphere maintained at a flow rate of 40 mL/min. Samples were heated to 300°C at 10°C/min to determine if degradation occurred.

3.2.2.2.2 Modulated differential scanning calorimetry (MDSC) analysis of PMs

Thermograms of pure drugs, polymers, PMs were recorded by TA DSC 2000 (TA Instruments, New Castle, DE). Samples (5-10 mg) were placed in hermetically sealed aluminum pans and heated at 2°C/min from 30-200°C. Inert atmosphere was maintained by nitrogen at a flow rate of 40 mL/min. An empty aluminum pan was used as a reference. The equipment was calibrated with Indium. Initiation and enthalpy of melting for pure drugs and polymers along with PMs were then determined for comparison. A second heating cycle was run solely for 70:30 (drug:polymer) w/w ratio. Modulated temperature was set to $\pm 0.2^\circ\text{C}/\text{min}$. The sample was initially heated to 150°C followed by a cooling cycle to 40°C and finally reheated to determine if recrystallization occurred.

3.2.2.3 Solubility Parameter Calculations

The solubility parameters were calculated using Hansen's method. The F_{di} , F_{pi} and E_{hi} of various functional groups of FLT and polymers were obtained from the values compiled by Van Krevelen. Functional group contributions for polymers were calculated based upon the single repeating monomer unit. Density and average

molecular weight of polymers were obtained from “Handbook of Pharmaceutical Excipients”.

3.2.2.4 Preparation of solid dispersions

FLT and polymer SDs were prepared at 70:30 (drug: polymer) w/w ratio. Weighed amounts of drug and polymer were placed in a 50 mL round bottomed flask and dissolved using methanol. To ensure complete dissolution of the mixtures containing HPMC and EPO, dichloromethane was used as a co-solvent. RotaVapor R-215 (Buchi, Flawil, Switzerland) was used to prepare SDs. Rota evaporation was carried out 60°C with a rotation speed of 150 rpm for 5-10 minutes or until a dry product remained. SDs were vacuum dried at room temperature overnight. The dispersions and the PMs were characterized by XRPD, MDSC, IR and Raman.

3.2.2.5 Characterization of solid dispersions

3.2.2.5.1 Modulated differential scanning calorimetry (MDSC) analysis of SDs

Thermograms of pure drugs, polymers, PMs, SDs were recorded by TA DSC 2000 (TA Instruments, New Castle, DE). Samples (5-10 mg) were placed in hermetically sealed aluminum pans. Inert atmosphere was maintained by nitrogen at a flow rate of 40 mL/min. Modulated temperature was set to $\pm 0.2^\circ\text{C}/\text{min}$. The sample was initially heated to 150°C followed by a cooling cycle to 40°C and finally reheated to determine if recrystallization occurred.

3.2.2.5.2 X-ray powder diffraction (xRPD)

The precipitate samples were analyzed by XRPD, Bruker AXS-XRD, (Billerica, Massachusetts) using Cu K α radiation. The XRPD patterns were collected in the angular range of $1 < 2\theta < 40^\circ$ in step scan mode and analyzed by EVA software

(Bruker, Billerica, MA). The XRPD was used to study the drug crystallinity and identify the precipitate polymorphic form.

3.2.2.5.3 Infrared (IR) Spectroscopy

Attenuated total reflectance (ATR) mode was used to obtain IR spectra using Bruker Vertex series 80 V IR spectrometer (Billerica, MA). Fifty scans were collected for each sample over a wave number region of 400-4000 cm^{-1} . IR spectroscopy was used for characterization of the precipitate and to explore the drug polymer interactions.

3.2.2.5.4 Raman spectroscopy

Raman spectra were obtained using Bruker Vertex series 80 V Raman spectrometer and data processing was performed using OPUS software (Billerica, MA). Data acquisition was done using an exposure time of 10 seconds for 10 accumulations and a laser power setting of 400 mW at 785 cm^{-1} . Raman spectroscopy was used for characterization of precipitate and to explore the drug polymer interactions in various mixtures and dispersions along with IR spectroscopy.

3.2.2.6 Molecular modeling studies

Jaguar (Schrodinger LLC, 2012) program was used to calculate the optimized geometries of the FLT-polymer complexes using the B3LYP/6-31G**. Calculations were performed with gradient-corrected density functionals and default convergence criteria for geometry optimization. Intermolecular energy values, E_{bind} , were computed by using Jaguar's hydrogen bond function to solve the following equation:

$$E_{\text{bind}} = [a\Delta E_{\text{bind}}(\text{cc} - \text{pvqz}) - b \Delta E_{\text{bind}}(\text{cc} - \text{pvtz})]/(a - b)$$

“[W]here $E_{\text{bind}}(\text{cc} - \text{pvqz})$ and $E_{\text{bind}}(\text{cc} - \text{pvtz})$ are the cc-pVQZ (-g) and cc-pVTZ (-f) counterpoise corrected binding energies, respectively. The values of the parameters a and b are determined by fitting to a ‘training set’ of molecular dimers, for which benchmark results have been obtained using conventional MP2 methods and ultra large basis sets.”

3.2.2.7 Flutamide precipitation studies

To gain an understanding of the effect of polymers on FLT precipitation, preparation of various concentrations of drug and polymer solutions were studied using a Synergy H1 Hybrid Reader (BioTek, Winooski, Vermont). First, FLT standard solutions (0.1 mg/mL, 0.05 mg/mL, 0.01 mg/mL, 0.005 mg/mL, 0.001 mg/mL) were prepared in methanol. Polymer stock solutions of similar concentrations were also prepared. EPO and HPMC were dissolved in methanol, while PVP and PEG were prepared in an aqueous medium. Four 96- well plates were designed to include triplicate 125 μL samples containing drug and an aqueous medium or drug, polymer, and an aqueous medium. FLT standard solutions and a methanol blank were included in each plate design. In the absence of polymer, 100 μL samples of each concentration of FLT stock solution were placed into wells using a micropipette. Wells containing drug alone were then precipitated out with 25 μL of water. To study the effect of polymer on the inhibition of precipitation, the volume of drug and polymer solution were varied. The volume of water added to each well, 25 μL , and the concentration of both drug and polymer solution remained constant. Wells containing drug and polymer were prepared at 90:10, 70:30, and 50:50 v/v

drug-polymer. Immediate formation of precipitate was noted upon addition of water. Plates were run at 37°C for a total of 5 hours with readings taken at 1, 2, 3, 5, 10, 20, 30, 60, 120, 180, 240, 300, and 360 minutes. The plate reader was set to an orbital shake in between readings to mitigate precipitate sedimentation. The percentage of drug in solution was analyzed for drug content utilizing Synergy H1 Hybrid Reader (BioTek, Winooski, Vermont) at λ_{max} 298 nm.

3.2.2.8 Flutamide dissolution study

In-vitro dissolution of powdered crystalline FLT or its equivalent amounts in PMs and SDs (70:30 drug-polymer, PVP, HPMC, EPO, PEG) was studied in a Vision Classic 6 dissolution apparatus (Hanson Research Corp., Chatsworth, CA) employing a paddle stirrer at 100 rpm using 90 mL of 0.1 N HCl, pH 1 as a dissolution medium at 37°C. 40 mg of FLT or PM equivalent was used in each test. At specified time intervals (15, 30, 45, 60, 90, 120 min) aliquots of 1 mL from each vessel were withdrawn and replaced with equal volume of fresh medium. The samples were obtained in triplicate and then filtered through a 0.45 μM Millipore filter. The percentage dissolved was analyzed for drug content utilizing Synergy H1 Hybrid Reader (BioTek, Winooski, Vermont) at λ_{max} 298 nm. The percentage cumulative amount of drug in solution was plotted against time. Precipitate of SDs were filtered and collected at completion of dissolution study for analysis.

3.3 Results and Discussion

3.3.1 Physiochemical properties of flutamide and polymers

Table 1. Physiochemical properties of FLT and polymers

Compound	MW (g/mol)	Density (g/cm ³)	Physical state	T _m (°C)	T _g (°C)	ΔH _{fus} (kJ/mol)
FLU	276.2	1.37	Crystalline	113	–	126
PVP K90	1,000,000	1.18	Amorphous	–	174.2	–
HPMC	10,000–1,500,000	1.326	Amorphous	–	145.2	–
EPO	100,000–250,000	0.816	Amorphous	–	49.2	–
PEG 8000	7000–9000	1.08	Crystalline	62	–	–

Data obtained from Elkhodairy, 2011 and Rowe, 2009.

Table 1 depicts the physiochemical properties of FLT and polymers. FLT has a characteristic melting temperature of 113°C and a calculated enthalpy of 126 kJ/mol. The polymers selected for this study were chosen because of their various physiochemical properties, characteristic T_m or T_g, and common use in pharmaceutical formulations. PVP, HPMC, and EPO are all amorphous polymers. PVP and HPMC have high T_g, while EPO has a low T_g. PEG is the only crystalline polymer used in this research and has a low T_m.

3.3.2 Thermal analysis of flutamide, polymers, and physical mixtures

3.3.2.1 Thermogravimetric analysis

TGA of pure drug and polymers showed that there was no significant weight loss when drug and polymer were heated to 350°C (Figure 11). It indicated that no degradation of drug and polymers happened in this temperature range. The slight weight loss observed in case of PVP and HPMC could be attributed to the evaporation of water due to the hygroscopic nature of these polymers.

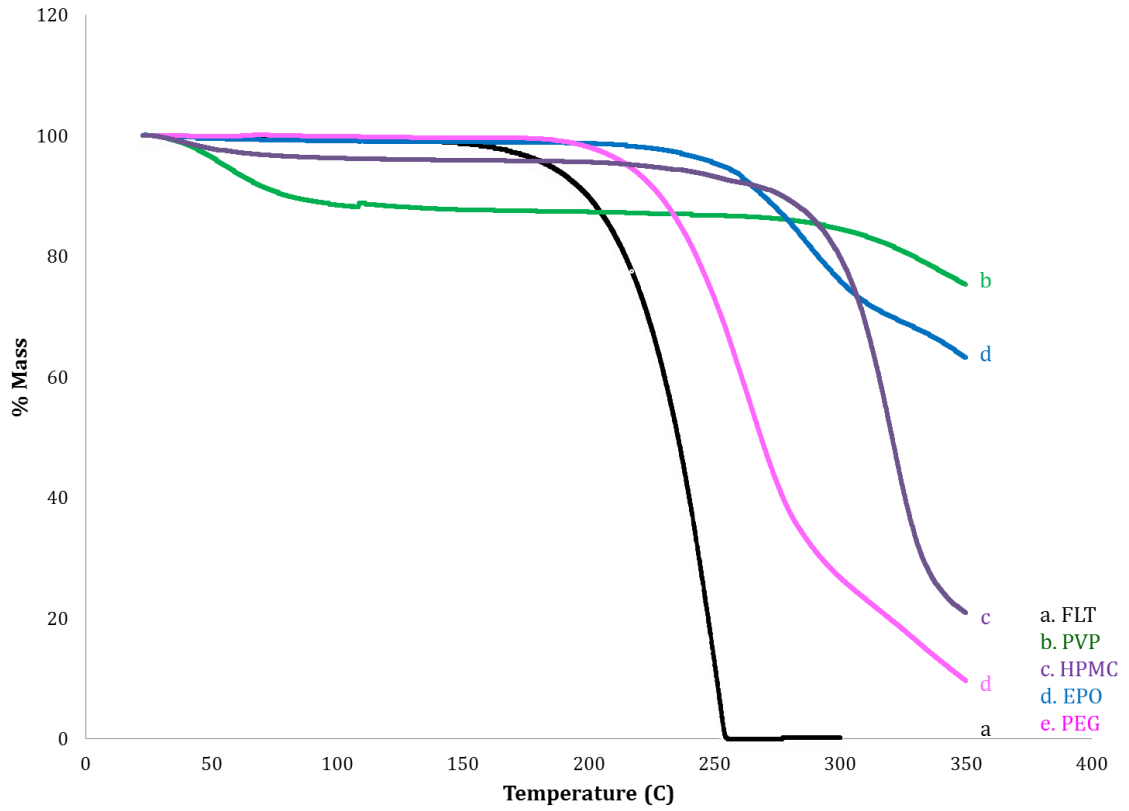


Figure 11. TGA of pure drugs and polymers. No significant degradation of FLT or polymers was observed below 200°C.

3.3.2.2 Modulated differential scanning calorimetry (MDSC) analysis of PMs

3.3.2.2.1 Drug Polymer Miscibility: First Heating Cycle (2°C/min)

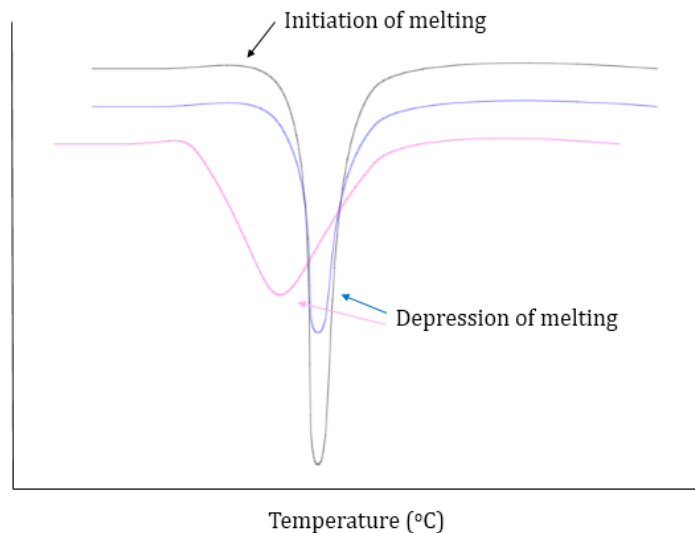


Figure 12. Example of MDSC thermogram from first heating cycle. Observed changes in the sharp characteristic peak of crystalline drug or polymer may include depression of melting endotherm or onset of melting initiation.

MDSC of the anticancer drug FLT, polymers, and their PMs were carried out to determine the miscibility between drug and polymers. Thermograms depict T_g and T_m of amorphous or crystalline products, respectively. MDSC thermograms of crystalline material produce sharp characteristic melting peaks or endotherms as seen in Figure 12. A change in this melting peak may be observed as a depression of the melting endotherm or decrease in the onset of melting. These changes indicate a reduction of drug crystallinity. T_g appear at levels equivalent to the baseline of the melting endotherms.

Figure 13 compares the DSC thermograms of FLT with different ratios of polymers viz. PVP, HPMC, Eudragit EPO and PEG 8000. Pure FLT showed a melting endotherm of 113.21°C which correlates well with the reported values (Elkhodairy, 2011). FLT-PVP and FLT-HPMC showed slight shift in melting depression characterized as either a decrease in melting endothermic peak, onset of melting or melting enthalpy, while FLT-EPO and FLT-PEG showed significant changes in melting depression. FLT-PVP, FLT-HPMC, FLT-EPO and FLT-PEG PMs showed decrease in melting initiation temperature of FLT at all the ratios. As expected, the decrease in melting initiation temperature of FLT becomes more significant with increase in the polymeric concentrations. FLT-EPO and FLT-PEG at 50:50 w/w PMs showed significant melting depression, which could be related to low T_g of EPO at 49°C and low T_m of PEG at 60°C, both of which occur before the melting of FLT at 113.21°C. It appears that the molecules of EPO and PEG were in a state of high molecular mobility prior to initiation of FLT melting which allowed the drug molecules to achieve molecular dispersion within these polymeric matrices resulting in disappearance of FLT endothermic melting peak. Compared to these polymers, PVP and HPMC molecules have low molecular mobility at the time of FLT melting owing to their high glass transition temperatures of 150°C and 160°C respectively.

The differences in the physicochemical properties of polymers may be indicative of their ability to be miscible with FLT. Based on these thermograms, it appears that the rank order of polymer effectiveness in achieving miscibility with FLT is as follows: PEG > EPO > PVP > HPMC. Despite this observation, it may be

unreasonable to compare these polymers using this approach given that PEG is the only polymer crystalline in nature. FLT-PEG 90:10 w/w PMs showed an additional endotherm at around 85°C along with the melting endotherms of FLT and PEG. This endotherm is absent at higher polymeric concentrations, namely 70:30 and 50:50 w/w PMs, along with the absence of FLT melting endotherms. The observed melting point depression may be due to the formation of a eutectic mixture rather than miscibility due to the crystalline nature of PEG. Moreover, the additional endotherm seen at 85°C in FLT-PEG 90:10 w/w PMs has not been reported in literature and may be due to the formation of a co-crystal. The significance of FLT-PEG co-crystal would be enhanced stability given that both drug and polymer are present in a thermodynamically stable crystalline state. Thus, comparison of polymers to determine miscibility is limited due to their physicochemical states.

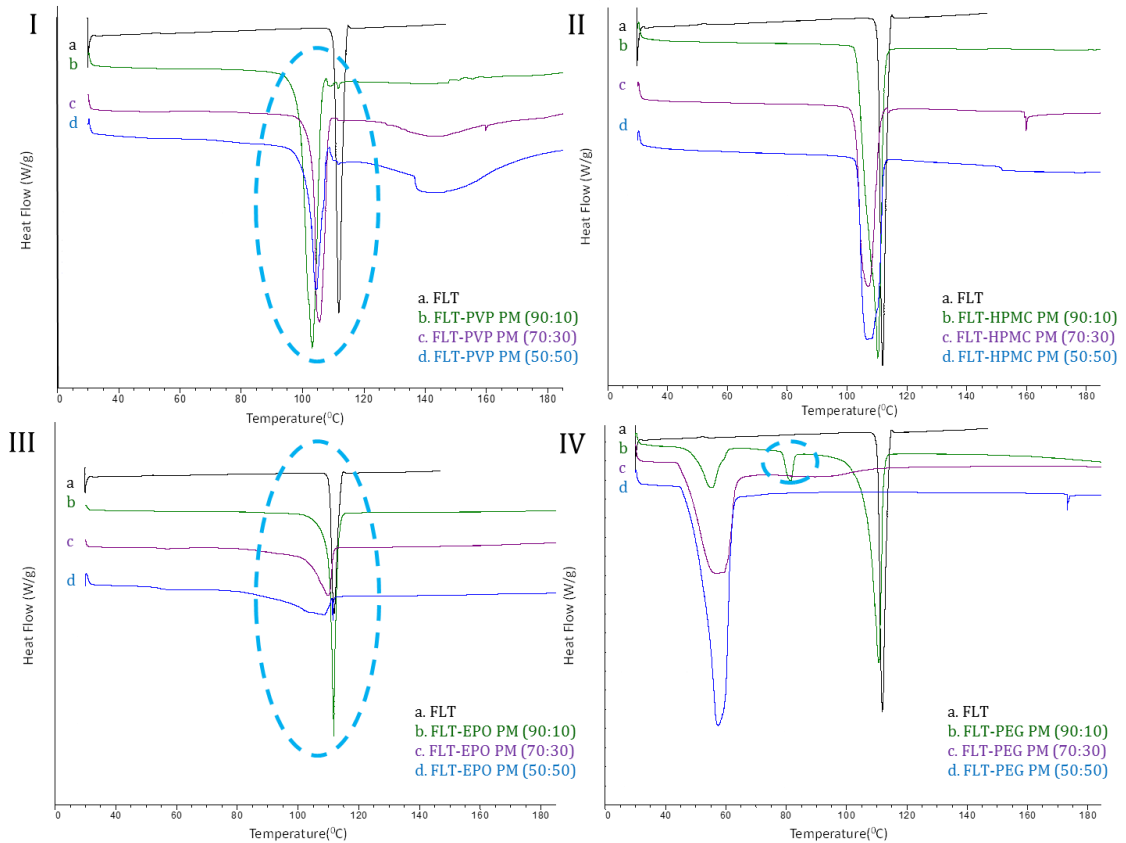


Figure 13. DSC thermograms of pure FLU, FLU-PVP 90:10, FLU-PVP 70:30, FLU-PVP 50:50 (I); pure FLU, FLU-HPMC 90:10, FLU-HPMC 70:30, FLU-HPMC 50:50 (II); pure FLU, FLU-EPO 90:10, FLU-EPO 70:30, FLU-EPO 50:50 (III); pure FLU, FLU-PEG 90:10, FLU-PEG 70:30, FLU-PEG 50:50 (IV). Depression of melting endotherm was more prominent at high polymer concentrations. FLT crystallinity was reduced in the presence of EPO and PEG.

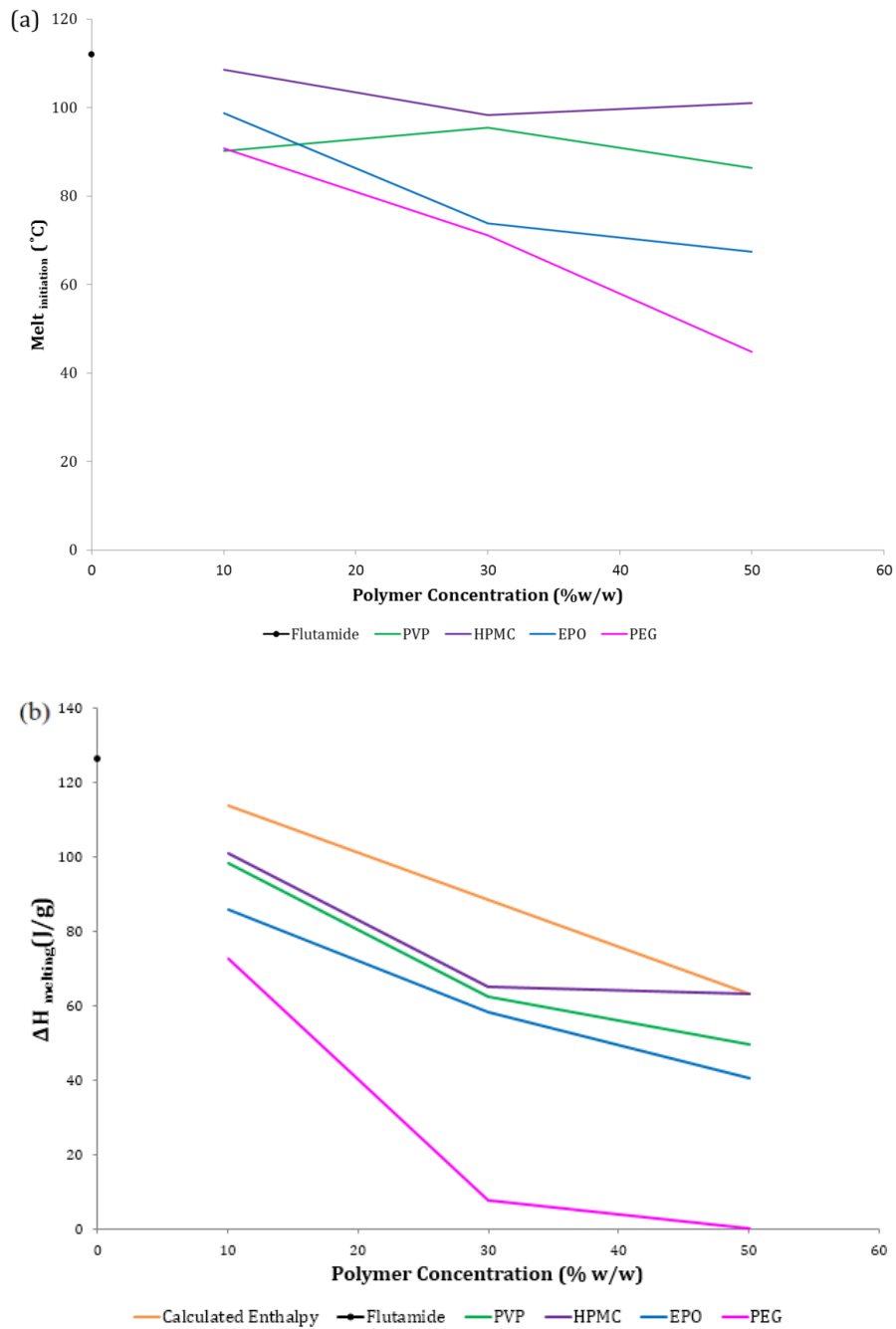


Figure 14. (a) Depression of melting point (initiation) of FLT in presence of various polymers. (b) Comparison of theoretical and experimental Enthalpy (melting) of pure FLT observed in presence of polymers. The melting temperature of FLT is 113°C and the calculated enthalpy of FLT is 126 J/g.

Drug enthalpy was found to decrease with increasing polymeric concentration indicative of a reduction in drug crystallinity (Figure 14). In the 50:50 w/w PMs, PVP and HMPC were found to reduce enthalpy less than EPO and PEG. Due to the high polymeric concentration and high T_g, PVP and HMPC were expected to form more stable SDs. However, PVP and HMPC were found to depress the melting initiation of FLT the least due to their high T_g. Thus PVP and HPMC may be less miscible than EPO and PEG. Miscibility of drug and polymer is important because the presence of polymer influences melting depression of the drug. Melting is more thermodynamically favorable because the presence of polymer results in the reduction of chemical potential of the drug (Baird Taylor, 2012). EPO and PEG were found to be more effective in decreasing the melting initiation of FLT and reducing enthalpy. Low enthalpy reflects a reduction in FLT crystallinity indicating that drug may be dispersed molecularly or dissolved within the polymer matrix (Elkhodairy, 2011). Similar phenomenon has been reported and explained by Elgindy et al for FLT-trehalose systems and FLT-chitosan systems. The rank order for the ability of polymers to reduce drug crystallinity is therefore PEG > EPO > PVP > HMPC.

3.3.2.2.2 Drug Polymer Miscibility: Second Heating Cycle ($\pm 0.2^\circ\text{C}/\text{min}$)

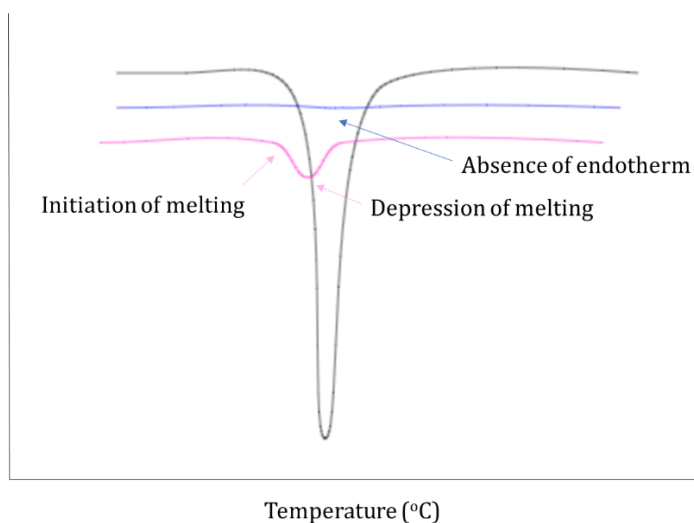


Figure 15. Example of MDSC thermogram from second heating cycle. The second heating cycle provides more information on the true physical state of its components as PMs are exposed to high temperatures and then cooled, which allows for mixing and potential formation of interactions.

Figure 15 depicts an example MDSC thermogram of a second heating cycle. The second heating cycle involves heating the sample to high temperatures and followed by a cooling phase. This modulation of temperature exposes the PM to higher temperatures resulting in increased molecular mobility. The subsequent cooling phase allows the molecules to slow down and potentially form interactions that contribute to miscibility. The absence of endotherms indicate the amorphous state, while endotherms with significant depression in melting are indicative of a small amount of crystalline drug.

Results of the second heating cycle are presented in Figure 16. The corresponding melting peak of pure crystalline FLT was absent in the FLT-PVP and

FLT-HPMC 70:30 PMs MDSC thermograms suggesting the formation of a single amorphous phase. The exposure to high temperatures above the T_g of these two polymers created an environment more suitable for the melting of FLT and interaction of drug and polymer due to increased molecular mobility. Subsequent cooling of the system decreased molecular mobility of both components to form an amorphous system. A study conducted by Meng and colleagues analyzed glass transition temperature changes that occurred when curcumin was in the presence of EPO and HMPc. It was determined that the efficacy of these polymers to bypass crystallization was due to similar kinetic changes involving molecular mobility upon exposure to high temperatures above T_g followed by a fast cooling cycle. FLT-EPO 70:30 PMs showed a slight shift and near disappearance of the FLT endotherm suggesting FLT may still be present in crystalline form and that FLT-PVP may be more miscible and stable than FLT-EPO. Contrary to the amorphous polymers (PVP, HPMc and EPO), FLT-PEG PMs showed a recrystallization exotherm at 37°C and a melting endotherm at 88°C. Glass transition occurred at 4.58°C and melting of drug occurred at 106.9°C. A similar theory can be used to account for these findings in relation to when the glass transition occurs. If T_g occurs prior to the melting of FLT, the polymer matrix may be more suitable to disperse the insoluble drug. However, if T_g occurs following FLT melting, an inadequate environment is available for drug to be miscible. As the only crystalline polymer being used in this research, PEG was the only polymer to undergo recrystallization. The amorphous form which is much higher in free energy compared to the crystalline form is more soluble and has faster dissolution rates. When subjected to cooler temperatures the likelihood of

recrystallization increases. Similarly, molecular mobility of the sample decreases with lower temperature (Trasi Taylor, 2012). In the first cycle, it appeared that FLT was completely miscible in the presence of PEG due to the observed loss of the characteristic endothermic peak of FLT. The shift away from equilibrium occurred when subsequently cooled to temperatures below FLT T_m and PEG T_g . Thus resulting in a transition back to the lower energy crystalline state, which may be attributed to the aforementioned formation of a FLT-PEG co-crystal.

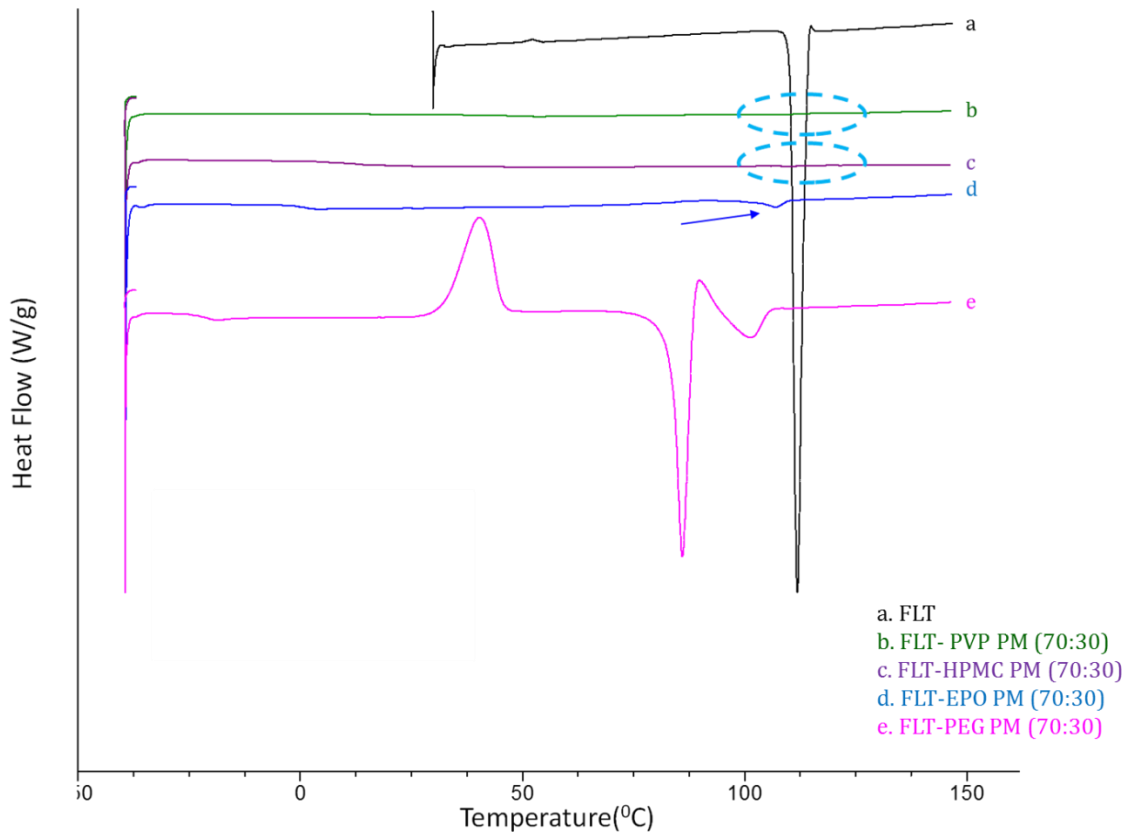


Figure 16. MDSC thermograms of 2nd heating cycling of FLT-polymer physical mixtures at 70:30 w/w drug to polymer concentration. The 2nd heating cycle may be more indicative of the physical state of FLT as drug and polymer have been exposed to a previous heating cycle. FLT is in the amorphous state in the presence of PVP and HPMC.

Based on these observations, it can be noted that PVP has the ability to decrease the melting initiation and enthalpy of FLT. Moreover, the MDSC thermogram of FLT-PVP in the second cycle (Figure 4) suggest the development of an amorphous system, which may be more effective than that of FLT-EPO. The

resultant rank order of the effectiveness of polymers to achieve miscibility is as follows PEG > PVP > HMPC > EPO.

3.3.3 Solubility parameters of FLT and polymers

The solubility parameters (δ) of FLT, polymers and their differences ($\Delta\delta$) are shown in Table 2 and 3. These calculations were performed to determine miscibility between drug and polymers. Drug-polymer combinations with lower $\Delta\delta$ are predicted to be more miscible than combinations with higher $\Delta\delta$. More specifically, if $\Delta\delta < 7.0 \text{ MPa}^{1/2}$, drug-polymer blends are likely to be miscible whereas if $\Delta\delta > 10.0 \text{ MPa}^{1/2}$, drug-polymer blends are likely to be immiscible (Archer, 1992; (Ghebremeskel, et al, 2007; Greenhalgh et al, 1999). All the $\Delta\delta$ values of FLT and polymers in this study were $< 7.0 \text{ MPa}^{1/2}$ suggesting miscibility with FLT. Based on these values, the rank order of miscibility predicted by solubility parameter is PVP > PEG > EPO > HPMC. While solubility parameters are useful for predicting miscibility, they may be less applicable to complex drug-polymer systems wherein hydrogen bonding or ionic interactions drive molecular interactions compared to simpler structures bound by van der Waals forces. Consequently, this theoretical model has its limitations in predicting miscibility (Baird Taylor, 2012; Marsac et al, 2006).

Table 2. Solubility parameter calculations of FLT

Group	Frequency	F_{di} ($J^{1/2} \text{ cm}^{3/2} \text{ mol}^{-1}$)	F_{pi}^2 ($J \text{ cm}^3 \text{ mol}^{-2}$)	E_{hi} (J/mol)
CH3	2	420	0	0
CH	1	80	0	0
C6H4 (2)	1	1,270	12,100	0
CO	2	290	592,900	2,000
C	2	-140	0	0
F	3	450	302,500	400
N	2	20	640,000	5,000
O	2	100	160,000	3,000
Σ	-	4,080	3,705,400	21,200
$\Delta = 23.1 \text{ MPa}^{1/2}$	-	$\delta_{di} = 20.2 \text{ MPa}^{1/2}$	$\delta_{pi} = 9.5 \text{ MPa}^{1/2}$	$\delta_{hi} = 10.3 \text{ MPa}^{1/2}$

Molecular weight = 276.2 g/mol, true density = 1.37, molar volume = 201.6 cm^3/mol

Table 3. Solubility parameters of FLT and polymers

Material	Solubility parameter ($\text{MPa}^{1/2}$)	$\Delta\delta$	Group Classification
FLU	23.1	-	-
PVP	21.7	1.4	Miscible
HPMC	28.1	5	Miscible
EPO	19.6	3.5	Miscible
PEG	21.3	1.8	Miscible

Drug-polymer blends with $\Delta\delta < 7.0 \text{ MPa}^{1/2}$ are expected to be miscible.

3.3.4 Characterization of solid dispersions

3.3.4.1 Thermal analysis of flutamide SDs

Figure 17 depicts the results obtained from MDSC of FLT-polymer 70:30 w/w SDs. In the case of FLT-PVP, the characteristic melting endotherm of FLT was absent confirming miscibility of drug and polymer and the formation of an amorphous system. The observed characteristic melting peak of FLT was shifted to lower temperatures and broadened in the presence of HPMC and EPO indicating decreased FLT crystallinity to a lesser extent than that of PVP. The thermogram for FLT-PEG SD shows absence of the FLT melting peak and two endothermic peaks

corresponding to the melting of PEG and a second endotherm at 85°C. The endothermic peak at 85°C was also observed in case of 90:10 w/w PM of FLT-PEG signifying the potential for formation of a FLT-PEG eutectic mixture, co-crystal or polymorph.

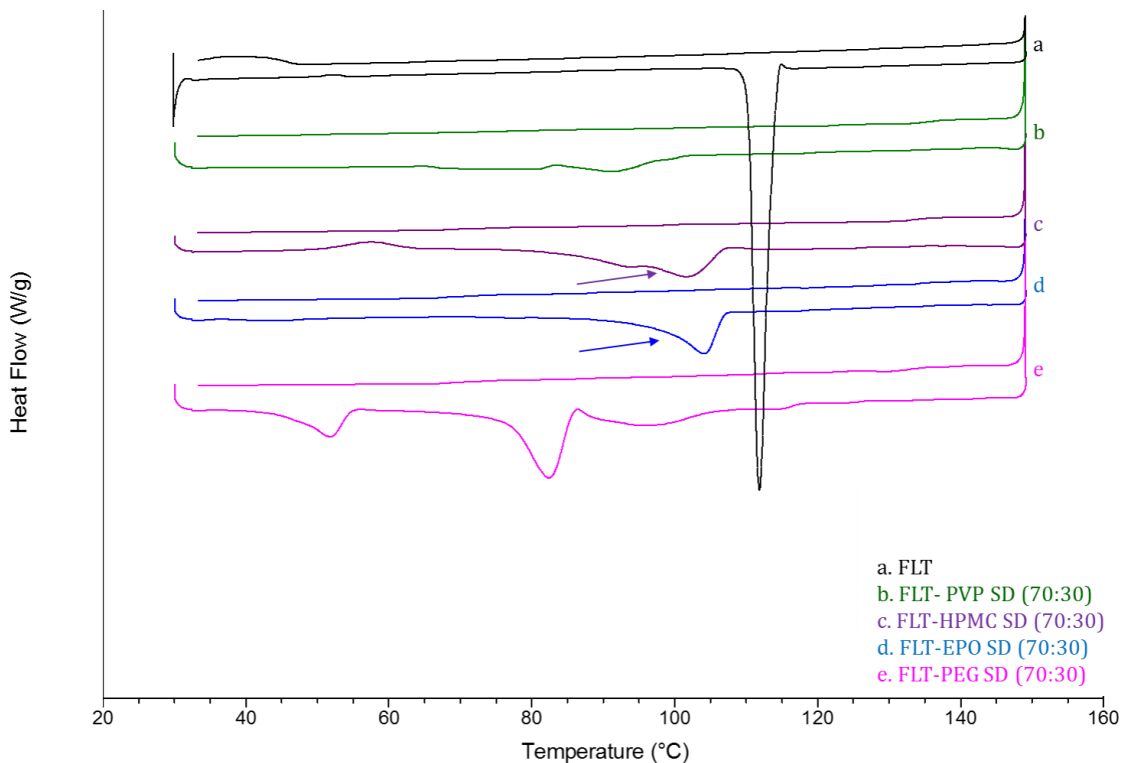


Figure 17. MDSC thermograms of FLT-polymer SDs (73:30 w/w): pure FLT, FLT-PVP, FLT-HPMC, FLT-EPO, FLT-PEG. PVP was able to reduce drug crystallinity to a greater extent than the remaining polymers. The lack of the FLT melting peak in the presence of PEG indicates miscibility between drug and polymer.

The profound changes of the FLT melting peak depicted in Figure 17 corresponds to improved solubilization of FLT at the 70:30 w/w SDs. Similar

observations were made by Kolasinac and coworkers in determining solubility enhancement of desloratidine and polyoxamer SDs at differing w/w ratios. The concentration of polymer in SDs resulted in peak smoothening, early initiation of melting or broadening of drug melting peaks. The latter corresponds to partial drug crystallization during preparation of SDs, in which after the cooling phase, the drug exists both in crystalline and amorphous phase (Kolašinac et al, 2012). Complete peak disappearance indicates that the drug is present in the amorphous state and the concentration of polymer was sufficient to solubilize the drug.

In the study by Kolasinac et al, increased w/w ratios of desloratidine (DSL) and poloxamer SDs were found to enhance DSL solubility. The present study only characterized FLT-polymer 70:30 w/w, but similar conclusions can be drawn from these observations. The rank order of polymer solubility enhancement is PVP > PEG > HPMC > EPO. Surface activity, solubilization and wetting effect of polymers can be correlated to enhanced solubility of FLT (Chen et al, 2004; Craig, 2002; Leuner Dressman, 2000; Rouchotas et al, 2000).

3.3.4.2 pXRD of pure FLT, polymers, PMs and SDs

The X-ray diffractograms of pure FLT, polymers, PMs and SDs are presented in Figure 18. Pure FLT showed sharp characteristic diffraction peaks at 2θ of 19° , 26° , and 41° . These same peaks were present in FLT-PVP, FLT-HPMC, and FLT-EPO PMs indicating FLT crystallinity within these systems. Additional peaks seen in the FLT-PEG PMs can be attributed to the crystalline nature and characteristic peaks of drug and polymer. In comparison to the FLT-polymer PMs, FLT-PVP SD was characterized as an amorphous system due to the lack of diffraction peaks and

presence of a halo pattern. Both FLT-HPMC and FLT-EPO binary SDs were found to be crystalline. Pure PEG has two characteristic peaks at 2θ of 19° and 23° . The peak at 2θ of 19° and 26° is present at a lower intensity in FLT-PEG SD. Since the former peak is characteristic of both FLT and PEG, decreased intensity may signify decreased crystallinity of the system. The characteristic peak of FLT at 2θ of 41° is absent in the FLT-PEG SD further implicating reduced drug crystallinity. The nature of FLT-PEG SD was difficult to ascertain given the overlap of diffraction peaks from the individual components. To confirm the physical states of FLT SDs MDSC was used. MDSC thermograms of FLT-PVP showed T_g instead of melting of FLT confirming FLT was present in amorphous state in this binary system. Initiation of melting occurred at lower temperatures in the FLT-HPMC and FLT-EPO SDs. Peak shift and broadening of these drug-polymer SDs indicated reduced FLT crystallinity and inability of these systems to achieve the amorphous state. Results of the FLT-PEG SD appear to confirm that FLT was present in the amorphous state. Present endotherms on the FLT-PEG SD thermogram are associated with the melting of pure PEG and potential FLT-PEG co-crystal or eutectic mixture. Therefore, the physical characterization of FLT SDs are in agreement with the ability of polymers to transform FLT into the amorphous form.

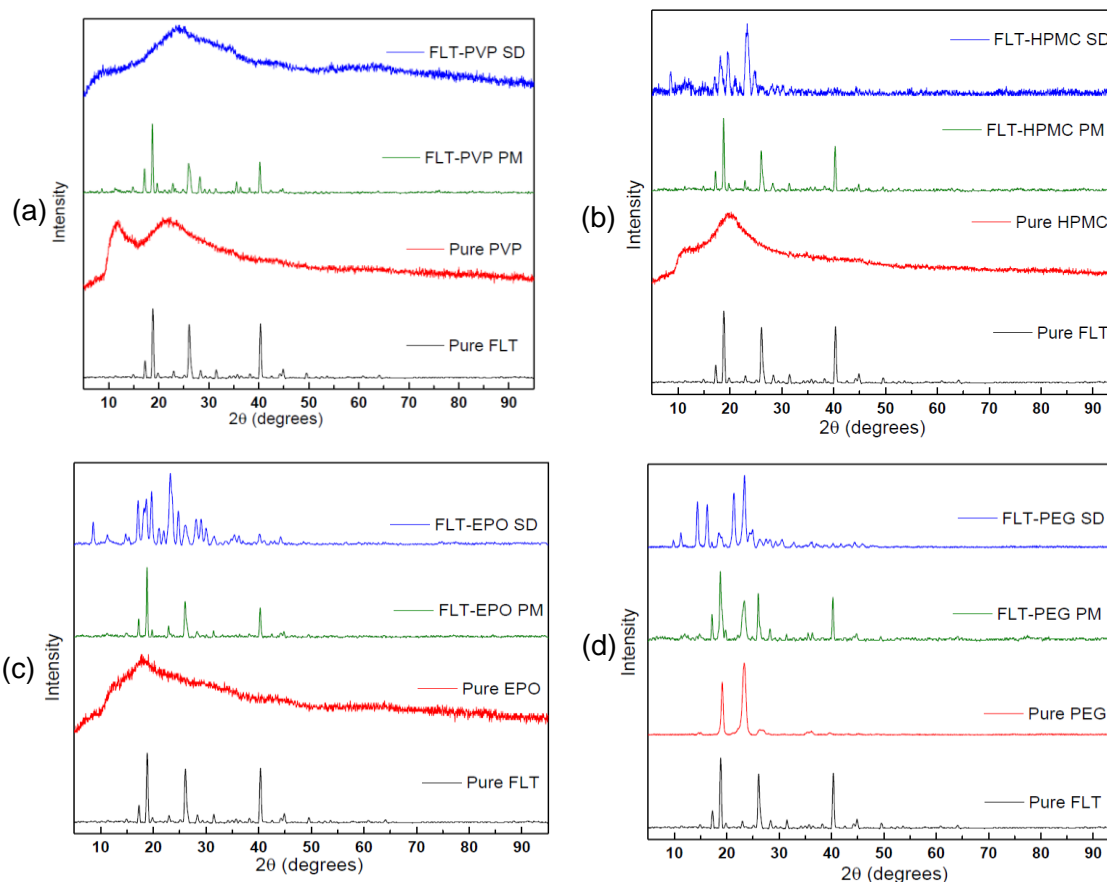


Figure 18. XRPD of pure FLT, polymers, physical mixtures (70:30 w/w) and SDs (70:30 w/w) (a) FLT-PVP; (b) FLT-HPMC; (c) FLT-EPO; (d) FLT-PEG. The halo pattern observed in the FLT-PVP SD indicates FLT is amorphous in this binary complex. Additional peaks present in the FLT-PEG SD are associated with the characteristic peaks of PEG as a crystalline polymer.

Table 4. Summary of PXRD and MDSC results

Drug	PXRD	MDSC
FLT-PVP	Amorphous	Amorphous
FLT-HPMC	Crystalline	Crystalline
FLT-EPO	Crystalline	Crystalline
FLT-PEG	Crystalline*	Crystalline*

Table 4 summarizes PXRD and MDSC results of FLT-polymers. FLT is present in the amorphous state when prepared with PVP, while FLT is present in the crystalline state when prepared with PEG, the only crystalline polymer used in this study. Co-crystal formation may be a viable explanation for the improved performance of FLT with PEG. FLT remains crystalline in the presence of HPMC and EPO indicating less favorable formulation of FLT with these polymers.

3.3.5 Molecular interactions

3.3.5.1 IR spectroscopy of pure FLT, polymers, PMs and SDs

The characteristic peaks of pure FLT, polymers, PMs and SDs are shown in Figure 19 and summarized in Table 5. IR spectra of pure FLT contains sharp absorption peaks at 3356 cm^{-1} and 1713 cm^{-1} which are attributed to the amino and carbonyl group. The very strong band at 3356 cm^{-1} assigned as a secondary amide typically appears strong and broad in the $3390 \pm 60\text{ cm}^{-1}$ region. However, the lowering of the N-H stretching wavenumber indicates weakening of the N-H bond due to proton transfer with the neighboring oxygen on FLT (Mariappan Sundaraganesan, 2014). Resultant proton transfer between the amino and carbonyl

group suggests potential sites of interaction between FLT and polymer. FLT contains one hydrogen bond donor, the N-H group, and two acceptors, the carbonyl and the nitro group. These functional groups have significant tendency to interact with polymers (Trasi Taylor, 2012).

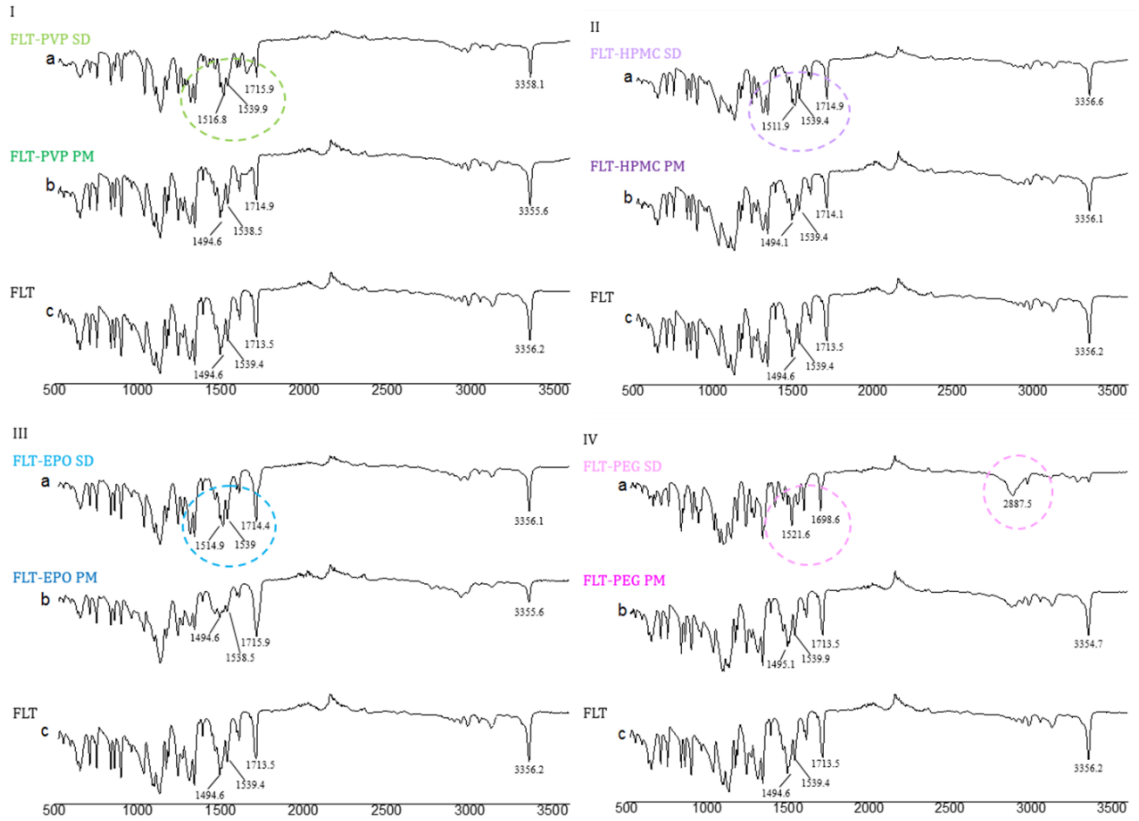


Figure 19. IR spectra of pure FLT, PMs, SDs of FLT-PVP (I), FLT-HPMC (II), FLT-EPO (III) and FLT-PEG (IV). Peak shifts observed in FLT-PVP SD and FLT-PEG SD may be indicative of interactions formed between drug and polymer.

Table 5. Peak positions of functional groups present in IR spectra for FLT and FLT binary SDs

FLT (cm ⁻¹)	FLT-PVP (cm ⁻¹)	FLT-HPMC (cm ⁻¹)	FLT-EPO (cm ⁻¹)	FLT-PEG (cm ⁻¹)	Assignment
3356	3358	3357	3356	2887	NH stretching
1713	1716	1715	1714	1699	CO stretching
1539	1540	1539	1539	1522	CC stretching + NO stretching + in-plane bending of HNC
1495	1517	1512	1515	----	In-plane bending HNC

FLT-polymer PM IR spectra have similar absorption patterns as that of pure FLT implicating the lack of significant interactions between drug and polymer. In contrast, the FLT-PVP SD IR spectrum show a shift of the carbonyl peak and peak associated with the HNC group indicating the presence of hydrogen bonds between drug and polymer. Moreover, the broadening of the HNC peak may be indicative of an intermolecular hydrogen bond between the amino group of FLT, a hydrogen bond donor, and the PVP carbonyl group, a hydrogen bond acceptor. Similar implications involving the FLT carbonyl group occurred in FLT-casein micelles in which the carbonyl stretching peak of FLT was shifted to a higher wavenumber as a result of suspected intermolecular hydrogen bond between the drug and protein due to a change in the environment of the carbonyl group in the preparation of nanoencapsulation (Elzoghby et al, 2013). In the SD of FLT-PEG, the characteristic amino and carbonyl peak was shifted to a lower wavenumber from 3356 cm⁻¹ to 2887 cm⁻¹ and from 1713 cm⁻¹ to 1699 cm⁻¹, respectively. These changes indicated the formation of molecular bonds between FLT and PEG. Moreover, in a study by Papadimitriou et. al., the carbonyl groups of PVP or oxygen atoms and hydroxyl groups of PEG were found to form hydrogen bonds with polar functional groups

(C=O, -Cl, NH) present on feldopine. These interactions contributed to the successful preparation of amorphous feldopine SDs ensuring improved physical stability and high solubility (Papadimitriou et al, 2012). Interactions between drug and polymer or drug and protein as in the Elzoghby and colleagues study, would prevent drug-drug interactions that would lead to potential recrystallization of FLT and thus enhance the stability of these binary systems. As minimal to no changes were observed in the IR spectra of FLT-HMPC and FLT-EPO SDs, the rank order of molecular interactions determined by IR spectroscopy is PVP, PEG > HPMC > EPO.

3.3.5.2 Raman spectroscopy of pure FLT, polymers, PMs and SDs

Confirmation of molecular interactions observed in IR spectroscopy was obtained using Raman spectroscopy. Figure 20 shows Raman peaks of pure FLT, PMs, and SDs. The corresponding peak assignments are shown in Table 6. Pure FLT showed four characteristic peaks: (1) in-plane bending of HCC and CC stretching at 1245 cm^{-1} , (2) ON stretching and in-plane bending of HCC at 1344 cm^{-1} , and (3) ON stretching and CC stretching at 1598 cm^{-1} . In FLT-PVP SD, peak changes were noted at all three characteristic vibration peaks of FLT. Though peaks were shifted to one wave number higher or lower than the pure FLT Raman spectrum, these changes imply potential interaction between FLT and PVP. Similar minimal changes were observed in the SDs of EPO (peaks 1 and 3) and PEG (peaks 1 and 2) in which only two peak shifts were observed in comparison to pure FLT. Thus EPO and PEG may form potential interactions with FLT, but to a lesser extent than FLT-PVP systems. In contrast to these binary SDs, only one change was visible in the Raman spectrum of HPMC associated with peak 2. This suggests little to no interaction with FLT occurs,

which may be attributed to polymeric steric hindrance preventing drug-polymer interactions. Thus, the rank order for molecular interaction based on Raman spectroscopy is PVP > PEG, EPO > HPMC. Similar conclusions from IR results were drawn for PVP and PEG. However, Raman results suggest greater possibility of molecular interaction with EPO versus HPMC.

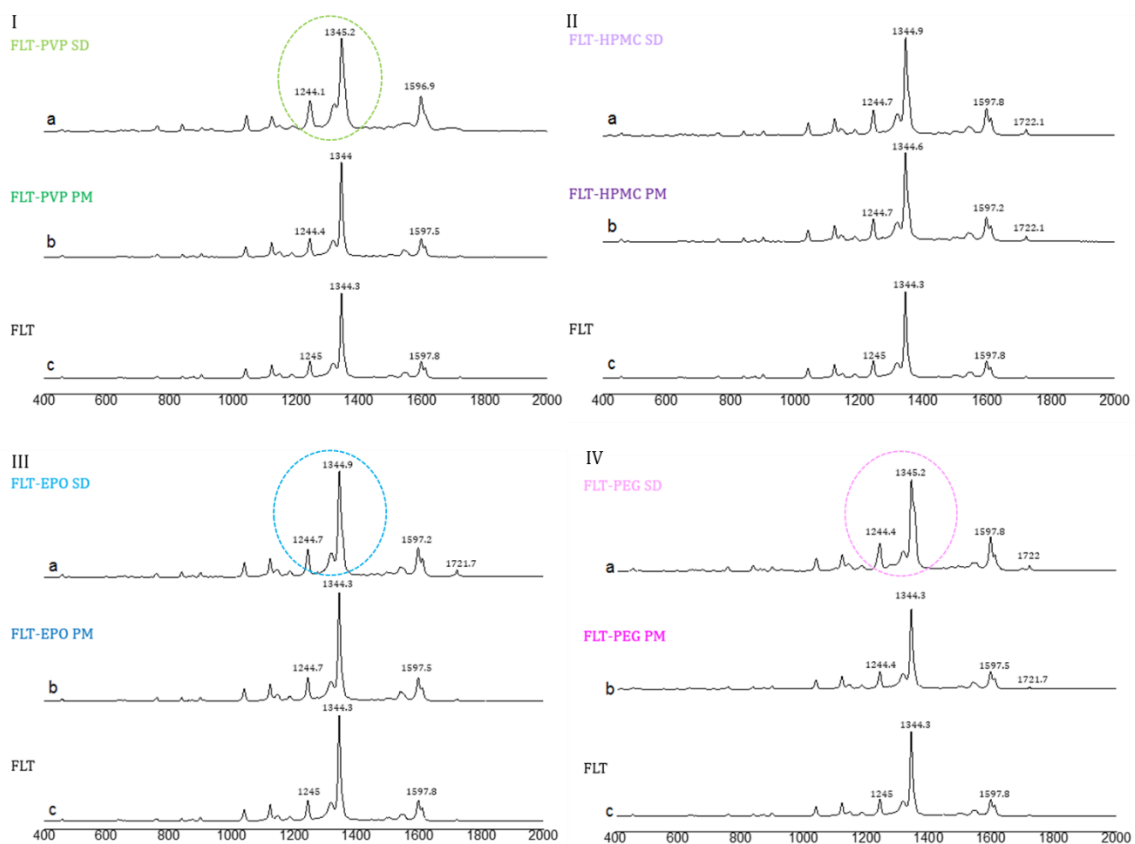


Figure 20. Raman spectra of pure FLT, PMs, and SDs of FLT-PVP(I), FLT-HPMC (II), FLT-EPO (III) and FLT-PEG (IV). Potential FLT and polymer interactions were more likely formed in the presence of PVP and PEG evidenced by peak shift changes. This correlates well with the results observed from IR spectra.

Table 6. Raman peak assignments of FLT and FLT-polymer SDs

FLT (cm ⁻¹)	FLT-PVP (cm ⁻¹)	FLT-HPMC (cm ⁻¹)	FLT-EPO (cm ⁻¹)	FLT-PEG (cm ⁻¹)	Assignment
1245	1244	1245	1245	1244	In-plane bending of HCC + CC stretching
1344	1345	1345	1345	1345	ON stretching + in-plane bending of HCC
1598	1597	1598	1597	1598	ON stretching + CC stretching

3.3.5.3 Molecular modeling

Table 7 shows the molecular modeling results of geometrically optimized calculations of hydrogen bond lengths, binding energies, and the atoms involved in these respective interactions. Figure 21 depicts the hydrogen bonds formed between FLT and monomer units of the studied polymers at optimized geometries. PVP has been shown to provide the greatest potential for molecular interaction with FLT based on results from IR, Raman and thermal analysis. Molecular modeling results are complimentary to these findings as FLT-PVP was calculated to have the highest binding energy. Comparison of binding energies for the remaining polymers ability to form interactions with FLT would rank PVP (-12.05 Å) > EPO (-10.2 Å) > HPMC (-8.39 Å) > PEG (-6.69 Å). Further, hydrogen bond lengths of FLT-PVP (2.038 kcal/mol), FLT-HPMC (2.212 kcal/mol), FLT-EPO (2.054 kcal/mol), and FLT-PEG (1.896 kcal/mol) were calculated. The rank order of increasing bond distance is as follows: HPMC > EPO > PVP > PEG. Based on the notion that shorter bond length indicates a stronger single bond, discrepancies arise between these molecular modeling calculations. Since these simulations were carried out using only monomer units, it should be noted that these results are only estimations and other factors, such as steric hindrance should be taken into account. Inconsistency of

molecular modeling results was also seen between curcumin (CUR) and EPO SDs, which had the lowest calculated H-bond binding energy (-5.68 Å) in comparison to PVP (-11.12 Å), HPMC (-10.64 Å) , and PEG (-9.95 Å) (Meng et al, 2015). Results from IR, Raman, and thermal analysis of this study had proven the strongest interaction was formed between CUR-EPO. This discrepancy was attributed to the potential formation of an ionic interaction between the acidic phenol hydroxyls of CUR and the dimethylamino groups of EPO (Aggarwal Harikumar, 2009; Meng et al, 2015). Therefore, molecular modeling results may supplement IR, Raman and thermal analyses, but steric hindrance and the formation of alternative intermolecular interactions (ionic bonds, van der Waals forces) must also be taken into consideration.

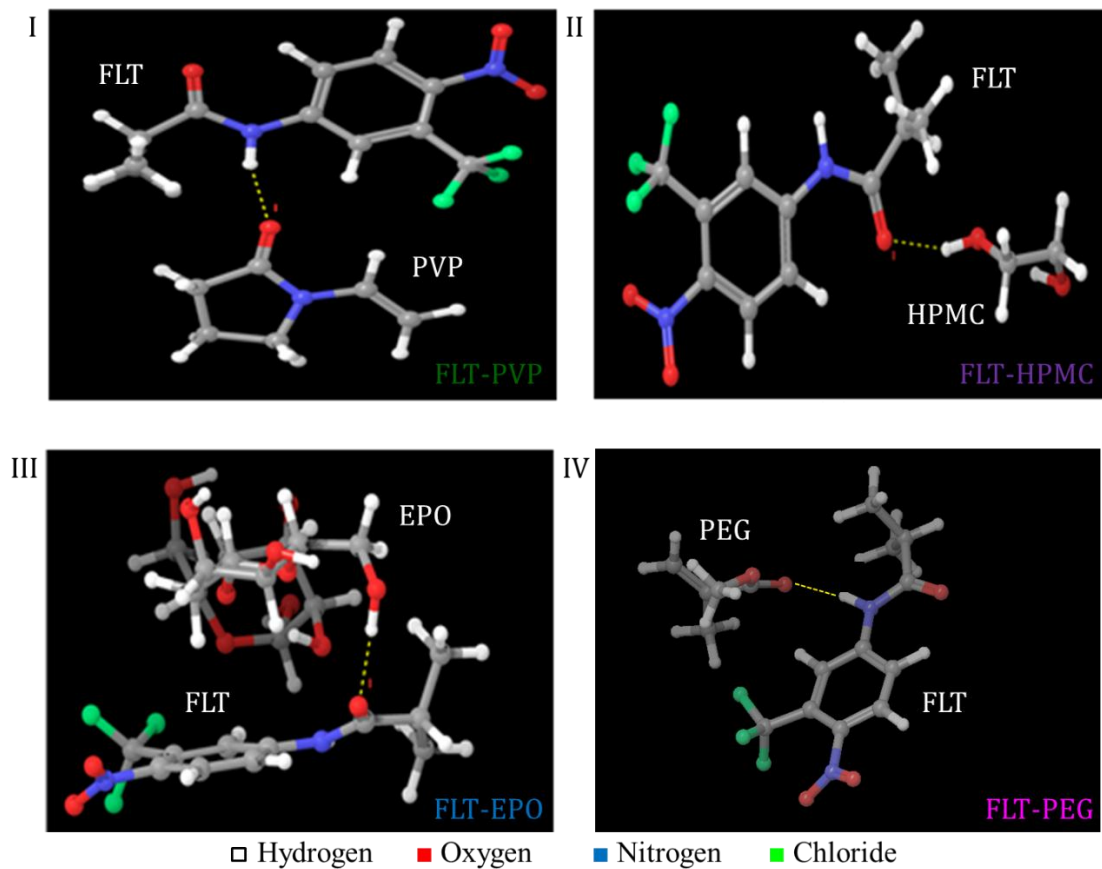


Figure 21. Molecular modeling results depicting hydrogen bonds formed between FLT-PVP (I), FLT-HPMC (II), FLT-EPO (III) and FLT-PEG (IV) complexes after geometric optimization.

Table 7. Molecular modeling results of FLT and monomers

Parameters	FLT-PVP	FLT-HPMC	FLT-EPO	FLT-PEG
R' (Angstroms)	2.038	2.212	2.054	1.896
E _{bind} (kcal/mol)	-12.05	-8.39	-10.2	-6.69
Bond made between FLT-polymer	NH-O	O-H	O-H	NH-O

The high binding energy calculated between FLT-PVP and FLT-EPO may be indicative of H-bond formation between drug and polymers. However in comparison to bond distance, interactions may be present in FLT-PEG and FLT-HPMC complexes as a result of close proximity.

3.3.6 Precipitation inhibition studies

FLT precipitation in the absence and presence of polymers from a concentration of 0.1 mg/mL and 0.05 mg/mL (70:30 w/w) is depicted in Figure 22 and Figure 23. In the absence of polymers, 100% of FLT was present in solution at 10 min with subsequent decline in concentration to 90% (30 min), 43% (120 min) and 4% (300 min). The addition of PVP sustained concentrations of FLT within solution at 100% (10 min), 99% (30 min), 83% (120 min), and 49% (300 min). FLT-HPMC and FLT-EPO exhibited rapid precipitation rates as FLT concentration at 30 min to 120 min decreased from 85% to 29% (0.62 mg/min) and 92% to 60% (0.27 mg/min), respectively. No FLT was present in solution at 300 min for these PMs. In contrast, the initiation of FLT precipitation was prolonged in the presence of PEG. The concentration of FLT precipitation remained at 100% at 30 min with concentrations of 90% and 58% at 120 min and 300 min, respectively. Similar

conclusions were drawn from the precipitation studies involving FLT-polymer 0.05 mg/mL (70:30 w/w). As expected, the ability to maintain FLT concentration in solution was less efficacious in the presence of decreased polymer concentration. PVP maintained 100% of FLT in solution at 30 min, but declined to 76% (120 min) then 0% (300 min). HPMC and EPO sustained high concentrations of FLT for 30 min. The rate of precipitation following this was 0.99 mg/min and 0.94 mg/min in the following 90 min of exposure for HMPC and EPO, respectively. PEG sustained FLT concentration in solution analogous to PVP for 30 min and decreased to 66% (120 min) and 5% (300 min). Based on these observations, the rank order of polymer efficiency to inhibit precipitation and prolong the concentration of FLT in solution is PEG > PVP > EPO > HMPC.

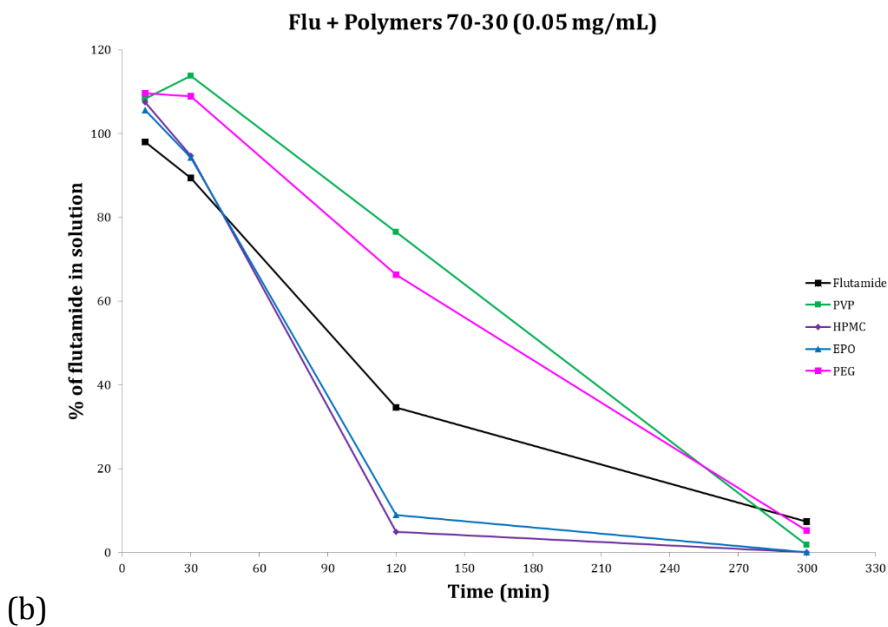
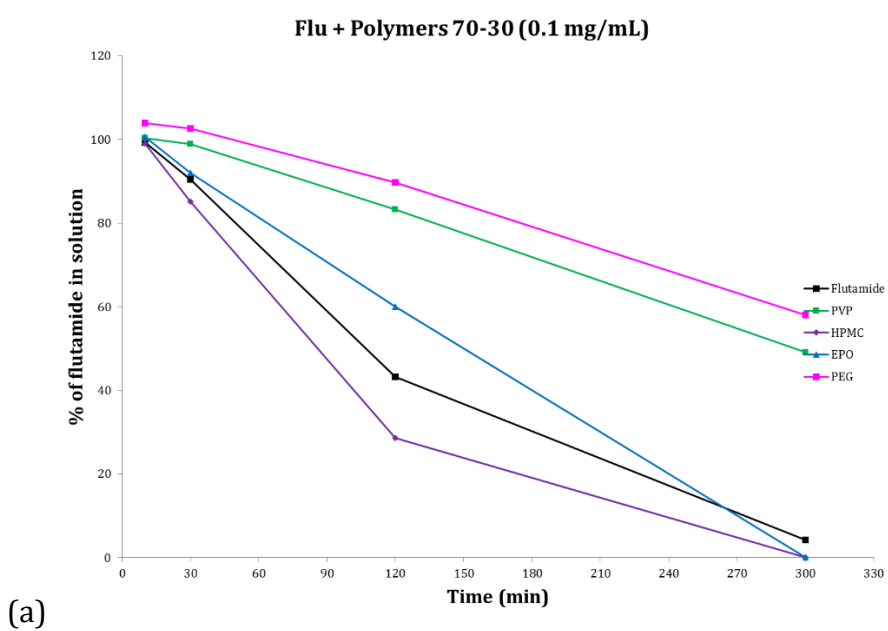


Figure 22. (a) FLT precipitation in absence and presence of various polymers (70:30 w/w) from a concentration of 0.1 mg/ml (a) 0.05 mg/ml(b). The percent of FLT in solution was sustained at higher concentrations in the presence of PVP and PEG.

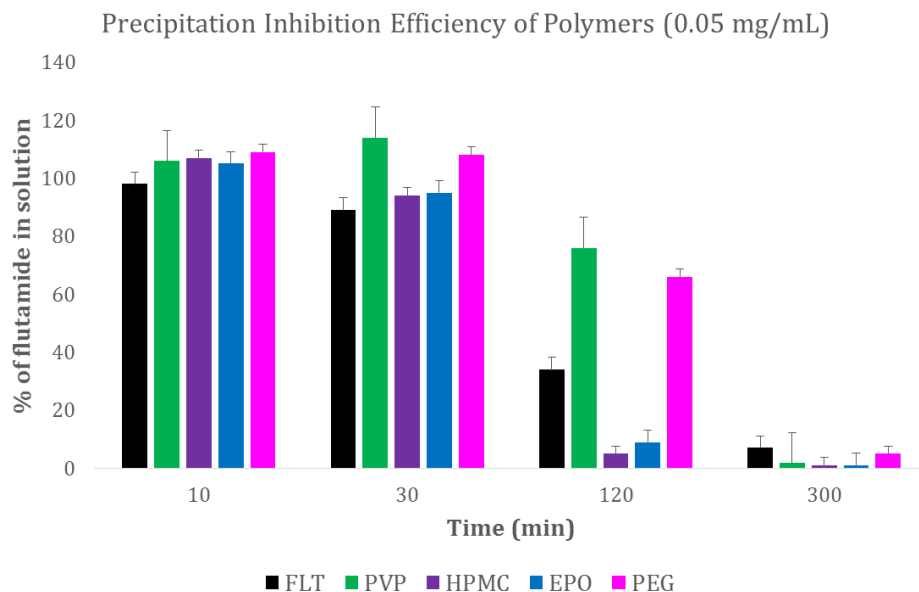
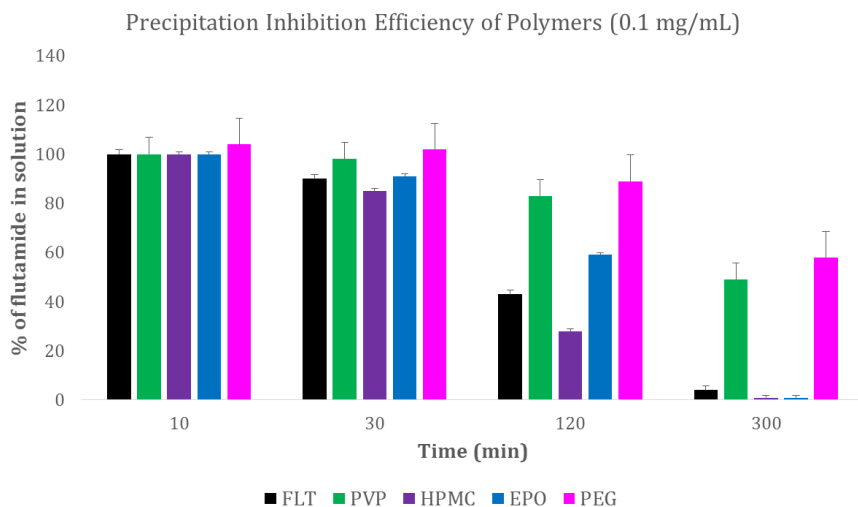


Figure 23. Precipitation inhibition efficiency of polymers. PVP and PEG sustained higher concentrations of FLT in solution in comparison to pure FLT, FLT-HPMC and FLT-EPO.

Molecular interaction between drug and polymer plays a significant role in polymer precipitation inhibition efficiency in solution state (Chauhan et al, 2013).

Chauhan et. al. found that PVP K90 > Eudragit E100 > HMPC were effective precipitation inhibitors and stabilizers of indomethacin (IMC) SDs, which attributed these effects to the type and strength of drug-polymer interactions. Hydrogen bonds formed between PVP K90 or HMPC to IMC resulted in the prevention of drug-drug associations, while the ionic potential of Eudragit E100 was thought to contribute to its precipitation inhibitory efficiency. PEG 8000 was also used, but was considered relatively hydrophobic in comparison to the other polymers studied. Its limited ability to interact with polar functional groups present on IMC favored other reports suggesting the ability of polymer to form interactions with solute. Such interactions would prevent crystallization (Chauhan et al, 2014). Similar importance of molecular interactions on polymer ability to inhibit precipitation was reported in dipyridamole (DPD) SDs (Chauhan et al, 2013).

In this study, it is evident that molecular interactions theorized between FLT and PVP or PEG contribute to successful precipitation inhibition efficiency of these two polymers based on IR and Raman. Molecular modeling studies support this conclusion based on high binding energy calculated for a hydrogen bond between FLT-PVP. However, FLT-PEG had the lowest binding energy suggesting the formation of another type of bond or molecular interaction with minimal steric hindrance given the shortest calculated distance between drug and polymer.

3.3.7 In vitro dissolution studies of FLT SDs

The dissolution profile of pure FLT, PMs and SDs (70:30 w/w) are shown in Figure 24. Pure FLT had the slowest dissolution rate with less than 9% of FLT dissolved within 5 hours. The poor dissolution behavior of FLT can be attributed to

poor wettability, low aqueous solubility, and/or agglomeration (Elkhodairy, 2010; Elkhodairy, 2011). Slight improvement of dissolution rates was observed with FLT PMs as less than 20% of FLT dissolved within the same time frame. In comparison, FLT SDs displayed enhanced dissolution rate and sustained concentration of FLT in solution. Within the first 60 min, the extent of dissolution for FLT-PVP increased from 69% to 95%. High concentrations above 90% were sustained for 2 hours within this system. Though FLT-HPMC and FLT-EPO binary SDs displayed improved dissolution in comparison to PMs, these polymers exerted less of an influence on the dissolution of FLT as only 35-55% of drug dissolved over a 5 hour period. Like PVP, PEG demonstrated a great influence on drug dissolution. The extent of dissolution within the first 60 min of FLT-PEG increased from 60% to 91%. In contrast to PVP, which sustained high concentration of FLT in solution, PEG displayed an initial burst release of drug after 1 hour with sudden decline to 58% at 2 hours. Despite this behavior, the extent of dissolution in the FLT-PEG system exhibited a slight rise to 65% at the end of 5 hours. The rank order of polymer ability to enhance FLT dissolution in prepared SDs is PVP > PEG > HPMC > EPO.

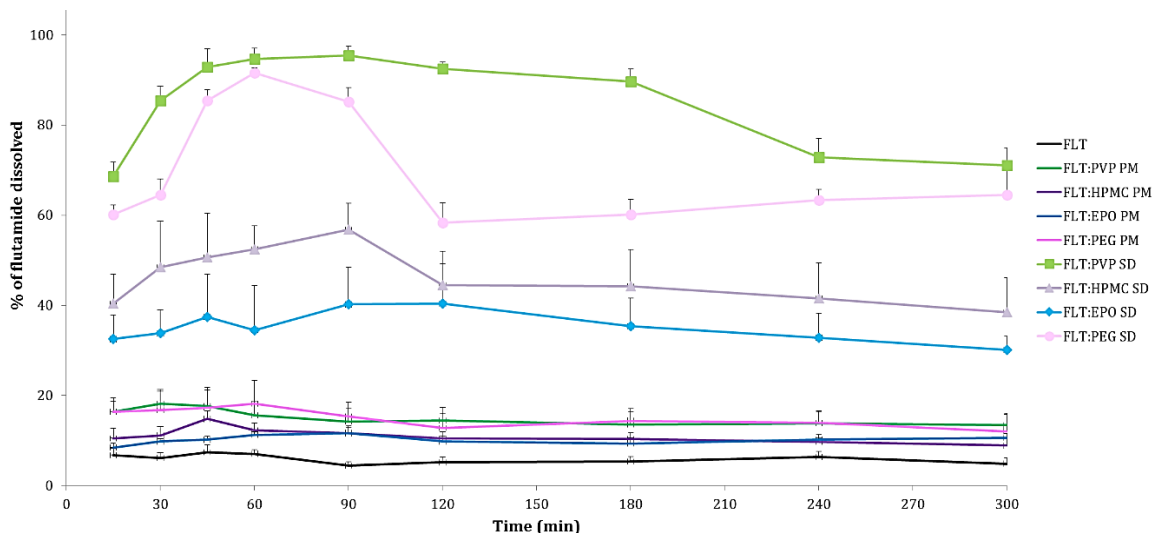


Figure 24. Dissolution profiles of pure FLT, PMs, and SDs (70:30 w/w). FLT SDs showed greater extent of dissolution in comparison to FLT PMs. FLT-PVP SD and FLT-PEG SD exhibited the greatest percent of FLT in solution.

Some of the mechanisms through which SDs can improve the dissolution profile of drugs include particle size reduction, improved wettability, the reduction or absence of crystal structure, and decreased aggregation of drug particles post-introduction of SD system into the dissolution medium (Craig, 2002; Elkhodairy, 2010; Elkhodairy, 2011; Leuner Dressman, 2000; Meng et al, 2015).

These results complimented IR and Raman, which designated the strongest molecular interactions were formed between FLT-PVP and FLT-PEG. The hydrophilic character of these polymers may have also strengthened intermolecular bonds with the aqueous solvent. This solubilizing effect would thus increase the dissolution rate of FLT. A similar conclusion was drawn in a study conducted by Gines and colleagues, which studied the effects of mannitol on triameterene

dissolution profile. Mannitol was found to form hydrogen bonds with water increasing the dissolution of the hydrophobic drug (Gines, 1993). Moreover, the transition of FLT to the amorphous state was achieved in the presence of PVP and PEG as previously characterized by pXRD and thermal analysis implying improved dissolution in the absence of a crystalline lattice. Thus, no energy is required to promote dissolution (Vasconcelos et al, 2007).

3.8 Conclusions

Our study evaluated the efficiency of chemically diverse polymers on the improvement of the physicochemical properties of an anticancer drug, FLT, in order to successfully formulate stable amorphous dispersions. PMs of various drug to polymer ratios identified FLT miscibility in PEG and EPO. These polymers had a melting temperature and glass transition temperature below that of FLT potentially altering the environment or forming complexes in which the insoluble drug could be molecularly dispersed. Subsequent studies identified PVP and PEG to prolong precipitation of FLT, which was significant for use in the formulation of SDs. Characterization of the amorphous dispersions using MDSC and pXRD concluded that FLT transformed from crystalline to amorphous form in the presence of PVP and PEG. Furthermore, high binding energies associated with FLT and PVP showed the strong correlation between binding strength and dispersion stability *in silico*. Amorphous dispersions formulated with PVP and PEG were more stable and thus, more water soluble, an important property necessary to improve the physicochemical properties and drug delivery of FLT.

3.9 References

- Aggarwal, B. B., & Harikumar, K. B. (2009). Potential therapeutic effects of curcumin, the anti-inflammatory agent, against neurodegenerative, cardiovascular, pulmonary, metabolic, autoimmune and neoplastic diseases. *The International Journal of Biochemistry & Cell Biology*, 41(1), 40-59.
- Archer, W.L . (1992). Hansen Solubility Parameters for Selected Cellulose Ether Derivatives and Their Use in the Pharmaceutical Industry. *Drug Development and Industrial Pharmacy*, 18, 599-616.
- Baird, J. A., & Taylor, L. S. (2012). Evaluation of amorphous solid dispersion properties using thermal analysis techniques. *Advanced Drug Delivery Reviews*, 64(5), 396-421.
- Caraballo, M. A. (2002). Stability study of flutamide in solid state and in aqueous solution. *Drug Development and Industrial Pharmacy*, 28(4), 413-422.
- Chauhan, H., Hui-Gu, C., & Atef, E. (2013). Correlating the behavior of polymers in solution as precipitation inhibitor to its amorphous stabilization ability in solid dispersions. *Journal of Pharmaceutical Sciences*, 102(6), 1924-1935.
- Chauhan, H., Kuldipkumar, A., Barder, T., Medek, A., Gu, C., & Atef, E. (2014). Correlation of inhibitory effects of polymers on indomethacin precipitation in solution and amorphous solid crystallization based on molecular interaction. *Pharmaceutical Research*, 31(2), 500-515.
- Chen, Y., Zhang, G. G. Z., Neilly, J., Marsh, K., Mawhinney, D., & Sanzgiri, Y. D. (2004). Enhancing the bioavailability of ABT-963 using solid dispersion containing pluronic F-68. *International Journal of Pharmaceutics*, 286(1-2), 69-80.
- Craig, D. Q. M. (2002). The mechanisms of drug release from solid dispersions in water-soluble polymers. *International Journal of Pharmaceutics*, 231(2), 131-144.
- Elkhodairy, E. N. (2010). Lyophilization monophasic solution technique for improvement of the physicochemical properties of an anticancer drug, flutamide. *European Journal of Pharmaceutics and Biopharmaceutics: Official Journal of Arbeitsgemeinschaft Für Pharmazeutische Verfahrenstechnik E.V*, 74(2), 397-405.
- Elkhodairy, E. N. (2011). Lyophilization monophasic solution technique for preparation of amorphous flutamide dispersions. *Drug Development and Industrial Pharmacy*, 37(7), 754-764.
- Elkhodairy, E. N. (2011). Lyophilized flutamide dispersions with polyols and amino acids: Preparation and in vitro evaluation. *Drug Development and Industrial Pharmacy*, 37(4), 446-455.

Elzoghby, A. O., Helmy, M. W., Samy, W. M., & Elgindy, N. A. (2013). Spray-dried casein-based micelles as a vehicle for solubilization and controlled delivery of flutamide: Formulation, characterization, and in vivo pharmacokinetics. *European Journal of Pharmaceutics and Biopharmaceutics*, 84(3), 487-496.

Ghebremeskel, A. N., Vemavarapu, C., & Lodaya, M. (2007). Use of surfactants as plasticizers in preparing solid dispersions of poorly soluble API: Selection of polymer-surfactant combinations using solubility parameters and testing the processability. *International Journal of Pharmaceutics*, 328(2), 119-129.

Gines, J.M., Arias, M.J., Rabasco, A.M. (1993). Elaboration and dissolution study of solid dispersions triamterene-D-mannitol. Summary of presentations. *Congressus Pharmaceutics Hungaricus IX*, 85, 19-22.

Greenhalgh, D. J., Williams, A. C., Timmins, P., & York, P. (1999). Solubility parameters as predictors of miscibility in solid dispersions. *Journal of Pharmaceutical Sciences*, 88(11), 1182-1190.

Gupta J, Nunes C, Vyas S, Jonnalagadda S 2011. Prediction of solubility parameters and miscibility of pharmaceutical compounds by molecular dynamics simulations. *The Journal of Physical Chemistry B* 115:2014-2023.

Ivanisevic I, Bates S, Chen P 2009. Novel Methods for the Assessment of Miscibility of Amorphous Drug-Polymer Dispersions. *Journal of Pharmaceutical Sciences* 98(9):3373-3386.

Jones, D. (2004). *Pharmaceutical applications of polymers for drug delivery* (Volume 15, Number 6 ed.). Shrewsbury, GBR: Smithers Rapra.

Kaminski, G. A.; Maple, J. R.; Murphy, R. B.; Braden, D. A.; Friesner, R. A. Pseudospectral Local Second-Order Møller-Plesset Methods for Computation of Hydrogen Bonding Energies of Molecular Pair. *J. Chem.*

Katila, P. J. (2000). Dissolution rate limited bioavailability of flutamide, and in vitro - in vivo correlation. *European Journal of Pharmaceutics and Biopharmaceutics: Official Journal of Arbeitsgemeinschaft Für Pharmazeutische Verfahrenstechnik E.V*, 49(1), 35-39.

Kolašinac N, Kachrimanis K, Homšek I, Grujić B, .urić Z, & Ibrić, S. (2012). Solubility enhancement of desloratadine by solid dispersion in poloxamers. *International Journal of Pharmaceutics*, 436(1-2), 161-170.

Leuner, C., & Dressman, J. (2000). Improving drug solubility for oral delivery using solid dispersions. *European Journal of Pharmaceutics and Biopharmaceutics*, 50(1), 47-60.

Lodge TP, Wood ER, Haley JC, 2005. Two Calorimetric Glass Transitions Do Not Necessarily Indicate Immiscibility: The Case of PEO/PMMA. *Journal of Polymer Science* 44:756-763.

Mariappan, G., & Sundaraganesan, N. (2014). Spectral and structural studies of the anti-cancer drug flutamide by density functional theoretical method. *Spectrochimica Acta Part A: Molecular and Biomolecular Spectroscopy*, 117(0), 604-613.

Marsac, P., Shamblin, S., & Taylor, L. (2006). Theoretical and practical approaches for prediction of Drug Polymer miscibility and solubility. *Pharmaceutical Research*, 23(10), 2417-2426.

Meng, F., Trivino, A., Prasad, D., & Chauhan, H. (2015). Investigation and correlation of drug polymer miscibility and molecular interactions by various approaches for the preparation of amorphous solid dispersions. *European Journal of Pharmaceutical Sciences*, 71(0), 12-24.

Millqvist, D. C. (2010). Polymer-drug interactions and wetting of solid dispersions. *European Journal of Pharmaceutical Sciences: Official Journal of the European Federation for Pharmaceutical Sciences*, 39(1-3), 125-133.

Newman A, Engers D, Bates S, Ivanisevic I, Kelly RC 2008. Characterization of Amorphous API: Polymer Mixtures Using X-ray Powder Diffraction. *Journal of Pharmaceutical Sciences* 97 (11):4840-56.

Papadimitriou, S. A., Barmpalexis, P., Karavas, E., & Bikiaris, D. N. (2012). Optimizing the ability of PVP/PEG mixtures to be used as appropriate carriers for the preparation of drug solid dispersions by melt mixing technique using artificial neural networks: I. *European Journal of Pharmaceutics and Biopharmaceutics*, 82(1), 175-186.

Rumondor ACF, Ivanisevic I, Bates S, Alonzo DE, Taylor LS 2009. Evaluation of Drug-Polymer Miscibility in Amorphous Solid Dispersion Systems. *Pharmaceutical Research* 26:2523-2534.

Sarmiento, V. T. (2007). Solid dispersions as strategy to improve oral bioavailability of poor water soluble drugs. *Drug Discovery Today*, 12(23-24), 1068-1075.

STAT!Ref, & Teton Data Systems. (2012). *AHFS drug information 2012*. Bethesda, MD: American Society of Health-System Pharmacists.

Taskinen, P. K. (2010). Predicting the formation and stability of amorphous small molecule binary mixtures from computationally determined flory-huggins interaction parameter and phase diagram. *Molecular Pharmaceutics*, 7(3), 795-804.

Trasi, N. S., & Taylor, L. S. (2012). Effect of additives on crystal growth and nucleation of amorphous flutamide. *Crystal Growth & Design*, 12(6), 3221-3230.

Van Krevelen, D.W. (1990). Properties of polymers. Amsterdam: Elsevier 189-225.

Vasconcelos, T., Sarmiento, B., & Costa, P. (2007). Solid dispersions as strategy to improve oral bioavailability of poor water soluble drugs. *Drug Discovery Today*, 12(23-24), 1068-1075.

Verma, A., Singh, M. K., & Kumar, B. (2011). Development and characterization of flutamide containing self-microemulsifying drug delivery system (smedds). *International Journal of Pharmacy & Pharmaceutical Sciences*, 3, 60-65.

Williams, P. J. (2004). Solid-state solubility influences encapsulation and release of hydrophobic drugs from PLGA/PLA nanoparticles. *Journal of Pharmaceutical Sciences*, 93(7), 1804-1814.

CHAPTER 4

Preparation and characterization of flutamide solid lipid nanoparticles

The purpose of this research is to study the correlation between miscibility of drug, lipids and surfactant on the particle size of SLNs. Solid lipid mixtures of lipids namely glyceryl monooleate (GMO), Precirol® (glyceryl palmitostearate, PRE), glyceryl monostearate (GMS) and Compritol® (glyceryl dibehenate, COM) were prepared with Gelucire® (stearoyl polyoxyl-32 glycerides, GEL) 50/13 as surfactant. Also, PMs of FLT and lipids/surfactant were prepared in a similar manner. These PMs were prepared in 5:2 w/w ratio (lipid:surfactant) and 2:1 w/w (FLT:lipids/surfactants) respectively by co-melting them at controlled temperature. Miscibility studies of drug, lipids and surfactant PMs were investigated using modulated differential scanning calorimetry in a temperature range of -40°C to 125°C at a ramp rate of 2°C/min. SLNs with and without drug loading were prepared by ultrasonication method and characterized for particle size analysis. Further, drug loaded nanoparticles were lyophilized and characterized by particle size.

MDSC experiments showed that GMO, PRE, GMS and COM melted at around 22°C, 54°C, 59°C and 71°C, respectively. These lipids showed exothermic crystallization peak at -13°C, 52°C, 56°C and 71°C, respectively. Melting of FLT and GEL 50/13 were observed at 115°C and 60°C, respectively. Physical mixture of GMO-GEL 50/13 showed decrease in the melting temperature to 35°C. Similarly, decreases in melting and crystallization temperature of GEL were observed with GMS and PRE. In case of COM-GEL 50/13 physical mixture, individual melting and crystallization peak were observed indicating immiscibility. Similarly, MDSC data suggests good miscibility of FLT in GMO, GMS and GEL. The particle size of SLNs

prepared from GMO and GMS with GEL 50/13 was found to be 70.2 ± 5.4 and 92.6 ± 8.5 compared to >200 nm particles obtained from PRE and COM. No increase in particle size was observed with GMO whereas increase in particles size was observed with COM on lyophilization.

Good correlation between drug, lipids and surfactants miscibility and particle size of SLNs was observed.

4.1 Introduction

Many new chemical entities (NCE) are poorly water soluble posing a challenge for the pharmaceutical industry to develop therapeutically efficacious solid dosage forms. Oral drug delivery is of high interest due to ease and convenience of administration, reduced health care resources, decreased frequency of hospital or clinic visits, and improved patient quality of life. Though the oral route has been the preferred method of treatment for various chronic disease states, further development of 40% of NCEs are limited due to low aqueous solubility (Verma et al, 2011). Issues that arise as a result of poor solubility include poor and variable bioavailability, high intra and inter subject variability, and lack of dose proportionality (Jeevana Sreelakshmi, 2011; Verma et al, 2011).

To overcome these challenges, other drug delivery formulations have been utilized. One such strategy is the development of SLNs. SLNs are a type of drug carrier system formulated as submicron-sized lipid emulsions composed of a solid lipid and emulsifier (surfactant). Advantages of SLNs include the possibility of controlled drug release and drug targeting, physical stability, ease of large-scale production, protection of labile drugs from degradation, low toxicity due to avoidance of organic

solvents, and high drug load (Jabir et al, 2012; Sultana et al, 2013). Improved bioavailability of the encapsulated drug can be explained by these properties offered by SLNs and thus is an important formulation study for hydrophobic drugs (Licciardi et al, 2012).

FLT (2-Methyl-*N*-[4-nitro-3-(trifluoromethyl)phenyl]-propanamide) is classified as an acetanilide, nonsteroidal drug used in the treatment of prostate cancer (Murthy Umrethia, 2004). FLT inhibits the uptake and or binding of dihydrotestosterone to target cell receptors exhibiting its antiandrogenic activity (Verma et al, 2011). Poor oral bioavailability of this anticancer agent can be attributed to low aqueous solubility, high hydrophobicity, poor wettability and permeability along with rapid first pass hepatic metabolism (Jeevana Sreelakshmi, 2011). Hence, FLT was selected as the model drug for this study.

The main objective of this study was to develop optimal SLNs through selection of miscible drug-lipid-emulsifier tertiary systems and analysis of particle size and stability of these formulations of FLT. Four lipids, GMO, PRE, GMS and COM along with two surfactants, GEL 44/14 and GEL 50/13 were used in various combinations for the preparation of FLT SLNs. Thus, this study proposed to formulate SLNs of FLT to enhance oral bioavailability by correlating the effects of particle size to improved therapeutic outcomes.

4.2 Materials and Methods

4.2.1 Materials

FLT was purchased from TGI America (Portland, Oregon). GEL 44/14 and 50/13 along with COM 888 ATO, and PRE ATO 5 were purchased from Gattefosse

(St. Priest, France). The two other lipids used, glyceryl monostearate (GMS) and glyceryl monooleate (GMO) were purchased from Spectrum Chemical Mfg. Corp (Gardena, CA).

4.2.2 Preparation of lipids and surfactants physical mixtures

PMs were prepared in 5:2 w/w ratio (lipid:surfactant). Accurately weighed quantity of the surfactant and solid lipid was placed in a glass vial. This mixture was heated to 90°C for all PMs, except for COM PM which was heated to 125°C and maintained at this the temperature until both the components melted completely. Homogenization of this mixture was performed with aid of stirbar. The solution was cooled to room temperature. All PMs were stored at room temperature in screw-capped vials until use.

4.2.3 Modulated differential scanning calorimetry (MDSC)

Modulated differential scanning calorimetry was performed by DSC Q2000 (TA Instruments, New Castle, DE). The equipment was calibrated with Indium. Inert atmosphere was maintained by nitrogen flow rate of 40 mL/min. An empty aluminum pan was used as a reference. Samples in MDSC were modulated at a ramp rate of 2°C/min. Thermal behavior of pure lipids and surfactants, PMs, and drug-loaded PMs were characterized by a series of heating and cooling cycles. Samples were heated from room temperature to 90°C (Cycle 1), cooled from 90°C down to -40°C (Cycle 2), and then reheated to 90°C (Cycle 3).

4.2.4 Preparation of nanoparticles

Nanoparticles were prepared using 500 mg of lipid (GMO, PRE, GMS, COM) and 200 mg of surfactant (GEL 50/13). Accurately weighed lipid and surfactant

were placed in a screw-capped vial and heated to 90°C until melted. To ensure complete melting of Compitrol, the temperature was increased to 125°C. As this mixture was heated, distilled water was placed into a separate beaker and heated to 90°C and 125°C, respectively. Addition of water to the lipid-surfactant mixture was carried out at a similar temperature to prevent recrystallization of both components. A stir bar was added to the screw-capped vial to help create a homogeneous mixture and stirred at 300 rpm. Once melted, 20 mg of FLT was added to the lipid and surfactant. Clarity of the mixture was ensured before proceeding. With the vial still on the hot plate, 10 mL of the heated, distilled water was added dropwise to the vial loaded with drug to create a primary emulsion. Ultrasonication of the primary emulsion was performed using the Sonicator 3000 (Misonix, Farmingdale, New York) at 18W with an output setting of 4.0 for 5 minutes to create a secondary emulsion. This method was performed in triplicate.

4.2.5 Characterization of nanoparticles

4.2.5.1 Particle size

Particle size of the prepared secondary emulsions were obtained to characterize the FLT nanoparticles. Data was acquired from a ZetaPlus, Zeta Potential Analyzer (Brookhaven Instruments Corp., Holtsville, New York). To attain these values, 10 µL of the secondary emulsion was placed in a test tube and diluted with 10 mL of water. The test tube was placed on a Genie 2 vortex (Fisher Scientific, Hampton, New Hampshire) to ensure homogenous mixing. The test tube containing the sample was then sonicated for 5 minutes using a Sonicator FS60 (Fisher Scientific, Hampton, New Hampshire).

4.2.5.2 Raman spectroscopy

Raman spectra were obtained using Bruker Vertex series 80 V Raman spectrometer and data processing was performed using OPUS software (Billerica, MA). Data acquisition was done using an exposure time of 10 seconds for 10 accumulations and a laser power setting of 400 mW. Raman spectroscopy was used for characterization of precipitate and to explore the drug polymer interactions in various mixtures

4.2.6 Stability studies

To study the stability of the prepared nanoparticles, particle size of the secondary emulsions were obtained on the day of preparation and 14 days after preparation. Secondary emulsions containing GMS formed a gel-like consistency upon cooling. GMS emulsions were reheated at 90°C to liquefy the mixture. The samples were prepared in a test tube with 10 µL of the secondary emulsion and 10 mL of water. The samples were mixed on a Genie 2 vortex (Fisher Scientific, Hampton, New Hampshire) and sonicated for 5 minutes using a Sonicator FS60 (Fisher Scientific, Hampton, New Hampshire). Particle size was obtained using the ZetaPlus, Zeta Potential Analyzer (Brookhaven Instruments Corp., Holtsville, New York).

4.3 Results

4.3.1 Physicochemical properties of flutamide, lipids, and surfactants

Table 8. Physicochemical properties of FLT, lipids, and surfactants

		Molecular weight (g/mol)	Melting temperature (°C)	Crystallization temperature (°C)
Drug	FLT	276.2	113	-
Lipids	GMO	356.54	14, 22	-13
	PRE	633	50-55	54
	GMS	358.57	58-60	56
	COM	1059.8	68-72	71
Surfactant	GEL 44/14	-	44	26
	GEL 50/13	-	50	26, 43

Data obtained from Elkhodairy, 2011; Rowe, 2009

Table 8 lists the physicochemical properties of FLT, lipids, and surfactants used in the study. FLT is a poorly water soluble anticancer drug with a molecular weight of 272.2 g/mol and characteristic melting temperature of 113°C. The extent of changes observed in melting temperature of pure FLT in comparison to FLT prepared SLN signified miscibility of these ternary complexes and potential improved performance of SLN as discussed in thermal analysis.

Formulation of SLN required the use of solid lipids, which included GMO, PRE, GMS, and COM. These lipids were selected due to the variation in molecular weight, melting and crystallization temperatures along with their common use in the pharmaceutical industry. GMO is a polar lipid used as an emulsifying agent and stabilizer, gelling agent, and surfactant (Rowe, 2009). PRE is classified as an oral formulation diluent and lubricant, coating and gelling agent. The effect of PRE on drug release rates is dependent upon concentration; the lower the concentration of

PRE in the formulation, the faster the release rate (Rowe, 2009). GMS is an emulsifier, solubilizer, stabilizer and lubricant. COM has the largest molecular weight of all the lipids used in the study with the least difference in melting temperature when compared to FLT. COM is amphiphilic and its high melting temperature is a desirable property for its use in colloidal dispersions, such as SLN. COM is used as a tablet binder, lubricant, and coating agent (Rowe, 2009). The rank order of increasing lipid molecular weight is as follows $GMO < GMS < PRE < COM$. The rank order of melting temperature difference compared to FLT is $COM < GMS < PRE < GMO$.

GEL 44/14 and 50/13 were used as surfactants in the formulation of SLN composed of triglycerides containing lauric acid (12-carbon chain) and stearic acid (18-carbon chain), respectively. As polyoxyglycerides, GEL 44/14 and 50/13 are used as dissolution enhancers, self-emulsifying and solubilizing agents for oral formulations (Rowe, 2009). Aside from their differences in structure, the other variances are defined by their name. The first value designates melting temperature, while the second value is the hydrophilic lipophilic balance (HLB) of a surfactant. The HLB values of the selected GEL correspond to more hydrophilic character associated with detergents and oil in water emulsifiers (Sinko, 2011). These higher HLB surfactants are composed of partial saturated glycerides and PEG esters (Bandari et al, 2014).

4.3.2 Thermal analysis

4.3.2.1 DSC for pure lipids and surfactants

MDSC of pure lipids, surfactants and their PMs were carried out to determine the miscibility between lipids and surfactants. Figure 25 compares the DSC thermograms of pure lipids, surfactants and PMs. MDSC experiments showed that GMO, PRE, GMS and COM melted at around 22°C, 54°C, 59°C and 71°C, respectively. These lipids showed exothermic crystallization peak at -13°C (GMO), 52°C (PRE), 56°C (GMS) and 71°C (COM). Similar melting of GEL 44/14 and GEL 50/13 was observed at 43°C with crystallization peaks at 22 and 25°C, respectively. Furthermore, GEL 50/13 showed an additional crystallization exotherm at 43°C not seen in GEL 44/14.

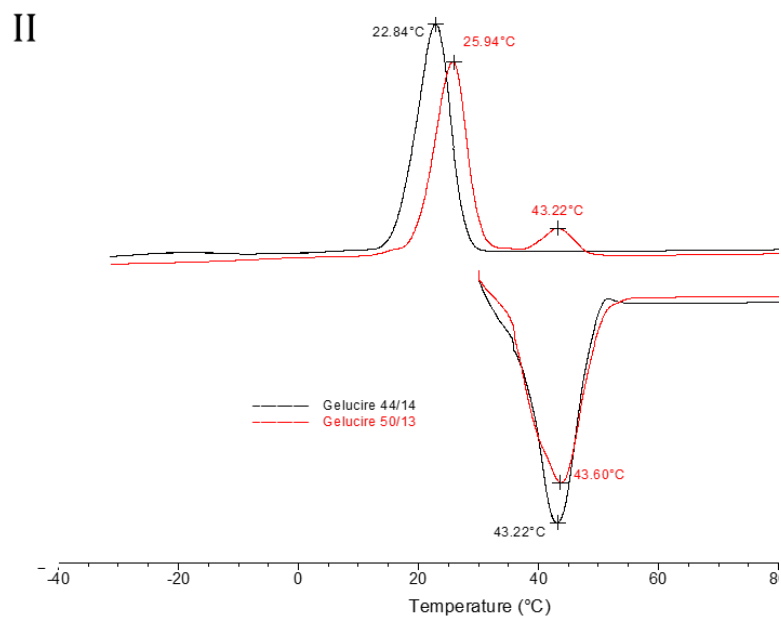
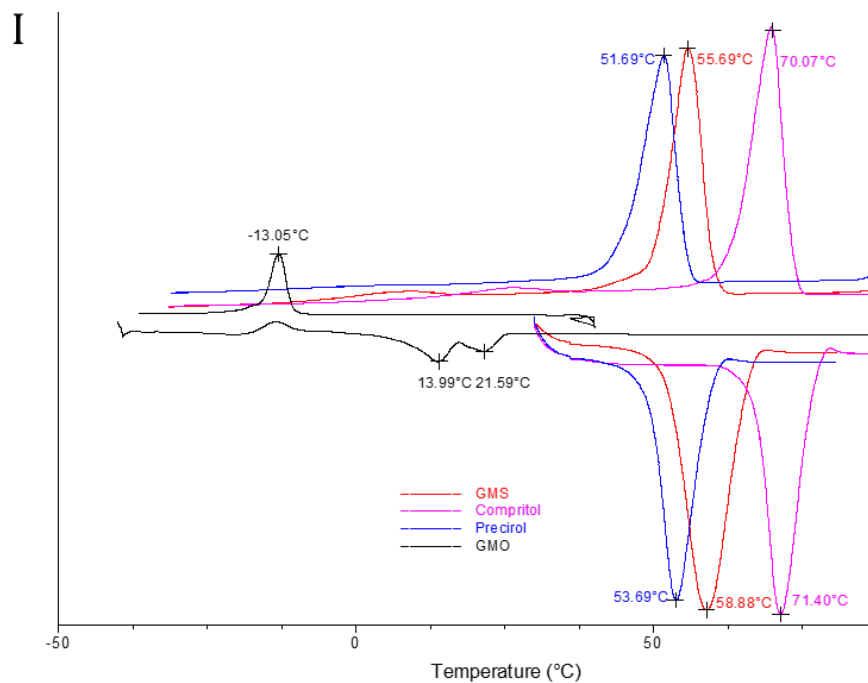


Figure 25. MDSC thermograms of pure lipids (I) pure surfactants (II). Characteristic melting endotherms and crystallization exotherms of these individual materials are observed in respective thermograms.

4.3.2.2 Miscibility of lipids with surfactants (GEL 44/14, 50/13)

MDSC thermograms of lipid-surfactant PMs shown in Figure 26 were assessed for subsequent changes to assess miscibility of these components. Physical mixture of GMO-GEL 44/14 and GMO-GEL 50/13 exhibited a decrease in the characteristic endotherm of GMO from 22°C to 20°C in the presence of GEL 44/14, but an increase from 22°C to 28°C was seen in the GEL 50/13 PM. GMO-GEL PMs showed decrease in the melting temperature of both the GELs from 43°C to 35°C. No crystallization peak was seen in case of GMO-GEL 44/14 PM, while the absence of one characteristic exotherm at 43°C of GEL 50/13 was observed in GMO-GEL 50/13 indicating miscibility of GMO and GELs. Minimal decreases in melting and crystallization temperature of PRE and GELs were seen in PRE-GEL PMs; although multiple endothermic peaks were observed in the case of PRE. PRE-GEL 50/13 displayed an additional endotherm and exotherm at 38°C and 18°C, respectively, which was not characteristic of either lipid or surfactant. A second exotherm was also seen in the PRE-GEL 44/14 PM at 11°C. Miscibility between PRE and GELs was considered less favorable than GMO. In the case of GMS-GEL, similar decreases in melting and crystallization temperature of both lipid and surfactant were observed. Melting endotherms of GMS in the presence of GEL 44/14 and GEL 50/13 were seen at 54°C and 55°C, respectively. Both endothermic peaks of surfactant were present at lower temperatures at 36°C (GEL 44/14) and 41°C (GEL 50/13). The absence of GEL crystallization peaks along with a decrease in the exothermic peaks of GMS in GMS-GEL PMs indicate good miscibility between GMS and GELs. In contrast, COM-GEL PMs displayed separate melting and crystallization peaks signifying

immiscibility of these two components. Thermal data indicates good miscibility between GMO and GMS with GEL. Thus, the rank order of lipid miscibility with GEL is GMO, GEL > PRE > COM.

Initial miscibility studies assessing lipid-surfactant PMs prepared were prepared with GEL 44/14 and GEL 50/13. Since both GEL have similar physiochemical properties, further miscibility studies with FLT were prepared with GEL 50/13.

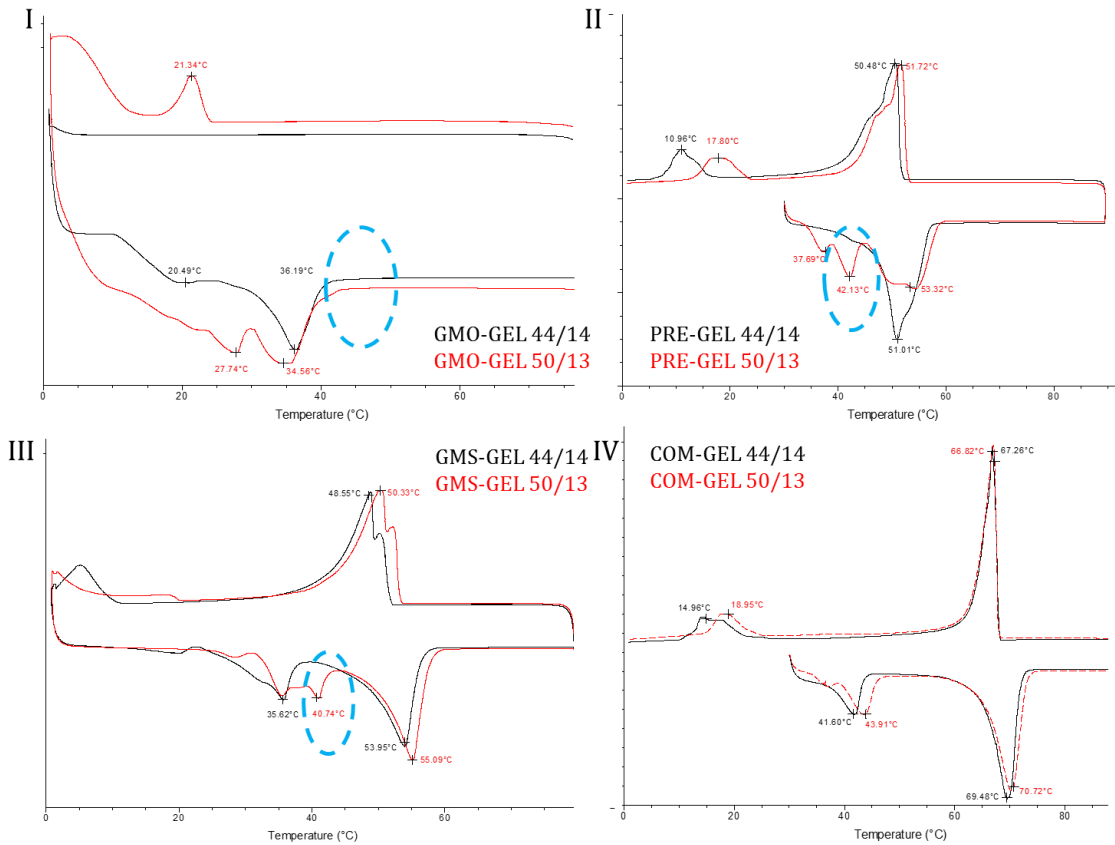


Figure 26. MDSC thermograms of physical mixtures: GMO and GELs (I) PRE and GELs (II) GMS and GELs (III) COM and GELs (IV). The absence of GMO and GMS crystallization peaks and presence of melting endotherms at lower temperatures indicated good miscibility between GMO-GEL and GMS-GEL.

4.3.2.3 Miscibility study of FLT with lipids and surfactant (GEL 50/13)

Figure 27 depicts the DSC thermograms of FLT-loaded lipids and surfactant (GEL 50/13). Pure FLT has a characteristic sharp, melting endotherm at 113°C. The absence of this peak in the presence of GMS, GMO, or GEL is indicative of the conversion of FLT from the crystalline to amorphous state and miscibility between drug and lipid or surfactant. Moreover, these observations correlate well with the MDSC results obtained from analysis of PMs as GMO and GMS were determined to be miscible with GEL. Miscibility of FLT within these systems suggests successful formulation of FLT SLNs. In contrast, reduced FLT crystallinity is observed in the FLT-PRE and FLT-COM systems evidenced by the near disappearance and broadening of the characteristic FLT endotherm. PRE appears to reduce drug crystallinity to a greater extent than COM. These results are in agreement with thermal analysis of PRE and COM PMs. Overall, the rank order of lipid ability to reduce FLT crystallinity is GMO, GMS > PRE > COM.

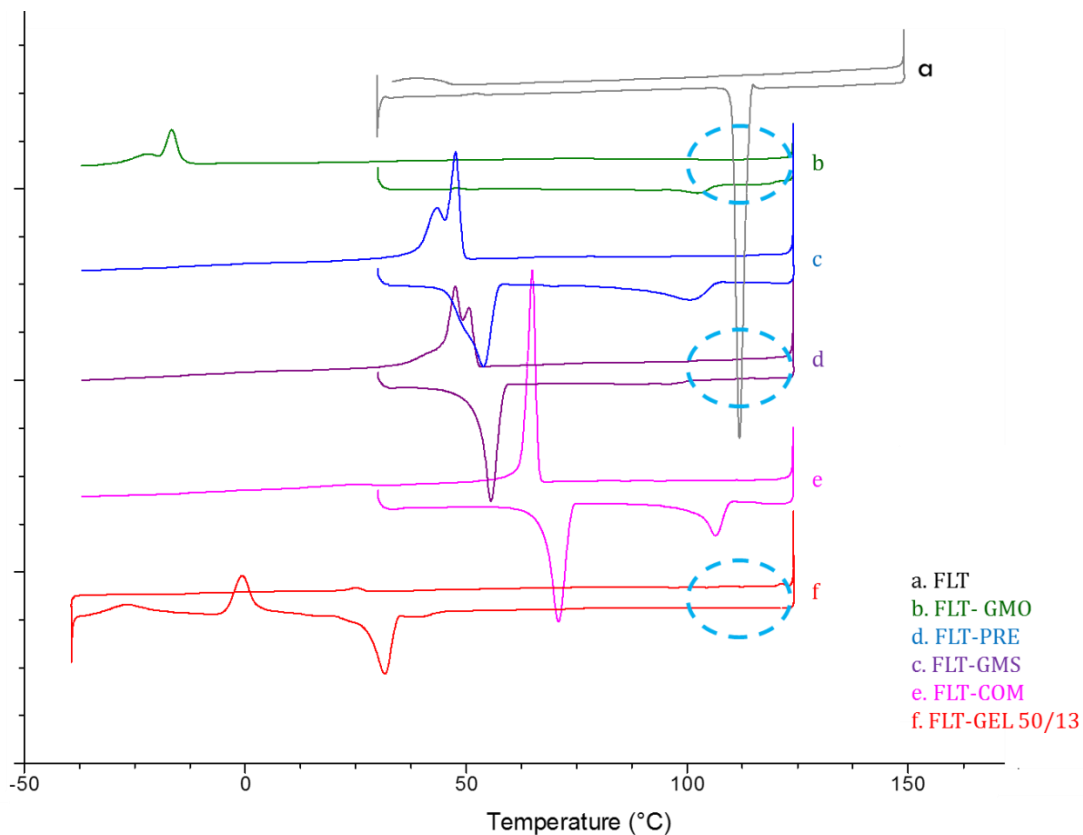


Figure 27. MDSC thermograms of pure FLT (a) FLT-GMO (b) FLT-PRE (c) FLT-GMS (d) FLT-COM (e) FLT-GEL 50/13. The absence of the characteristic melting peak of FLT is observed in the presence of GMO, GMS, and GEL 50/13 indicating miscibility of FLT with these lipids and surfactant.

4.3.3 Particle size analysis

4.3.3.1 Unloaded solid lipid nanoparticles

Figure 28 depicts the particle size of unloaded SLNs. The particle size of prepared GMO and GMS nanoparticles with GEL 50/13 was found to be 70.2 ± 5.4 and 92.6 ± 8.5 compared to >200 nm particles obtained from PRE and COM. The reduced particle size observed in GMO and GMS SLNs correlates well with the

results obtained from miscibility studies of lipid and surfactant PMs as GMO and GMS were found to be miscible in the presence of GEL. Miscible compounds were thus expected to incorporate FLT, maintain small particle size and stability.

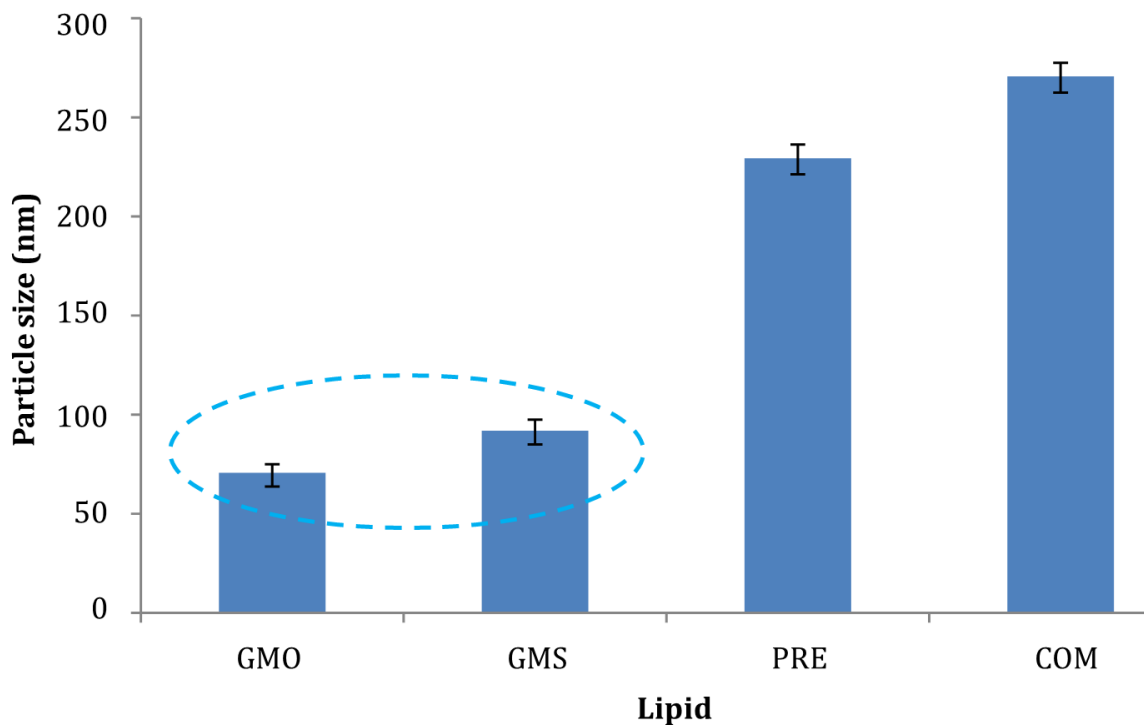


Figure 28. Particle size of unloaded SLNs. The resultant particle size of GMO and GMS prepared SLN was lower than PRE and COM.

4.3.3.2 Drug loaded solid lipid nanoparticles

Figure 29 shows the particle size of loaded SLNs. SLNs containing FLT (Day 1) displayed similar particle size trends compared to the unloaded SLNs. GMO and GMS prepared SLNs had smaller particle size compared to PRE and COM. The rank order of increasing particle size for FLT loaded SLNs was found to be $GMO < GMS < COM < PRE$.

Miscibility of lipid and surfactant PMs showed promising results in terms of preparing optimal SLNs. GMO-GEL and GMS-GEL PMs were able to create a favorable matrix for encapsulation of FLT. With a reduction of particle size there is an increase in surface area around each nanoparticle; consequently, the extent of dissolution is expected to increase along with bioavailability of the drug.

4.3.4 Raman spectroscopy of lipids and surfactants

Raman spectroscopy was obtained for PRE, COM, GELs and their PMs as seen in Figure 26. Three characteristic peaks of PRE are seen at 1459, 1438, and 1102 cm^{-1} . These respective peaks are shifted to higher wavenumbers at 1464, 1440, and 1103 cm^{-1} when mixed with GEL 44/14, but remain unchanged in the presence of GEL 50/13. Miscibility studies of PRE with GELs displayed an additional endotherm or exotherm not associated with pure PRE or GEL. This may be indicative of complex formation between lipid and surfactant and thus potential interaction may be possible. Minor peak shifts seen in PRE-GEL 44/14 spectra correlated well with the notion that interactions may have formed. This minimal change or lack of change as observed with PRE and GEL 50/13 were in agreement with the results obtained from miscibility studies. Miscibility of GELs with PRE was considered less favorable in comparison to GMO and GMS.

The Raman spectrum of pure COM had several characteristic peaks located at 1460, 1439, 1130, and 1062 cm^{-1} . These peaks remained unchanged in the presence of both GELs. This suggested the lack of potential interactions formed between lipid and surfactant. These results correlated well with miscibility studies, which showed that COM was immiscible with GEL 44/14 and GEL 50/13.

Further studies to obtain the Raman spectra of pure GMO, GMS, GELs and their PMs would significantly contribute the conclusions of this research.

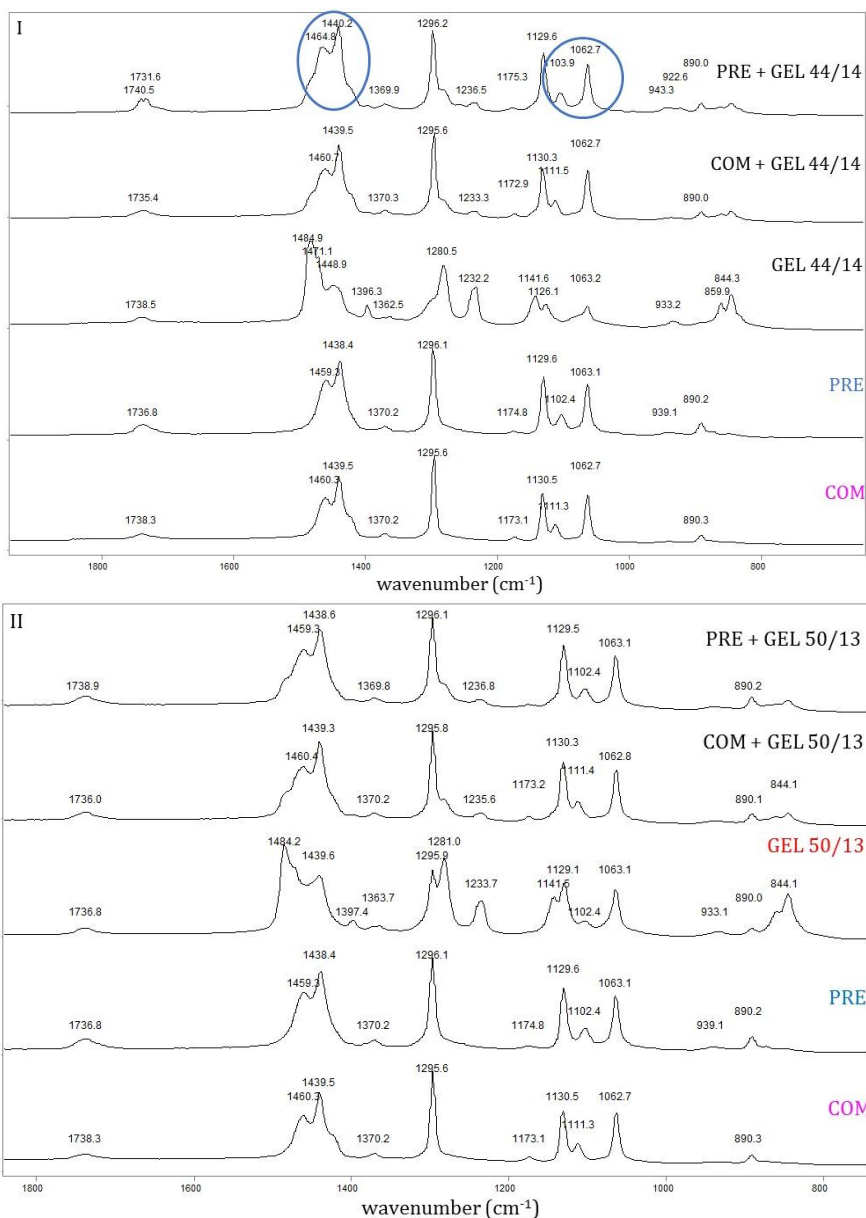


Figure 29. Raman spectra of pure lipids, surfactants and PMs. No peak changes observed in COM with GELs indicated no potential interactions formed between these compounds. Minimal changes were seen in the characteristic peaks of PRE with GEL 44/14 indicating the potential for interactions.

4.3.5 Stability studies of drug loaded solid lipid nanoparticles

Particle size of the prepared drug loaded SLNs was obtained on the Day 1 after preparation and subsequently on Day 14 as seen in Figure 30. No increase in particle size after two weeks was observed with GMO and GMS SLNs. A more prominent increase in particle size after two weeks was observed in PRE and COM SLNs. It was determined that FLT SLNs prepared with GMO and GMS were more stable compared to FLT SLNs prepared with PRE and COM due to miscibility and ability of the former lipids to reduce FLT crystallinity.

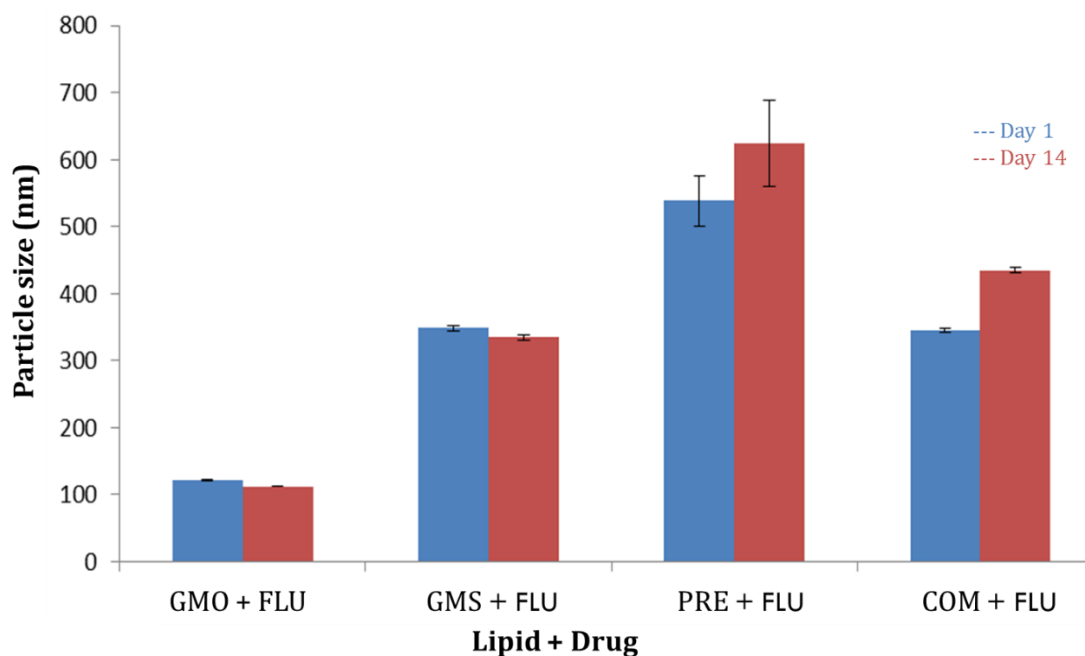


Figure 30. Particle size of loaded SLNs on Day 1 and Day 14. Drug-loading did not affect particle size of GMO and GMS-prepared SLN. Smaller particle size and minimal change in particle size was observed in GMO and GMS SLN.

4.4 Discussion

SLNs are mixtures of solid lipids and surfactants capable of containing poorly water soluble drugs. It was considered that the excipients selected for formulation of SLNs could enhance the dissolution and permeability of the drug by decreasing particle size. To develop the optimal formulation of SLNs, it was necessary to evaluate drug and excipient miscibility along with particle size and stability.

Miscible lipid and surfactant combinations, as observed between GMO-GEL and GMS-GEL, contributed to the reduction of particle size and stability of SLNs. These excipients reduce interfacial energy, increase absorption at the interface, and decrease free energy of the system. This leads to a decrease in the tendency for nanoparticles to coalesce and improvement of thermodynamic stability (Verma et al, 2011). Moreover, utilization of a solid lipid component prevents nanoparticles from coalescing (Siekmann Westesen, 1998). Incorporation of FLT into SLNs immobilizes the drug within the lipid matrix and minimizes drug exposure to the aqueous environment. Encapsulation of the drug also protects FLT from degradation (Wong et al, 2007). Since PRE-GEL and COM-GEL produced larger-sized nanoparticles, it can be stated that miscibility plays a significant role in the maintenance and production of smaller SLNs.

Preparation of SLN with the selected lipids and surfactant was advantageous because of their physiological compatibility, thus reducing inherent toxicity, an added benefit for anticancer agents like FLT. GEL is widely used due to its emulsifying and amphiphilic properties. In a study by Bandari and colleagues, GEL 50/13 was used to prepare loratidine SDs. As a BCS class II drug, loratidine

exhibited poor solubility and slow dissolution rate. The investigation determined that solubility of loratidine increased by 100-fold in the presence of 10% concentration of GEL 50/13 compared to pure loratidine. Additionally, the mean dissolution time of loratidine also decreased meaning improvement in dissolution rate (Bandari et al, 2014). Other studies involving GEL 44/14 have been found to increase dissolution rate of poorly water soluble drugs, such as curcumin, fexofenadine hydrochloride and ritonavir (Zhang et al, 2014). The resultant increase in bioavailability of these agents warranted use of GEL in this research for application with FLT.

The study aimed to evaluate the performance of SLNs through assessment of particle size. As an anticancer agent, bioavailability of FLT is dependent upon its therapeutic efficacy. The advantages of SLNs in relation to anticancer therapy include facilitated deposition into tumors, increased accumulation and cellular uptake of cancer cells, and decreased systemic toxicity (Moghimi et al, 2001; Doijad et al, 2007; Goutayer et al, 2010). Reddy et. al. conducted a study that examined tumor uptake of etoposide SLNs. Tumor uptake of free etoposide was found to be less than that of etoposide SLNs. It was concluded that the SLN design increased site-specific targeting. Furthermore, this resulted in fewer adverse toxicity effects of anticancer therapy (Reddy et al, 2005). Preparation of docetaxel-loaded SLNs was performed by Yuan et. al. to study the effects of SLN formulation on therapeutic efficacy and toxicity. Docetaxel SLNs were advantageous due to their ease of preparation, better stability, use of safe materials, and potential for controlled release. Myelosuppression is a common side effect of therapy with docetaxel and

SLNs were found to produce a lower incidence of myelosuppression along with other dose-limiting side effects while maintaining anticancer activity (Yuan et al, 2014). Therapeutic efficacy and avoidance of side effects are significant benefits of SLN for the treatment of cancer.

FLT was selected as the model drug of this study because of its poor water solubility and thus low bioavailability. The ability of SLN to incorporate hydrophobic drugs provided additional rationale for selection of this formulation for optimal performance of FLT. Since many NCE are classified as poorly water soluble, additional study of FLT SLNs could contribute to the advancement of other novel agents. This study concluded that GMO and GMS prepared SLNs showed promising results, including decreased particle size and stability. GMS was also used to prepare efavirenz SLN in a study conducted by Gaur and colleagues. The mean particle size of efavirenz SLN was 124.5 ± 3.2 nm, which was achieved with the addition of Tween 80 as surfactant (Gaur, 2014). Tween 80 was found to stabilize the interfacial film of the SLNs resulting in increased drug entrapment efficiency, but limited drug release. A similar rationale was used for selection of GEL in this study. The reduced particle size and stability displayed by FLT SLN prepared with GMO and GMS along with GEL may provide essential bioavailability and physiochemical properties necessary for optimal formulation and treatment of prostate cancer with FLT.

4.5 Conclusion

MDSC provided useful information about the melting (endothermic transition) and crystallization (exothermic transition) of lipids and surfactants.

Lipids having good miscibility with surfactants as evidenced by a decrease or broadening of melting and crystallization transition were found to have smaller particle size. Drug loading did not affect order of particle size (GMO < GMS < COM < PRE) of prepared SLNs. Good correlation between miscibility of lipid-surfactant and particle size was observed. GMO and GMS showed good miscibility with GELs and were used successfully in the formulation of SLNs.

4.6 References

Bandari, S., Jadav, S., Eedara, B., Dhurke, R., & Jukanti, R. (2014). Enhancement of solubility and dissolution rate of loratadine with gelucire 50/13. *Journal of Pharmaceutical Innovation*, 9(2), 141-149.

Doijad, R. C., Manvi, F. V., Godhwani, D. M., Joseph, R., & Deshmukh, N. V. (2007). Formulation and targeting efficiency of cisplatin engineered solid lipid nanoparticles. *Indian Journal of Pharmaceutical Sciences*, 70(2), 203-207.

Gaur, P. K., Mishra, S., Bajpai, M., & Mishra, A. (2014). Enhanced oral bioavailability of efavirenz by solid lipid nanoparticles: In vitro drug release and pharmacokinetics studies. *BioMed Research International*, 2014, 363404.

Goutayer, M., Dufort, S., Josserand, V., Royère, A., Heinrich, E., Vinet, F., . . . Texier, I. (2010). Tumor targeting of functionalized lipid nanoparticles: Assessment by in vivo fluorescence imaging. *European Journal of Pharmaceutics and Biopharmaceutics*, 75(2), 137-147.

Jabir, N. R., Tabrez, S., Ashraf, G. M., Shakil, S., Damanhour, G. A., & Kamal, M. A. (2012). Nanotechnology-based approaches in anticancer research. *International Journal of Nanomedicine*, 7, 4391-4408.

Jeevana, J. B., & Sreelakshmi, K. (2011). Design and evaluation of self-nanoemulsifying drug delivery system of flutamide. *Journal of Young Pharmacists : JYP*, 3(1), 4-8.

Licciardi, M., Di Stefano, M., Craparo, E. F., Amato, G., Fontana, G., Cavallaro, G., & Giammona, G. (2012). PHEA-graft-polybutylmethacrylate copolymer microparticles for delivery of hydrophobic drugs. *International Journal of Pharmaceutics*, 433(1-2), 16-24.

Moghimi S, Hunter A, Murray J. (2001). Long-circulating and target-specific nanoparticles: theory to practice. *Pharmacol Rev*, 53, 283-318.

Murthy, R. S. R., & Umrethia, M. L. (2004). Optimization of formulation parameters for the preparation of flutamide liposomes by 33 factorial 26-term logit model. *Pharmaceutical Development & Technology*, 9(4), 369-377.

Reddy L, Sharma R, Chuttani K, Mishra A, Murthy R. (2005). Influence of administration route on tumor uptake and biodistribution of etoposide loaded solid lipid nanoparticles in Dalton's lymphoma tumor bearing mice. *J Control Release*, 105, 185-198.

Rowe, R., Sheskey, P., Quinn, M. American Pharmacists Association. (2009). *Handbook of pharmaceutical excipients*. London: Pharmaceutical Press.

Siekmann B, Westersen K. (1998). Submicron emulsions in drug targeting and delivery. The Netherlands: Horwood Academic Publishers, 205-218.

Sinko, P., Singh, Y. (2011). Martin's physical pharmacy and pharmaceutical sciences. Philadelphia: Wolters Kluwer, Lippincott Williams and Wilkins.

Sultana, S., Khan, M. R., Kumar, M., Kumar, S., & Ali, M. (2013). Nanoparticles-mediated drug delivery approaches for cancer targeting: A review. *Journal of Drug Targeting*, 21(2), 107-125.

Verma, A., Singh, M. K., & Kumar, B. (2011). Development and characterization of flutamide containing self-microemulsifying drug delivery system (smedd). *International Journal of Pharmacy & Pharmaceutical Sciences*, 3, 60-65.

Wong, H. L., Bendayan, R., Rauth, A. M., Li, Y., & Wu, X. Y. (2007). Chemotherapy with anticancer drugs encapsulated in solid lipid nanoparticles. *Advanced Drug Delivery Reviews*, 59(6), 491-504.

Yuan, Q., Han, J., Cong, W., Ge, Y., Ma, D., Dai, Z., . . . Bi, X. (2014). Docetaxel-loaded solid lipid nanoparticles suppress breast cancer cells growth with reduced myelosuppression toxicity. *International Journal of Nanomedicine*, 9, 4829-4846.

Zhang, H., Huang, X., Mi, J., Huo, Y., Wang, G., Xing, J., & Gao, Y. (2014). Improvement of pulmonary absorptions of poorly absorbable drugs using gelucire 44/14 as an absorption enhancer. *Journal of Pharmacy and Pharmacology*, 66(10), 1410-1420.

CHAPTER 5

Correlation of drug-polymer miscibility to solubility of amorphous solid dispersions and drug-lipid miscibility to particle size of solid lipid nanoparticles

5.1 Summary and conclusions

Miscibility is an important factor to consider for the selection of a polymer or lipid that would produce the optimal formulation of amorphous SDs and SLNs, respectively. The polymers and lipids used in this study were chosen due to their variance of physicochemical properties and frequent use in the pharmaceutical industry. Physicochemical properties of interest included length, weight, polar and nonpolar functional groups, physical state, as well as, melting temperature or glass transition temperature. Miscibility and solubility are expected to decline with increasing polymer or lipid length and weight as a result of changes in entropy. Similar entropic effects can be related to melting and glass transition temperatures. For excipients with T_m or T_g below that of the desired drug's T_m or T_g , entropy increases resulting in an increase in internal energy thus providing a favorable environment for the drug to be dispersed within the melt. Analysis of functional groups present on drug and excipient may be indicative of probable interactions formed between components, which lead to miscibility and stability of the binary compound. Though there are numerous excipients available for study, methods such as calculation of solubility parameter can be used to quickly identify excipients with the potential to achieve kinetic stability and provide chemical potential necessary for successful formulation of SDs and SLNs.

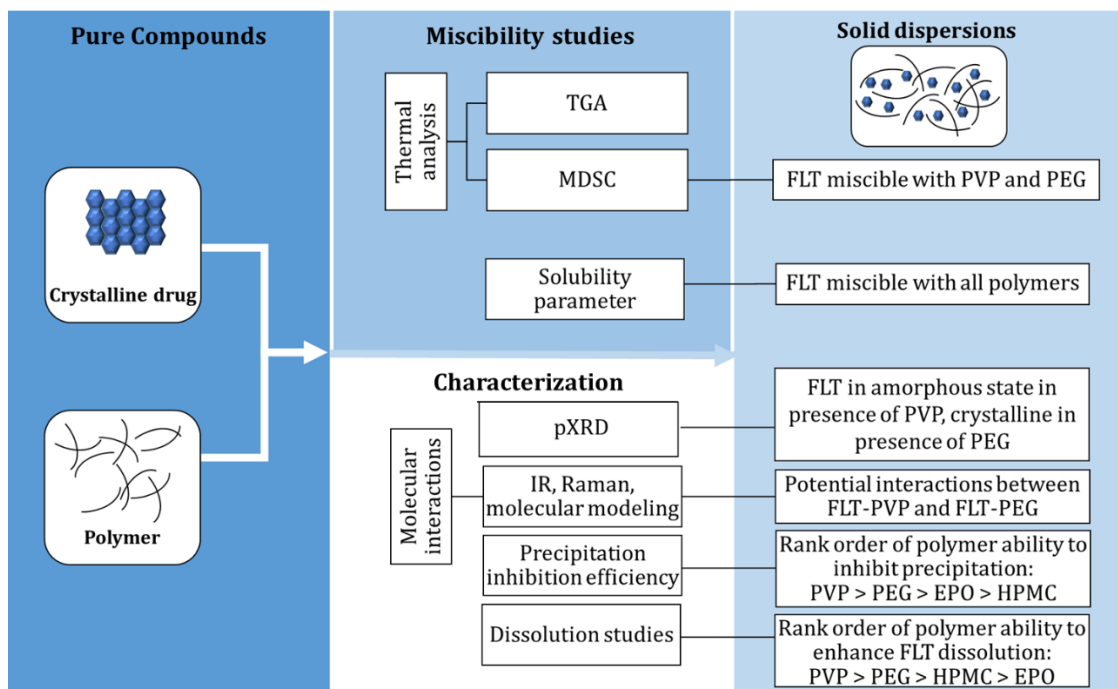


Figure 31. Summary of the methods and results of FLT SDs. Miscibility of FLT with PVP and PEG was correlated to improved precipitation inhibition efficiency and dissolution enhancement. Potential interactions formed between FLT-PVP and FLT-PEG were believed to contribute to these improvements displayed by FLT.

Figure 31 depicts a summary of the studies and results carried out in the preparation and characterization of FLT SDs. Amorphous SDs in this study were prepared with PVP, HPMC, EPO and PEG. Solubility parameter calculations showed promising results that all four polymers were miscible with FLT. However, miscibility studies of PMs and SDs using MDSC suggested good miscibility between PVP and PEG due to the depression of melting point initiation and melting enthalpy of FLT with these polymers. The reduction of enthalpy was indicative of reduced drug crystallinity suggestive of an improved dissolution profile due to the lack of a

crystalline lattice and decreased need for energy to promote dissolution. Moreover, potential hydrogen bond formation between FLT-PVP and FLT-PEG were identified through IR, Raman and molecular modeling studies. These interactions were assumed to play significant roles in the ability of these polymers to achieve miscibility with FLT. Additionally, interactions between drug and polymer were thought to improve the physical stability of SDs as this meant fewer interactions were formed between drug-drug molecules. This study found that hydrogen bonding parameter was most influential in predicting drug-polymer miscibility.

Based on these findings, improved physiochemical properties of FLT were expected with FLT-PVP and FLT-PEG binary compounds. This was in fact the case as PVP and PEG were found to be efficient precipitation inhibitors allowing FLT to remain in solution for a prolonged period of time. An increased percentage of FLT in solution implied increased drug available for absorption and thus improved bioavailability. Consequently, PVP and PEG were also shown to enhance the dissolution profile of FLT. In comparison to PMs, SDs improved the extent of dissolution considerably. Conversion of FLT from the crystalline to amorphous form in the presence of PVP was attributed to improved dissolution. However, FLT crystallinity was maintained in the presence of PEG. This negated the notion that reduced drug crystallinity promoted dissolution. Thus the contribution of molecular interactions may play a more significant role in miscibility than previously thought. Overall, good miscibility of drug and polymer was found to increase solubility of FLT evidenced by the increased amount of drug in solution and the improvement of the extent of drug dissolution.

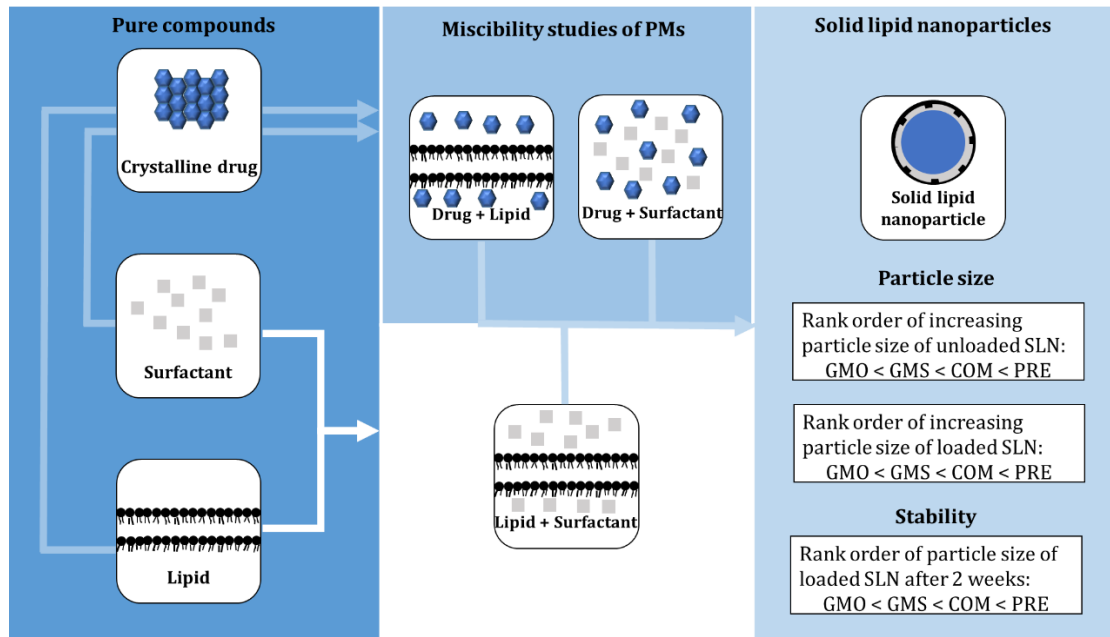


Figure 32. Summary of the methods used to prepare FLT SLNs. Miscibility exhibited by FLT with lipid and surfactant along with miscibility of lipid with surfactant was ideal for the formulation of FLT SLNs. Assessment of SLNs performance was focused on particle size. Both GMO and GMS were able to maintain lower particle size in comparison to PRE and COM.

Figure 32 shows an overview of the methods used to prepare FLT SLNs. SLNs were prepared with GMO, PRE, GMS and COM. Initial MDSC studies between lipid and surfactant, GEL, were conducted to determine miscibility between these two components. Based on the comparison of the physiochemical properties, it was predicted that increased dissimilarities between components implied immiscibility. The apparent differences between COM and GEL supported this conclusion as the characteristic endotherms and exotherms of both these compounds were observed

in the MDSC thermogram indicating poor miscibility; on the contrary, the characteristic melting and crystallization peaks were decreased or absent in the presence of GMO-GEL and GMS-GEL. Good miscibility was seen between GMO-GEL and GMS-GEL. Combinations of FLT with lipid or surfactant were then studied to assess drug crystallinity. Reduced FLT crystallinity was apparent in the presence of GMO, GMS and Gel, which supported miscibility studies between lipid and surfactant. A reduction of FLT crystallinity suggested reduced particle size and therefore, improved bioavailability. This study predicted that preparation of SLN between miscible lipid and surfactant would enhance the performance of SLN through analysis of particle size.

Particle size analysis and stability studies of prepared SLNs correlated well to the conducted miscibility results. Lipids exhibiting good miscibility with surfactants were shown to have smaller particle size. Furthermore, drug loading did not affect particle size. Thus, miscibility is a good indicator of optimal performance demonstrated by SLNs. Miscibility favorably affects drug-carrier stability, drug load and drug dissolution due to an increase in surface area.

CHAPTER 6

Future Directions

6.1 Potential Future Studies

This study theorized that amorphous SDs would enhance the solubility and stability of FLT, a crystalline, poorly water soluble drug. The method used to assess FLT conversion from the crystalline to amorphous state was MDSC and further characterization was performed using pXRD. Miscibility studies of drug-polymer PMs and SDs concluded that PVP and PEG exhibited enhanced stability, dissolution, and solubility. Interestingly, PEG was the only crystalline polymer used in this study and results confirmed these improvements in the physiochemical properties of FLT. Amorphous SDs have high internal energy and are prone to revert to the crystalline state. Thus, the existence of both drug and polymer in the crystalline state warrant further studies be carried out to determine whether sustaining crystalline FLT could contribute to the development of an optimal formulation.

Furthermore, miscibility studies of FLT-PEG depicted an additional endotherm unrelated to the characteristic melting peaks of drug or polymer. Quantitative analysis using pXRD, IR and Raman to confirm the presence of a FLT-PEG co-crystal would provide valuable research. The significance of co-crystal formation would indicate the potential adjustment of drug crystallinity, melting point, dissolution, solubility and thereby bioavailability through alteration of physiochemical properties of the drug. Improved solubility can be influenced by the strength of the crystal lattice and solvation of the co-crystal components. Molecular interactions between drug and co-former subsequently affect the strength of the crystal lattice. Moreover, solid state materials are more thermodynamically and physically stable.

Molecular modeling studies using Jaguar software was used in this study to identify potential interactions made between drug and polymers. IR and Raman spectroscopy were then used to confirm the presence of these potential interactions. More extensive molecular modeling studies could be conducted to identify which atoms are involved in bond formation and how specific functional groups present on both drug and polymer necessitate a particular configuration or surrounding environment in order to form these interactions. Computational data, such as vibrational or rotational frequencies, can be calculated to identify characteristic peaks of drug, polymer, and co-crystal products. Chemical conformation of compounds and stretching peaks could also be calculated. Correlation of this data to the observed changes in IR and Raman spectra would strengthen our findings.

This study did not analyze the potential interactions formed between FLT and lipids used in the formulation of SLNs. Molecular modeling studies along with IR and Raman spectroscopy could be used to identify bonds made between drug and lipid, which contributed to miscibility and stability of these binary compounds. Further studies providing this data would confirm the significant contribution of molecular interactions in the successful formation of SLNs. Additionally, drug entrapment efficiency and drug dissolution studies would provide insight to the prospective advantages or improvements of FLT physiochemical properties as a result of preparation of SLNs.